Low Energy Constants from a Ginsparg-Wilson type operator in lattice QCD

Dissertation

zur Erlangung des akademischen Grades
Doktor der Naturwissenschaften

vorgelegt von
Philipp Huber

Betreuung:
Univ. Prof. Dr. C. B. Lang

Juni 2007

Präambel

Ich, Philipp Huber, bestätige, dass es sich bei dieser Dissertation um eine Originalarbeit handelt, die von mir selbständig verfass wurde.

Introduction

Quantum Chromodynamics (QCD) is a field theory formulated in terms of quarks and gluons and is believed to describe strong interactions. We live in space-time with Minkowski metric, but it is possible to formulate QCD in space-time with Euclidean metric, which is better suited for numerical simulations. The results can then be related to a formulation in Minkowski space-time.
Quantization of QCD in four dimensions leads to divergent contributions. In the process of regularization the theory is manipulated, such that it is mathematically well-defined. There are different regularization methods available that are more or less suited for different physical situations. Each of them keeps some of the symmetries of the original theory intact and destroys others. The lattice regularization is one that does not affect the gauge symmetry, which is a vital ingredient of QCD. Instead of continuous space-time, the theory is formulated on a lattice of space-time points with a specific lattice spacing. Additionally only a finite set of points in each direction is considered and periodic (or anti-periodic) boundaries are imposed, which makes the theory suitable for numerical simulations.
Among others, chiral symmetry, that is that left- and right-handed fermions decouple, is a symmetry of the massless Lagrangian of QCD and an approximate symmetry for the light quark sector. Upon quantization an additional spontaneous breaking of chiral symmetry occurs. For a long time it has been unclear how to translate chiral symmetry to the lattice. The original lattice formulation proposed by Wilson has the problem of generating 16 lattice fermions from one fermion in the continuum, but only one has the correct dispersion relation. This issue is called the fermion doubling problem. The additional doublers decouple from the theory when taking the continuum limit, but spoil the realization of chiral symmetry at finite lattice spacing. In 1981 Nielsen and Ninomiya showed that it is not possible to use the con-

tinuum version of chiral symmetry while maintaining other vital properties on the lattice.
Shortly thereafter in 1982 Ginsparg and Wilson suggested a relation that defines a lattice version of chiral symmetry, but the first realization of an operator satisfying this relation took until the 1990's. The so-called chirally improved Dirac operator is constructed as a general expansion of an operator in terms of paths on the lattice containing all 16 Clifford algebra elements. The expansion parameters are constrained by symmetries and the Ginsparg-Wilson relation. For numerical applications the expansion is usually truncated to contain paths up to length four, hence the chirally improved Dirac operator obeys the Ginsparg-Wilson relation only approximately.
Meson propagators can be computed using lattice QCD where especially for the light quark sector chiral symmetry is of great importance. Therefore actions with good chiral properties are supposed to provide reliable results for quantities like the pion propagator when going to small quark mass parameters.
Chiral perturbation theory is believed to be a valid low energy effective theory for QCD defined in the chiral limit. Mesonic chiral perturbation theory uses pseudoscalar fields as fundamental degrees of freedom that are massless in the chiral limit. In order to include non-vanishing quark and therefore also meson masses a symmetry breaking term can be included in the Lagrangian of the theory. Every interaction term, that is not excluded by the symmetries can be included in the Lagrangian and the terms are ordered according to the number of powers of momentum and mass. For this application only first order terms are included.
Lattice QCD computations are typically performed at unphysically high quark masses, whereas results obtained in chiral perturbation theory have the best quality close to the chiral limit. There one hopes that higher order corrections do not have a strong impact. Two parameters appear in the lowest order of mesonic chiral perturbation theory: the pseudoscalar decay constant, the parameter that determines the pion's coupling to the weak current, and the chiral condensate, which can be considered as order-parameter. Correlation functions can be evaluated in both frameworks and provide a means of using ab-initio results from lattice QCD to compute the low energy parameters of chiral perturbation theory.
Results in lattice QCD always come with the regularization scale attached. For quantities where the absolute value of the propagator plays a role, proper normalization and renormalization is an issue. In [1] and [2] the renormal-

ization factors for the chirally improved action are computed and allow to determine quark masses and the low energy parameters for this action in a continuum renormalization scheme and a comparison to other approaches is possible.
The outline of this thesis is as follows. Chapter 1 gives a short overview over the basic properties of Euclidean QCD. The focus lies on the basic symmetries of QCD. In Chapter 2 the main ideas for formulating a gauge theory on the lattice are collected. The symmetries of QCD in this framework are worked out in Chapter 3. The emphasis lies on chiral symmetry and a lattice formulation of this symmetry, the Ginsparg-Wilson relation. The Dirac operator used for numerical simulations is introduced there. In Chapter 4 formulae for meson propagators from lattice quark propagators are worked out and also the quenched approximation is explained. Chiral perturbation theory and its basic formulae are introduced in Chapter 5. The connection between a continuum effective theory for mesons and the ab-initio computations performed in lattice QCD is established in this Chapter. Numeric results from our quenched lattice calculation are presented in Chapter 6, which is heavily based on [3] and [4]. Starting from properly (re)normalizing quark and meson propagators results for the quark mass, chiral condensate and the pseudoscalar decay constants for pion and kaon are computed. The lattice sizes range from $8^3 \times 24$ to $20^3 \times 32$ with lattice spacings between 1.2 fm and 2.4 fm. The mass of the pion extends down to around 330 MeV. In the Appendices properties of Pauli, Gell-Mann and Dirac matrices along with the coefficients of the chirally improved action are collected. Additionally the fitting method used is explained.

Contents

Chapter 1

General introduction to QCD

1.1 Euclidean QCD

Quantum Chromo Dynamics (QCD) [5] is believed to be the right description of strong interactions on the level of quarks and gluons in a quantum field theoretic framework. Here we define it straightaway in a Euclidean framework, i.e., we replace the Minkowski time by imaginary time. Thereby we also modify anti-commutation relations and the structure of the Dirac matrices (see Sect. A.2 for definition of the matrices). In order to transform correlation functions from Euclidean back to Minkowski metric, they have to satisfy several conditions, among them one called reflection positivity [6].

1.1.1 The fields

In this description quarks and antiquarks are massive spin-$\frac{1}{2}$ fermionic fields that have spatial, Dirac, flavor and color structure. We can denote them by

$$\psi^f_{\alpha c}(x),\ \bar{\psi}^f_{\alpha c}(x) \tag{1.1}$$

where x is the space-time position of the field, $\alpha = 1, \ldots, 4$ gives the Dirac index, $c = 1, 2, 3$ the color index and $f = 1, \ldots, N_f$ the flavor of the quark in consideration. Quark fields and the renormalized mass are no observables, i.e., they have to be defined within a theoretical framework, but we may order quarks such that they fall into light and heavy sections compared to the typical scale of QCD (e.g., the mass of the nucleon or $4\pi f_\pi$, which is both

roughly 1 GeV) in a specific scheme, the $\overline{\text{MS}}$ scheme [7, 8]

$$\begin{pmatrix} m_u = 0.0015 - 0.003\,\text{GeV} \\ m_d = 0.003 - 0.007\,\text{GeV} \\ m_s = 0.070 - 0.120\,\text{GeV} \end{pmatrix} \ll 1\,\text{GeV} \ll \begin{pmatrix} m_c = 1.16 - 1.34\,\text{GeV} \\ m_b = 4.13 - 4.27\,\text{GeV} \\ m_t = 170.9 - 177.5\,\text{GeV} \end{pmatrix}. \tag{1.2}$$

We can combine the quark masses to a matrix defined in flavor space, namely the quark mass matrix

$$\mathcal{M} = \text{diag}\,(m_u, m_d, m_s, m_c, m_b, m_t) \tag{1.3}$$

and truncate it to the light (i.e., $N_f = 3$) or light, non-strange (i.e., $N_f = 2$) sector for our purposes. The fact that the light quarks are so much lighter than, e.g., masses of nucleons leads to an approximate global $SU(2)$ and to a lesser extent $SU(3)$ symmetry of the QCD-Lagrangian. For the $SU(2)$ and $SU(3)$ sector using the unit matrix plus the Pauli and Gell-Mann matrices, respectively, the mass matrix reads the following way

$$\begin{aligned} \mathcal{M} &= \frac{m_u - m_d}{2}\lambda_3 + \frac{m_u + m_d}{2}\mathbb{1} && \text{(1.4a)} \\ &= \mathcal{M}_3\lambda_3 + \mathcal{M}_0\mathbb{1}, \\ \mathcal{M} &= \frac{m_u - m_d}{2}\lambda_3 + \frac{m_u + m_d - 2m_s}{2}\lambda_8 + \frac{m_u + m_d + m_s}{3}\mathbb{1} && \text{(1.4b)} \\ &= \mathcal{M}_3\lambda_3 + \mathcal{M}_8\lambda_8 + \mathcal{M}_0\mathbb{1} \end{aligned}$$

with the definitions

$$\mathcal{M}_3 = \frac{m_u - m_d}{2}, \tag{1.5a}$$

$$\mathcal{M}_0 = \frac{m_u + m_d}{2} \tag{1.5b}$$

for $SU(2)$ and

$$\mathcal{M}_3 = \frac{m_u - m_d}{2}, \tag{1.6a}$$

$$\mathcal{M}_8 = \frac{m_u + m_d - 2m_s}{2}, \tag{1.6b}$$

$$\mathcal{M}_0 = \frac{m_u + m_d + m_s}{3} \tag{1.6c}$$

for $SU(3)$. In Minkowski space-time using the operator approach, the fermion fields are related by

$$\bar{\psi} = \psi^\dagger \gamma_0, \tag{1.7}$$

whereas in the Euclidean path integral we integrate over two independent Grassmann fields ψ and $\bar{\psi}$. Gluons on the other hand are incorporated in form of the gauge fields

$$A_{\mu cd}(x) \in \mathrm{su}(3) \tag{1.8}$$

having spatial (x), Dirac (μ) and color (c, d) structure, but no flavor content.

1.1.2 QCD action

The action can be split into a fermionic and a gauge or gluonic part

$$S_{QCD} = \int dt\, L_{QCD} = \int d^4x\, \mathcal{L}_{\mathrm{QCD}} = \int d^4x\, \left(\mathcal{L}_{\mathrm{F}} + \mathcal{L}_{\mathrm{G}}\right) \tag{1.9}$$

where the action is the integral of the Lagrangian L over the time direction. The Lagrangian itself is the spatial integral of the Lagrangian density $\mathcal{L}$.

Fermionic part

The fermionic contribution is bilinear in the quark fields and given by

$$\begin{aligned} S_F[\psi, \bar{\psi}, A] &= \int d^4x\, \bar{\psi}(x) \left(\gamma_\mu \left(\partial_\mu + ig\, A_\mu(x)\right) + \mathcal{M}\right) \psi(x) \\ &= \int d^4x\, \bar{\psi}^f_{\alpha c}(x) \Big((\gamma_\mu)_{\alpha\beta} \left(\delta_{cd}\, \partial_\mu + igA_{\mu cd}(x)\right) \\ &\qquad + \delta_{\alpha\beta}\, \delta_{cd}\, \mathcal{M}^{ff'} \Big) \psi^{f'}_{\alpha d}(x) \end{aligned} \tag{1.10}$$

where summation over Dirac flavor and color indices is implied. The constant g arises from the coupling of quark and gluon fields in the covariant derivative

$$D_\mu(x) = \partial_\mu + igA_\mu(x). \tag{1.11}$$

Gauge part

The gluonic part only depends on the gauge fields and reads

$$S_G[A] = \frac{1}{2g^2} \int d^4x\, Tr\left[F_{\mu\nu}(x) F_{\mu\nu}(x)\right]. \tag{1.12}$$

In contrary to the fermion fields, which are in the fundamental representation of the associated gauge group ($SU(3)$ for QCD), the gauge fields are in the adjoint with the Gell-Mann flavor matrices from Sect. A.1.3 as basis

$$A_\mu(x) = \sum_{i=1}^{N_f^2-1} A_\mu^{(i)}(x)\frac{\lambda_i}{2}. \tag{1.13}$$

The components can be retrieved using the projection property of the λ's

$$A_\mu^{(i)} = \frac{1}{2} Tr\left[\lambda_i A_\mu(x)\right]. \tag{1.14}$$

1.2 Path integral quantization

Up to that point we only dealt with the theory at the classical level. There are many ways to quantize a theory, all of them having advantages and disadvantages making them especially suitable for different classes of theories. We use the path integral formalism [9]. The generating functional for QCD reads

$$Z = \int d[\bar{\psi}]\, d[\psi]\, d[A]\, \mathrm{e}^{-\mathcal{S}_{\mathrm{QCD}}}, \tag{1.15}$$

where we integrate over all possible values of the fields $\bar{\psi}$, ψ and A. Note, that in the usual Minkowski metric we would have an additional imaginary unit in front of the action, which would cause rapid oscillations, but by going to Euclidean space we replaced this by a monotonic function. Expectation values of functions F can be computed using

$$\langle F \rangle = \frac{1}{Z} \int d[\bar{\psi}]\, d[\psi]\, d[A]\, F(\bar{\psi}, \psi, A)\, \mathrm{e}^{-\mathcal{S}_{\mathrm{QCD}}}, \tag{1.16}$$

with the Grassmann variables $\bar{\psi}$ and ψ.

1.3 Symmetries of the QCD Lagrangian

1.3.1 General transformations

In order to illustrate the symmetry properties of the Lagrangian it is useful to split the fermionic part into a massless ($\mathcal{L}_{\mathrm{F}}^0$) and a mass term ($\mathcal{L}_{\mathrm{F}}^{\mathcal{M}}$)

$$\mathcal{L}_{\mathrm{F}} = \mathcal{L}_{\mathrm{F}}^0 + \mathcal{L}_{\mathrm{F}}^{\mathcal{M}}. \tag{1.17}$$

For checking under which transformations the massless Lagrangian stays invariant, we define local unitary transformations on the quark fields

$$\psi' = \mathrm{e}^{i\epsilon(x)\Delta}\psi, \quad \bar{\psi}' = \bar{\psi}\mathrm{e}^{i\epsilon(x)\overline{\Delta}} \tag{1.18}$$

with the local parameter $\epsilon(x)$ and the global Hermitian operators Δ and $\overline{\Delta}$. For the global operators the following relations hold:

$$[\Delta, D_\mu] = 0, \tag{1.19a}$$

$$\left[\overline{\Delta}, D_\mu\right] = 0. \tag{1.19b}$$

The Lagrangian can now be expressed in terms of the transformed fields

$$\begin{aligned}
\mathcal{L}_\mathrm{F}^0[\bar{\psi}, \psi, A] =& \bar{\psi}'(x)\mathrm{e}^{-i\epsilon(x)\overline{\Delta}} D(x) \mathrm{e}^{-i\epsilon(x)\Delta}\psi'(x) \\
=& \bar{\psi}'(x)\mathrm{e}^{-i\epsilon(x)\overline{\Delta}}\gamma_\mu \mathrm{e}^{-i\epsilon(x)\Delta} D_\mu(x)\psi'(x) \\
=& \mathcal{L}_\mathrm{F}^0[\bar{\psi}', \psi', A] - i\epsilon(x)\bar{\psi}'(x)\left[\overline{\Delta}\gamma_\mu + \gamma_\mu\Delta\right] D_\mu(x)\psi'(x) \\
& - i\left(\partial_\mu\epsilon(x)\right)\bar{\psi}'(x)\gamma_\mu\Delta\psi'(x) + \mathcal{O}\left(\epsilon^2\right),
\end{aligned} \tag{1.20a}$$

$$\begin{aligned}
\mathcal{L}_\mathrm{F}^\mathcal{M}[\bar{\psi}, \psi, A] =& \mathcal{L}_\mathrm{F}^\mathcal{M}[\bar{\psi}', \psi', A] - i\epsilon(x)\bar{\psi}'(x)\left[\overline{\Delta}\mathcal{M} + \mathcal{M}\Delta\right]\psi'(x) + \mathcal{O}\left(\epsilon^2\right) \\
=& \mathcal{L}_\mathrm{F}^\mathcal{M}[\bar{\psi}', \psi', A] \\
& - i\epsilon(x)\bar{\psi}'(x)\left[\left(\Delta + \overline{\Delta}\right)\mathcal{M} + [\mathcal{M}, \Delta]\right]\psi'(x) + \mathcal{O}\left(\epsilon^2\right)
\end{aligned} \tag{1.20b}$$

resulting in

$$\begin{aligned}
i\,\delta\mathcal{L}_\mathrm{F}^0 =& \epsilon(x)\bar{\psi}(x)\left[\overline{\Delta}\gamma_\mu + \gamma_\mu\Delta\right] D_\mu(x)\psi(x) \\
& + \left(\partial_\mu\epsilon(x)\right)\bar{\psi}(x)\gamma_\mu\Delta\psi(x) + \mathcal{O}\left(\epsilon^2\right),
\end{aligned} \tag{1.21a}$$

$$i\,\delta\mathcal{L}_\mathrm{F}^\mathcal{M} = \epsilon(x)\bar{\psi}(x)\left[\left(\Delta + \overline{\Delta}\right)\mathcal{M} + [\mathcal{M}, \Delta]\right]\psi(x) + \mathcal{O}\left(\epsilon^2\right). \tag{1.21b}$$

We can utilize Nöther's theorem to identify contributions with currents J_μ and the derivative thereof

$$\begin{aligned}
J_\mu =& \frac{\partial\delta\mathcal{L}}{\partial\partial_\mu\epsilon} = -i\frac{\partial\mathcal{L}}{\partial\partial_\mu\psi}\Delta\psi \\
=& -i\bar{\psi}(x)\gamma_\mu\Delta\psi(x),
\end{aligned} \tag{1.22a}$$

$$\begin{aligned}
\partial_\mu J_\mu =& \frac{\partial\delta\mathcal{L}}{\partial\epsilon} = -i\frac{\partial\mathcal{L}}{\partial\psi}\Delta\psi - i\frac{\partial\mathcal{L}}{\partial\partial_\mu\psi}\Delta\partial_\mu\psi \\
=& -i\bar{\psi}(x)\left[\overline{\Delta}\gamma_\mu + \gamma_\mu\Delta\right] D_\mu\psi(x) \\
& - i\bar{\psi}(x)\left[\left(\Delta + \overline{\Delta}\right)\mathcal{M} + [\mathcal{M}, \Delta]\right]\psi(x).
\end{aligned} \tag{1.22b}$$

1.3.2 Chiral representation

Let us introduce right- and left-handed projection operators on the fields

$$P_R = \frac{1}{2}\left(\mathbb{1} + \gamma_5\right), \quad P_L = \frac{1}{2}\left(\mathbb{1} - \gamma_5\right) \tag{1.23}$$

with the following properties

$$\begin{aligned} P_R^2 = P_R, \quad P_L^2 = P_L, \quad P_R P_L = P_L P_R = 0, \\ P_R + P_L, = \mathbb{1} \quad \gamma_\mu P_L = P_R \gamma_\mu, \quad \gamma_\mu P_R = P_L \gamma_\mu. \end{aligned} \tag{1.24}$$

Due to these relations the action can be block-diagonalized

$$\begin{aligned} \mathcal{L}_{\mathrm{F}}^0[\bar{\psi}, \psi, A] &= \bar{\psi} P_R D P_R \psi + \bar{\psi} P_L D P_L \psi \\ &= \bar{\psi}_R D \psi_R + \bar{\psi}_L D \psi_L \end{aligned} \tag{1.25}$$

with the definitions

$$\psi_{R,L} = P_{R,L}\psi, \quad \bar{\psi}_{R,L} = \bar{\psi} P_{L,R} \tag{1.26}$$

denoting the left- and right-handed components of the Dirac fields. Let us consider operators for Δ and $\overline{\Delta}$ that can be built from left- and right-handed projectors, namely the vector and axial-vector combinations

$$\Gamma_{V_\mu} = \gamma_\mu \left(P_R + P_L\right) = \gamma_\mu \mathbb{1}, \tag{1.27a}$$
$$\Gamma_{V_\mu^i} = \tau_i \gamma_\mu \left(P_R + P_L\right) = \tau_i \gamma_\mu \mathbb{1}, \tag{1.27b}$$
$$\Gamma_{A_\mu} = \gamma_\mu \left(P_R - P_L\right) = \gamma_\mu \gamma_5, \tag{1.27c}$$
$$\Gamma_{A_\mu^i} = \tau_i \gamma_\mu \left(P_R - P_L\right) = \tau_i \gamma_\mu \gamma_5. \tag{1.27d}$$

Additionally we want to take a look at scalar and pseudoscalar combinations

$$\Gamma_S = \left(P_R + P_L\right) = \mathbb{1}, \tag{1.28a}$$
$$\Gamma_{S^i} = \tau_i \left(P_R + P_L\right) = \tau_i \mathbb{1}, \tag{1.28b}$$
$$\Gamma_P = \left(P_R - P_L\right) = \gamma_5, \tag{1.28c}$$
$$\Gamma_{P^i} = \tau_i \left(P_R - P_L\right) = \tau_i \gamma_5. \tag{1.28d}$$

Symmetry group of the massless Lagrangian

In Tab.s 1.2 and 1.1 the resulting properties for the different transformations are listed. We see that the massless fermionic action is invariant under left- and right-handed special unitary transformations, which can be rewritten due to the properties of the projectors in terms of scalar and pseudoscalar operators with vector and axial-vector, respectively, as the associated current. The resulting symmetry group can therefore be denoted as

$$SU(N_f)_L \times SU(N_f)_R = SU(N_f)_V \times SU(N_f)_A. \tag{1.29}$$

Similarly the unitary transformations for the flavor singlet can be given as

$$U(1)_L \times U(1)_R = U(1)_V \times U(1)_A. \tag{1.30}$$

So the chiral action is invariant under

$$SU(N_f)_L \times SU(N_f)_R \times U(1)_L \times U(1)_R = SU(N_f)_V \times SU(N_f)_A \times U(1)_V \times U(1)_A. \tag{1.31}$$

Symmetry group of the massive, iso-symmetric Lagrangian

As soon as the quarks in the Lagrangian are given a mass, some of the symmetries and the associated currents are no longer conserved. Let us discuss two scenarios. In the first one we have degenerate, but non-zero quark masses, i.e., $m_u = m_d = m_s = m$. The contributions to the mass matrix from (1.6) then read

$$\mathcal{M}_3 = 0, \quad \mathcal{M}_8 = 0, \quad \mathcal{M}_0 = m\mathbb{1}. \tag{1.32}$$

Hence the term containing $[\mathcal{M}, \Delta]$ in the derivative of the action vanishes. The Lagrangian is also no longer invariant under left- and right-handed rotations, neither is it under the axial-vector transformation but the vector current is still conserved. The symmetry group is thereby reduced to

$$SU(N_f)_V \times SU(N_f)_A \times U(1)_V \times U(1)_A \to SU(N_f)_V \times U(1)_V \times U(1)_A. \tag{1.33}$$

The broken axial $SU(N_f)$ symmetry results in the so-called axial Ward-Takahashi identities of the form

$$\partial_\mu A_\mu = 2mP, \tag{1.34a}$$

$$\partial_\mu A^i_\mu = 2mP^i. \tag{1.34b}$$

Note, however that this is only true on the classical level. Upon quantization the expression for the singlet picks up an additional anomalous term.

Symmetry group of the full Lagrangian

Now we also break flavor symmetry by giving the quarks individual masses. The only remaining conserved current is the flavor singlet vector current. The resulting Ward-Takahashi identities then read

$$\partial_\mu V_\mu^i = \bar{\psi}\left[\mathcal{M}, \tau_i\right], \tag{1.35a}$$

$$\partial_\mu A_\mu = 2\bar{\psi}\gamma_5\mathcal{M}\psi, \tag{1.35b}$$

$$\partial_\mu A_\mu^i = \bar{\psi}\gamma_5\left\{\mathcal{M}, \tau_i\right\}\psi. \tag{1.35c}$$

The symmetry group is reduced even further to

$$\underbrace{U(1)_V \times \cdots \times U(1)_V}_{N_f} \times U(1)_A. \tag{1.36}$$

Δ	$\overline{\Delta}$	$\gamma_\mu\Delta$	$\left[\overline{\Delta}+\Delta\right]\mathcal{M}$	$[\mathcal{M},\Delta]$
Γ_S	$-\Gamma_S$	Γ_{V_μ}	0	0
Γ_{S^i}	$-\Gamma_{S^i}$	$\Gamma_{V_\mu^i}$	0	$[\mathcal{M},\tau_i]$
Γ_P	Γ_P	Γ_{A_μ}	$2\Gamma_P\mathcal{M}$	0
Γ_{P^i}	Γ_{P^i}	$\Gamma_{A_\mu^i}$	$2\Gamma_{P^i}\mathcal{M}$	$\gamma_5[\mathcal{M},\tau_i]$
P_L	$-P_R$	$\gamma_\mu P_L$	$-\gamma_5\mathcal{M}$	0
$\tau_i P_L$	$-\tau_i P_R$	$\tau_i\gamma_\mu P_L$	$-\tau_i\gamma_5\mathcal{M}$	$P_L[\mathcal{M},\tau_i]$
P_R	$-P_L$	$\gamma_\mu P_R$	$\gamma_5\mathcal{M}$	0
$\tau_i P_R$	$-\tau_i P_L$	$\tau_i\gamma_\mu P_R$	$\tau_i\gamma_5\mathcal{M}$	$P_R[\mathcal{M},\tau_i]$

Table 1.1: Transformation properties for the dynamic part of the QCD Lagrangian on the classical level before quantization. All of the above transformations satisfy $\overline{\Delta}\gamma_\mu + \gamma_\mu\Delta = 0$.

Δ	$\overline{\Delta}$	iJ_μ	chiral, $\mathcal{M}=0$ $i\partial_\mu J_\mu$	iso-symm. $\mathcal{M}=m\mathbb{1}$ $i\partial_\mu J_\mu$	full $i\partial_\mu J_\mu$
Γ_S	$-\Gamma_S$	V_μ	0	0	0
Γ_{S^i}	$-\Gamma_{S^i}$	V_μ^i	0	0	$\bar{\psi}\left\{\mathcal{M}_3\left[\tau_3,\tau_i\right]+\mathcal{M}_8\left[\tau_8,\tau_i\right]\right\}\psi$
Γ_P	Γ_P	A_μ	0	$2mP$	$2\bar{\psi}\Gamma_P\mathcal{M}\psi$
Γ_{P^i}	Γ_{P^i}	A_μ^i	0	$2mP^i$	$2\bar{\psi}\Gamma_P\mathcal{M}\psi+\bar{\psi}\gamma_5\left[\mathcal{M},\tau_i\right]\psi$ $=\bar{\psi}\left\{\Gamma_{P^i},\mathcal{M}\right\}\psi$
P_L	$-P_R$	$\psi\gamma_\mu P_L\psi$ $=V_\mu-A_\mu$	0	$-mP$	$-\bar{\psi}\Gamma_P\mathcal{M}\psi$
$\tau_i P_L$	$-\tau_i P_R$	$\bar{\psi}\tau_i\gamma_\mu P_L\psi$ $=V_\mu^i-A_\mu^i$	0	$-mP^i$	$-\bar{\psi}\Gamma_P^i\mathcal{M}\psi+\bar{\psi}P_L\left[\mathcal{M},\tau_i\right]\psi$
P_R	$-P_L$	$\bar{\psi}\gamma_\mu P_R\psi$ $=V_\mu+A_\mu$	0	mP	$\bar{\psi}\Gamma_P\mathcal{M}\psi$
$\tau_i P_R$	$-\tau_i P_L$	$\bar{\psi}\tau_i\gamma_\mu P_R\psi$ $=V_\mu^i+A_\mu^i$	0	mP^i	$\bar{\psi}\Gamma_P^i\mathcal{M}\psi+\bar{\psi}P_R\left[\mathcal{M},\tau_i\right]\psi$

Table 1.2: Transformation properties for the chirally symmetric, iso-symmetric and full QCD Lagrangian on the classical level before quantization.

Chapter 2

Lattice regularization

Quantizing a theory like QCD confronts us with a lot of mathematical challenges. For example, we need a way to compute all possible paths of propagation between two space-time points. One way to alter the theory such that it is mathematically well-defined is to replace continuous space-time with a space-time lattice. For this purpose we introduce an (artificial) regularization parameter a, the lattice-spacing. The canonical lattice Λ has a hypercubic symmetry,

$$\Lambda = \{x | x_\mu / a \in \mathbb{Z}\}. \tag{2.1}$$

Furthermore we restrict ourselves to a finite system, i.e., after some distance L_μ in a specific direction the boundaries are identified periodically such that we end up with a torus in spacetime. Now we need to find a way to define the elements appearing in the Lagrangian on Λ.

2.1 Gauge fields and action

Unlike fermion fields gauge fields are vector-fields and carry a space-time index μ. When a particle evolves, it picks up a (depending on the group and representation possibly matrix-valued) phase-factor determined by the gauge field

$$\psi \to P \exp\left(i \int_s dx_\mu A^\mu\right) \psi, \tag{2.2}$$

where P denotes path ordering and the coupling g has been absorbed into the definition of A. We introduce parallel-transporters of the form

$$U_\mu(x) = U_{x,x+a\hat{\mu}} = \exp\left(iaA_\mu(x)\right), \tag{2.3}$$

$$U_{x+a\hat{\mu},x} = U_\mu(x)^\dagger. \tag{2.4}$$

Doing this we changed from non-compact variables A^μ in the algebra su(3) to compact variables U_μ in the corresponding group SU(3). Elitzur's theo-

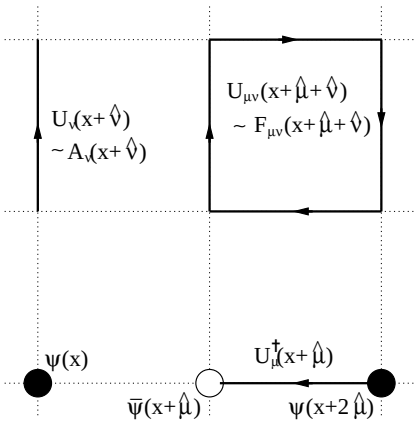

Figure 2.1: Different objects on the lattice

rem [10] states that only gauge-invariant quantities can have non-vanishing expectation values. Under gauge-transformations V our fields behave like

$$\bar{\psi}(x) \to \bar{\psi}(x)V^\dagger(x), \tag{2.5a}$$

$$\psi(x) \to V(x)\psi(x), \tag{2.5b}$$

$$U_\mu(x) \to V(x)U_\mu(x)V^\dagger(x + a\hat{\mu}). \tag{2.5c}$$

We can construct gauge-invariant quantities using link-variables U and fermionic fields $\bar{\psi}$ and ψ. Examples are (see Fig. 2.2) a quark created and annihilated at the same site

$$\bar{\psi}(x)\psi(x) \to \bar{\psi}V^\dagger(x)V(x)\psi(x) = \bar{\psi}(x)\psi(x), \tag{2.6}$$

a quark created and annihilated at different sites connected by a product of gauge link variables

$$\begin{aligned} &\bar{\psi}(x)U_\mu(x)\dots U_\nu(y - a\hat{\nu})\psi(y) \to \\ &\bar{\psi}V^\dagger(x)V(x)U_\mu(x)V^\dagger(x + a\hat{\mu})V(x + a\hat{\mu})\dots\psi(y) \\ &= \bar{\psi}(x)U_\mu(x)\dots U_\nu(y - a\hat{\nu})\psi(y), \end{aligned} \tag{2.7}$$

and a pure gluonic object, the so-called Wilson loop, a closed loop of path-ordered gauge links

$$\begin{aligned} Tr\left[U_\mu(x)U_\mu(x+a\hat{\mu})\dots U_\nu(x-a\hat{\nu})\right] \rightarrow \\ Tr\left[V(x)U_\mu(x)V^\dagger(x+a\hat{\mu})V(x+a\hat{\mu})\right. \\ \left.\times\, U_\mu(x+a\hat{\mu})V^\dagger(x-a\hat{\nu})\dots U_\nu(x-a\hat{\nu})V(x)\right] \\ = Tr\left[U_\mu(x)U_\mu(x+a\hat{\mu})\dots U_\nu(x-a\hat{\nu})\right]. \end{aligned} \tag{2.8}$$

In order to discretize the gauge action S_G of the theory, we have to find a

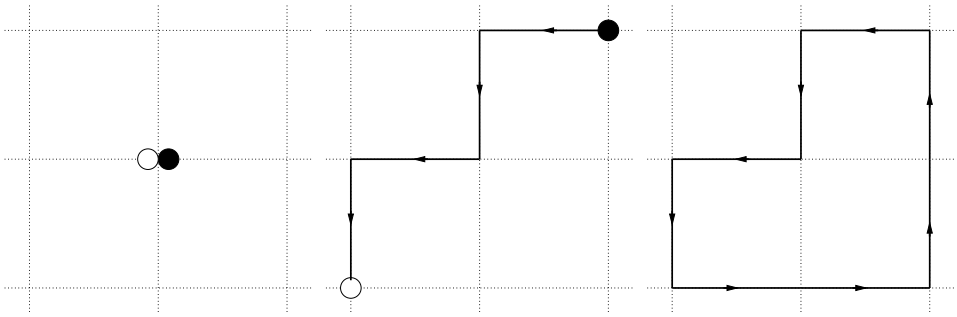

Figure 2.2: (a) A quark and anti-quark at the same site, (b) a quark and anti-quark at remote sites connected by gauge links, (c) a Wilson loop

prescription to define the field-strength tensor and the action

$$S_G = \frac{1}{4}\int d^4x F_{\mu\nu}F^{\mu\nu}, \tag{2.9a}$$

$$F_{\mu\nu}(x) = \partial_\mu A_\nu(x) - \partial_\nu A_\mu(x) - i\left[A_\mu(x), A_\nu(x)\right], \tag{2.9b}$$

on the lattice. A naïve discretization for the derivative modifies the field-strength tensor such that

$$\begin{aligned} F_{\mu\nu}(x) = \frac{1}{a}\left[A_\nu(x+a\hat{\mu}) - A_\nu(x)\right] - \frac{1}{a}\left[A_\mu(x+a\hat{\nu}) - A_\mu(x)\right] \\ - i\left[A_\mu(x), A_\nu(x)\right] + \mathcal{O}(a). \end{aligned} \tag{2.10}$$

A candidate for the gauge action is the plaquette, the smallest possible, 1×1 Wilson loop building block which reads

$$\begin{aligned} U_{\mu\nu}(x) &= U_\mu(x) U_\nu(x + a\hat{\mu}) U_\mu^\dagger(x + a\hat{\nu}) U_\nu^\dagger(x) \\ &= \mathrm{e}^{iaA_\mu(x)} \mathrm{e}^{iaA_\nu(x+a\hat{\mu})} \mathrm{e}^{-iaA_\mu(x+a\hat{\nu})} \mathrm{e}^{-iaA_\nu(x)} \\ &= \exp\left[ia\left(A_\mu(x) + A_\nu(x + a\hat{\mu})\right) - \frac{a^2}{2}\left[A_\mu(x), A_\nu(x + a\hat{\mu})\right] + \mathcal{O}\left(a^3\right)\right] \\ &\times \exp\left[-ia\left(A_\mu(x + a\hat{\nu}) + A_\nu(x)\right) + \frac{a^2}{2}\left[A_\mu(x + a\hat{\nu}), A_\nu(x)\right] + \mathcal{O}\left(a^3\right)\right] \\ &= \exp\Bigg[ia\left(A_\mu(x) - A_\mu(x + a\hat{\nu}) + A_\nu(x + a\hat{\mu}) - A_\nu(x)\right) \\ &\quad - \frac{a^2}{2}\left(\left[A_\mu(x), A_\nu(x + a\hat{\mu})\right] + \left[A_\mu(x + a\hat{\nu}), A_\nu(x)\right]\right) + \mathcal{O}\left(a^3\right)\Bigg]. \end{aligned} \tag{2.11}$$

In order to evaluate $U_{\mu\nu}(x)$ we used the Baker-Campbell-Hausdorff formula for multiplying the exponentials. The order a terms are the naïve lattice differentials of the fields in μ and ν direction and expanding the fields around site x allows us to write the commutators as

$$\left[A_\mu(x), A_\nu(x + a\hat{\mu})\right] + \left[A_\mu(x + a\hat{\nu}), A_\nu(x)\right] = 2\left[A_\mu(x), A_\nu(x)\right] + \mathcal{O}(a). \tag{2.12}$$

We end up with connecting $U_{\mu\nu}(x)$ with the field strength tensor

$$U_{\mu\nu}(x) = \mathrm{e}^{iga^2 F_{\mu\nu}(x)}. \tag{2.13}$$

2.1.1 Wilson gauge action

The plaquette action proposed by Wilson [11] reads

$$S[U] = \sum_x \sum_{1 \le \mu < \nu \le 4} S_P(U_{\mu\nu}(x)) \tag{2.14}$$

and can be related using (2.13) to the continuum expression

$$\begin{aligned} S_P(U_{\mu\nu}(x)) &= \frac{\beta}{3}\mathrm{Re}\,Tr\left(1 - U_{\mu\nu}(x)\right) \\ &= \frac{\beta}{3}\mathrm{Re}\,Tr\left(1 - \mathrm{e}^{iga^2F_{\mu\nu}(x)}\right) \\ &= \frac{\beta}{3}\mathrm{Re}\,Tr\left(-iga^2F_{\mu\nu}(x) + \frac{g^2a^4}{2}F_{\mu\nu}(x)F_{\mu\nu}(x) + \mathcal{O}\left(a^8\right)\right) \\ &= \frac{\beta}{3}Tr\frac{g^2a^4}{2}F_{\mu\nu}(x)F_{\mu\nu}(x) + \mathcal{O}\left(a^8\right), \end{aligned} \tag{2.15}$$

where the quantity β is related to the coupling

$$\beta = \frac{6}{g^2}. \tag{2.16}$$

Note that the order of correction is only due to the expansion of the exponential. But there are also other corrections as we could include different contributions to the field strength tensor that come with some order of a smaller than 8.

2.1.2 Lüscher-Weiss gauge action

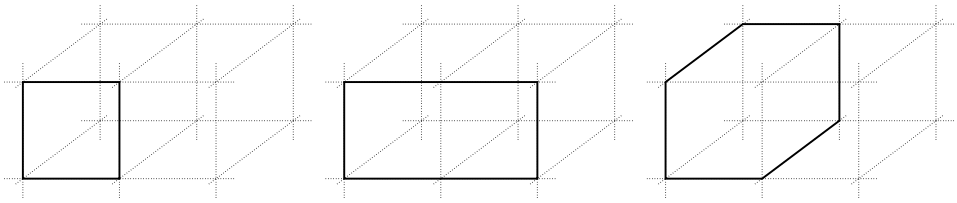

Figure 2.3: (a) The plaquette $U_{\mu\nu}$ (b) The 2×1 rectangle that leads to U_{rect} (c) A parallelogram that leads to U_{para}

In order to reduce lattice artefacts larger loops can be included to improve the gauge action. In addition to closed paths of length four as in the Wilson case, also length six paths are included in the Lüscher-Weiss gauge action [12, 13]. The new contributions are the planar 2×1 loop and the parallelogram

in 3 dimensions that each come with a new parameter (see Fig. 2.3). The action then reads

$$\begin{aligned} S[U] =& \beta_1 \sum_P \frac{1}{3}\mathrm{Re}Tr\left(1 - U_P\right) \\ &+ \beta_2 \sum_{rect} \frac{1}{3}\mathrm{Re}Tr\left(1 - U_{rect}\right) + \beta_3 \sum_{para} \frac{1}{3}\mathrm{Re}Tr\left(1 - U_{para}\right). \end{aligned} \tag{2.17}$$

The terms U_{rect} and U_{para} are constructed analogously to the plaquette. The coefficients β_2 and β_3 have been worked out to be [14]

$$\beta_2 = -\frac{\beta_1}{20u_0^2}\left[1 + 0.4805\alpha\right], \tag{2.18a}$$

$$\beta_3 = -\frac{\beta_1}{u_0^2}\,0.03325\alpha, \tag{2.18b}$$

with u_0 and α given in terms of the expectation value of the plaquette $\frac{1}{3}Tr\langle U_P\rangle$ in [15]

$$u_0 = \left(\frac{1}{3}\mathrm{Re}Tr\langle U_P\rangle\right)^{1/4}, \tag{2.19a}$$

$$\alpha = -\frac{\ln\left(\frac{1}{3}\mathrm{Re}Tr\langle U_P\rangle\right)}{3.06839}. \tag{2.19b}$$

2.2 Fermion fields and action

We can put fermion fields on the lattice in a straight-forward way. In the continuum the fields $\bar{\psi}^f_{\mu\, c}(x_\nu)$ and $\psi^f_{\mu\, c}(x_\nu)$ carry a Dirac (μ), color (c) and flavor (f) structure. We just adopt these properties, but restrict the values of the space-time index to $x_\mu \in \Lambda$ Eq. (2.1) instead of the whole Euclidean space $\mathbb{R}^4$.

2.2.1 Naïve discretization

There is no unique way to define the equivalent of a derivative operator on a discrete manifold. In principle all methods that approach the continuum expression in the limit $a \to 0$ are valid definitions. Let us first consider the 2-point difference operator.

The free case

Let us start with the free case, i.e., the case where all gauge fields are set to $A_\mu = 0$. In the continuum the action reads

$$-S_F[\bar{\psi}, \psi, A = 0] = -S_F^0[\bar{\psi}, \psi] = \int d^4x \, \bar{\psi}(x) \left[\gamma_\mu \partial_\mu + \mathcal{M}\right] \psi(x). \tag{2.20}$$

For the remaining discussion we only consider the iso-symmetric case where

$$\mathcal{M} = m \, \mathbb{1}. \tag{2.21}$$

On the lattice we have to introduce a discretized derivative operator, that approaches the continuum derivative operator when the lattice spacing is taken to zero. The symmetric difference operation

$$\lim_{a \to 0} \frac{1}{2a} \left(\psi(x + \hat{\mu}) - \psi(x - \hat{\mu})\right) = \partial_\mu \psi(x) \tag{2.22}$$

fulfills this requirement. This leads to the following free, naïve lattice action

$$S_F^0[\bar{\psi}, \psi] = a^4 \sum_{x \in \Lambda} \bar{\psi}(x) \left(\sum_{\mu=1}^{4} \gamma_\mu \frac{\psi(x + \hat{\mu}) - \psi(x - \hat{\mu})}{2a} + m\psi(x) \right). \tag{2.23}$$

The difference operator may also be written in the form

$$\Delta_\mu(x, y) = \frac{1}{2a} \left(\delta_{x, y - \hat{\mu}} - \delta_{x, y + \hat{\mu}}\right), \tag{2.24}$$

which acts on a fermionic field in the way described above by summing over the spatial index y

$$\sum_y \Delta_\mu(x, y) \psi(y). \tag{2.25}$$

Now let us transform this operator to momentum space. The discrete Fourier transform for the lattice reads

$$\tilde{f}(p) = \frac{1}{|\Lambda|} \sum_{x_\mu} f(x) \mathrm{e}^{iap_\mu x_\mu}, \tag{2.26}$$

where $|\Lambda| = L_1 L_2 L_3 L_4$ and the momentum space is defined as

$$\tilde{\Lambda} = \left\{ p | p_\mu = \frac{2\pi k_\mu}{a L_\mu}, k_\mu = -\frac{L_\mu}{2} + 1, \ldots, \frac{L_\mu}{2} \right\}. \tag{2.27}$$

The symmetric difference operator can then be evaluated

$$\begin{aligned}\tilde{\Delta}_\mu(p) &= \frac{1}{|\Lambda|^2}\sum_{x,y} \mathrm{e}^{-iap_\nu x_\nu}\Delta_\mu(x,y)\mathrm{e}^{iap_\rho y_\rho} \\ &= \frac{1}{|\Lambda|^2}\sum_{x,y} \mathrm{e}^{-iap_\nu(x_\nu-y_\nu)}\Delta_\mu(x,y) \\ &= \frac{1}{2a|\Lambda|^2}\sum_{x,y} \mathrm{e}^{-iap_\nu(x_\nu-y_\nu)}\left(\delta_{x,y-\hat{\mu}}-\delta_{x,y+\hat{\mu}}\right) \\ &= \frac{1}{2a|\Lambda|^2}\sum_{y} \left(\mathrm{e}^{iap_\mu}-\mathrm{e}^{-iap_\mu}\right) \\ &= \frac{i}{|\Lambda|}\sin(ap_\mu).\end{aligned} \tag{2.28}$$

Note that in the continuum $\tilde{\Delta}_\mu(p)$ would be proportional to p_μ. The free Dirac operator in momentum space then reads

$$\tilde{D}(p) = \frac{1}{|\Lambda|}\left(\sum_\mu i\gamma_\mu \sin(ap_\mu) + m\mathbb{1}\right), \tag{2.29}$$

and gives us the quark propagator

$$\tilde{D}(p)^{-1} = a|\Lambda|\frac{-\sum_\mu i\gamma_\mu\sin(ap_\mu)+am\mathbb{1}}{\sum_\mu \sin^2(ap_\mu)+a^2m^2}. \tag{2.30}$$

Poles in the quark propagator tell us the masses of the particles involved. In this case not only states at $p_\mu = 0$, but also states at $ap_\mu = \pi$ give poles in the propagator, so we have altogether we have 16 particles in the theory, but 15 of them are the so-called doublers, i.e., unphysical states in the theory.

The interacting case

The naïve discretization brings along a set of problems. But before turning our attention towards curing those, let us write down the lattice action for the interacting case. The link variables can be expanded in terms of the fields A_μ

$$U_\mu(x) = \mathrm{e}^{iaA_\mu(x)} \simeq 1 + iaA_\mu(x) + \mathcal{O}\left(a^2\right), \tag{2.31a}$$

$$U_{-\mu}(x) = U_\mu^\dagger(x-\hat{\mu}) = \mathrm{e}^{-iaA_\mu^\dagger(x-\hat{\mu})} \simeq 1 - iaA_\mu(x-\hat{\mu}) + \mathcal{O}\left(a^2\right), \tag{2.31b}$$

where we used $A_\mu = A_\mu^\dagger$. Plugging this into the action leads us to

$$\begin{aligned} S_F[\bar{\psi}, \psi, U] = a^4 \sum_{x \in \Lambda} \bar{\psi}(x) \Bigg(\sum_{\mu=1}^{4} \gamma_\mu \frac{1}{2a} \left(U_\mu(x) \psi(x + \hat{\mu}) \right. \\ \left. - U_{-\mu}(x) \psi(x - \hat{\mu}) + m\psi(x) \right) \Bigg). \end{aligned} \tag{2.32}$$

Note that this expression is invariant under gauge transformations

$$S_F[\bar{\psi}, \psi, U] = S_F[\bar{\psi}', \psi', U']. \tag{2.33}$$

2.2.2 The Wilson action

Wilson's suggestion to handle the problem doublers [16] was to add a term that allows us to distinguish between proper poles and unphysical ones as we approach the continuum limit. In momentum space the Wilson Dirac operator reads

$$\begin{aligned} \tilde{D}_W(p) &= \tilde{D}(p) + \tilde{W}(p) \\ &= \frac{1}{|\Lambda|} \left(\frac{i}{a} \sum_\mu \gamma_\mu \sin(a p_\mu) + \frac{1}{a} \sum_\mu \left(1 - \cos(a p_\mu)\right) + m \mathbb{1} \right). \end{aligned} \tag{2.34}$$

The additional "Wilson-term" $\tilde{W}(p)$ has no effect for $p_\mu = 0$, but adds a mass to the doublers that goes like

$$m + \frac{2l}{a}, \tag{2.35}$$

where l is the number of momentum components that are different from zero. Taking the continuum limit sends the mass of such modes to infinity and they decouple from the theory. Also the Wilson term itself is removed from the action. In position space the term looks like

$$W(x, y) = \frac{1}{a} \left[4\delta_{x,y} - \frac{1}{2} \sum_\mu \left(\delta_{x+\hat{\mu}, y} + \delta_{x-\hat{\mu}, y} \right) \right], \tag{2.36}$$

which leads to the full Wilson Dirac operator

$$D_W(x, y) = -\frac{1}{2a} \sum_{\mu \pm 1}^{\pm 4} (1 - \gamma_\mu) U_\mu(x) \delta_{x+\hat{\mu}, y} + \left(m + \frac{4}{a} \right). \tag{2.37}$$

Just like in the naïve case we added the link variables U, but also defined $\gamma_{-\mu} = -\gamma_\mu$ for $\mu = 1, 2, 3, 4$.

Chapter 3

Lattice symmetries

3.1 Chiral symmetry on the lattice

In the continuum the massless Dirac operator has, among others, symmetries under charge conjugation $\mathcal{C}$, parity transformation $\mathcal{P}$, chiral symmetry and fulfills the so-called γ_5-hermiticity. Transferring these properties to the lattice confronts us with a number of problems.

3.1.1 Nielsen-Ninomiya theorem

The Nielsen-Ninomiya theorem [17, 18] states the following. It is not possible to find a Dirac operator with the following four conditions satisfied simultaneously:

1. The Dirac operator $D(x, x+r)$ is bounded by $C\mathrm{e}^{-\gamma|r|}$.
2. The Dirac operator in the continuum limit can be written as $\tilde{D}(p) = \sum_\mu i\gamma_\mu a p_\mu + \mathcal{O}\left(a^2 p_\mu^2\right)$ for small momenta.
3. The massless Dirac operator can be inverted for any momentum $p \neq 0$, i.e., there are no massive doublers.
4. The Dirac operator fulfills the naïve (continuum) version of chiral symmetry $\{D, \gamma_5\} = 0$.

According to this theorem the Wilson Dirac operator cannot describe light fermions reliably. Let us examine the last property for the massless case

$$\begin{aligned}\left\{\tilde{D}_W(p), \gamma_5\right\} &= \frac{i}{a}\sum_\mu \{\gamma_\mu, \gamma_5\}\sin(ap_\mu) + \frac{1}{a}\sum_\mu (1-\cos(ap_\mu))\{\mathbb{1}, \gamma_5\} \\ &= \frac{2}{a}\gamma_5 \sum_\mu (1-\cos(ap_\mu))\,.\end{aligned} \tag{3.1}$$

The Wilson term breaks chiral symmetry explicitly and the term cannot be modified such that the operator fulfills all the property stated above.

3.1.2 The Ginsparg-Wilson relation

In [19] a first method to overcome the restrictions imposed by the Nielsen-Ninomiya theorem was worked out. The so-called Ginsparg–Wilson relation redefines chiral symmetry on the lattice. One commonly used version of it reads

$$\{\gamma_5, D\} = aD\gamma_5 D. \tag{3.2}$$

On the right-hand side there is a soft (local) symmetry-breaking term that vanishes in the continuum limit. It can be viewed as a remnant chiral symmetry present on the lattice. We now want to analyze an operator that fulfills the GW-relation. Together with γ_5-hermiticity

$$D^\dagger = \gamma_5 D \gamma_5 \tag{3.3}$$

we can establish a relation

$$D + D^\dagger = aDD^\dagger = aD^\dagger D, \tag{3.4}$$

which reveals the eigenvalue structure for this operator. With $D\,|\lambda\rangle = \lambda\,|\lambda\rangle$ we can relate the eigenvalues

$$\begin{aligned}\lambda + \lambda^\dagger &= a|\lambda|^2 \\ x + iy + x - iy &= ax^2 + ay^2 \\ (x - \frac{1}{a})^2 + y^2 &= \frac{1}{a^2},\end{aligned} \tag{3.5}$$

which are located on a circle with radius $1/a$ around $(1/a, 0)$ in the complex plane. Note that this holds for the massless Dirac operator. If we include a mass term, the circle gets shifted on the positive real axis by the mass. Again, taking the continuum limit the eigenvalues lie on the imaginary axis only.

3.2 Ginsparg-Wilson type operators

Some time passed between the proposal of the GW relation and the first realization of an operator obeying this relation. In this section we present only two of them.

3.2.1 The overlap operator

The overlap operator [20, 21, 22] is an explicit solution of the Ginsparg-Wilson equation. The explicit form reads

$$D_{\mathrm{ov}} = \frac{1}{a}\left(\mathbb{1} - \gamma_5 \,\mathrm{sign}(\gamma_5 A)\right) \tag{3.6}$$

with A being a suitable γ_5-hermitian Dirac operator used as kernel. A possible choice is to use

$$A = (1+s)\,\mathbb{1} - aD_{\mathrm{W}} \tag{3.7}$$

with the the massless Wilson operator D_{W} and a real parameter s. This accords to projecting all the eigenvalues of the Wilson operator to the Ginsparg-Wilson circle and therefore exact chiral properties. One of the drawbacks is the numerically costly evaluation of the sign function, though.

3.2.2 The chirally improved Dirac operator

A different approach is to construct an operator that satisfies this equation only approximately, hence has only approximate chiral symmetry. The chirally improved Dirac operator D_{CI} [23, 24] is such an operator. The starting point is to write down a general form of the discretized derivative operator, not only including nearest neighbors, but also more remote connections. Each pair of such points is connected via gauge links and can be viewed as path with a certain length. Each such path can come up with a certain prefactor and different Dirac structures attached, not only the unit matrix and vectors γ_μ as in the Wilson case, but all possible elements of the Clifford algebra (see Sect. A.2). In order for the operator to obey the symmetries of the system we get restrictions for the coefficients. The general expression

reads

$$
\begin{aligned}
D_{\mathrm{CI}} =& \mathbb{1}\left[s_1\langle\rangle + s_2 \sum_{l_1} \langle l_1\rangle + s_3 \sum_{l_2\neq l_1} \langle l_1, l_2\rangle + s_4 \sum_{l_1} \langle l_1, l_1\rangle + \dots \right] \\
&+ \sum_{\mu} \gamma_\mu \sum_{l_1=\pm\mu} \mathrm{sign}(l_1) \left[v_1\langle l_1\rangle + v_2 \sum_{l_2\neq\pm\mu} \left[\langle l_1, l_2\rangle + \langle l_2, l_1\rangle\right] + v_3\langle l_1, l_1\rangle + \dots \right] \\
&+ \sum_{\mu<\nu} \gamma_\mu\gamma_\nu \sum_{\substack{l_1=\pm\mu \\ l_2=\pm\nu}} \mathrm{sign}(l_1)\,\mathrm{sign}(l_2) \sum_{i,j=1}^{2} \epsilon_{ij} \left[t_1\langle l_i, l_j\rangle + \dots \right] \\
&+ \sum_{\mu<\nu<\rho} \gamma_\mu\gamma_\nu\gamma_\rho \\
&\quad \times \sum_{\substack{l_1=\pm\mu, l_2=\pm\nu \\ l_3=\pm\rho}} \mathrm{sign}(l_1)\,\mathrm{sign}(l_2)\,\mathrm{sign}(l_3) \sum_{i,j,k=1}^{3} \epsilon_{ijk} \left[a_1\langle l_i, l_j, l_k\rangle + \dots \right] \\
&\quad + \gamma_5 \sum_{\substack{l_1=\pm1, l_2=\pm2 \\ l_3=\pm3, l_4=\pm4}} \mathrm{sign}(l_1)\,\mathrm{sign}(l_2)\,\mathrm{sign}(l_3)\,\mathrm{sign}(l_4) \\
&\qquad \times \sum_{i,j,k,n=1}^{4} \epsilon_{ijkn} \left[p_1\langle l_i, l_j, l_k, l_n\rangle + \dots \right]
\end{aligned}
\tag{3.8}
$$

with $\langle l_1, l_2, \dots l_n\rangle$ denoting paths of length n and the l_i's denoting the directions. The real coefficients s_i, p_i, v_i, a_i and t_i used in this work listed in the Sect. A.3. In principle Eq. (3.8) contains an infinite set of paths, but for practical purposes we have to truncate the series to finite path lengths, usually of the order of 4. This is the reason why the operator is only an approximate GW-operator.

3.3 Axial Ward identity

Just like in the continuum we want to establish the Ward identity for the axial current on the lattice. Let us define transformations on the lattice,

$$\psi' = (1 + \epsilon\Delta)\,\psi + \mathcal{O}\left(\epsilon^2\right), \tag{3.9a}$$

$$\bar{\psi}' = \bar{\psi}\left(1 + \epsilon\overline{\Delta}\right) + \mathcal{O}\left(\epsilon^2\right), \tag{3.9b}$$

where just as in the continuum case Δ and $\overline{\Delta}$ denote operators for the deviation from an identical transformation and ϵ denotes a local parameter matrix, i.e., a diagonal matrix in space-time with the entries $\epsilon(x)$. Note, that we do not demand that the ψ and $\bar{\psi}$ fields transform equally. The fermionic action can then be expressed in terms of the transformed fields analogously to the continuum case

$$\begin{aligned}
-S_F\left[\bar{\psi},\psi\right] =& \bar{\psi}\left(D+m\right)\psi \\
=& -S_F\left[\bar{\psi}',\psi'\right] - \bar{\psi}'\epsilon\left[\overline{\Delta}\left(D+m\right)+\left(D+m\right)\Delta\right]\psi' \\
&+\bar{\psi}'\left[\epsilon,D\right]\Delta\psi' + \mathcal{O}\left(\epsilon^2\right) \\
=& -S_F\left[\bar{\psi}',\psi'\right] - \bar{\psi}'\epsilon\left[\overline{\Delta}D + D\Delta\right]\psi' \\
&-m\bar{\psi}'\epsilon\left[\overline{\Delta}+\Delta\right]\psi' + \bar{\psi}'\left[\epsilon,D\right]\Delta\psi' + \mathcal{O}\left(\epsilon^2\right)
\end{aligned} \tag{3.10}$$

In addition to the fields in the action also the fields in the measure of the generating functional Z have to be transformed, so let us take a look at those. The condition for invariance looks like

$$\begin{aligned}
Z &= \int [dA][d\bar{\psi}][d\psi]\exp\left(-S_F[\bar{\psi},\psi,A]\right)\exp\left(-S_G[A]\right) \\
&= \int [dA][d\bar{\psi}'][d\psi']\exp\left(-S_F[\bar{\psi}',\psi',A]\right)\exp\left(-S_G[A]\right)
\end{aligned} \tag{3.11}$$

and therefore we have to investigate the effect of the Jacobian of the transformation matrices M

$$d\bar{\psi}\,d\psi = d\bar{\psi}'d\psi'\det\begin{pmatrix} \frac{d\bar{\psi}}{d\bar{\psi}'} & \frac{d\bar{\psi}}{d\psi'} \\ \frac{d\psi}{d\bar{\psi}'} & \frac{d\psi}{d\psi'} \end{pmatrix} = d\bar{\psi}'d\psi' M, \tag{3.12}$$

which can be broken down to

$$\begin{aligned}
M = \det\left[1+\epsilon\Delta\right]\det\left[1+\epsilon\overline{\Delta}\right] &= \exp\left[Tr\log\left(1+\epsilon\Delta\right)\right]\exp\left[Tr\log\left(1+\epsilon\overline{\Delta}\right)\right] \\
&= \exp\left[Tr\sum_{n=0}^{\infty}\frac{\epsilon^n}{n}\Delta^n\right]\exp\left[Tr\sum_{n=0}^{\infty}\frac{\epsilon^n}{n}\overline{\Delta}^n\right] \\
&= 1 + Tr(\epsilon)\left(Tr\Delta + Tr\overline{\Delta}\right) + \mathcal{O}\left(\epsilon^2\right).
\end{aligned} \tag{3.13}$$

The parameter matrix ϵ behaves as a diagonal matrix in real space with no Dirac or flavor structure, hence the trace can be written as a sum over

the spatial index. Let us make a special choice for the transformation, the so-called Lüscher-rotation [25] with τ being a matrix in flavor space

$$\Delta = \tau\gamma_5 \left(1 - \frac{a}{2}D\right), \tag{3.14a}$$

$$\overline{\Delta} = \left(1 - \frac{a}{2}D\right)\tau\gamma_5. \tag{3.14b}$$

This choice leads to

$$\begin{aligned} M &= 1 + 2Tr\tau \sum_x \epsilon(x) \left[Tr\gamma_5 - \frac{a}{2}Tr\left[\gamma_5 D\right]\right] \\ &= 1 - Tr\tau \sum_x \epsilon(x) Tr\left[\gamma_5 D\right]. \end{aligned} \tag{3.15}$$

If we now take a singlet operator for τ (e.g., $\tau = 1$) the trace gives the number of flavors N_F. The trace over the Dirac operator can be replaced by the topological charge density $q(x)$ leading to the following $U(1)$ transformation of the integral measure

$$d\psi\, d\bar{\psi} = d\psi' d\bar{\psi}' \left[1 - N_F \sum_x \epsilon(x) q(x)\right], \tag{3.16a}$$

$$\begin{aligned} q(x) &= \frac{a}{2} Tr\left[\gamma_5 D(x,x)\right] \\ &= \frac{1}{32\pi^2} F_{\mu\nu}(x) \widetilde{F}_{\mu\nu}(x) + \mathcal{O}\left(a^2\right), \end{aligned} \tag{3.16b}$$

where the definition using the field-strength tensor comes from the continuum definition. Considering a constant ϵ matrix and the chiral limit we can show that the Lüscher-rotation leaves the action of a Ginsparg-Wilson operator invariant. It leads to a cancellation of the term involving the Dirac operator in expression (3.10)

$$\begin{aligned} \left[\overline{\Delta}D + D\Delta\right] &= \tau\gamma_5 D - \tau\frac{a}{2}D\gamma_5 D + \tau D\gamma_5 - \tau\frac{a}{2}D\gamma_5 D \\ &= \tau\left[\gamma_5 D + D\gamma_5 - aD\gamma_5 D\right] = 0, \end{aligned} \tag{3.17}$$

for an operator satisfying the Ginsparg-Wilson (3.2) relation exactly. Allowing a non-vanishing mass and non-constant matrix ϵ we can identify terms in (3.10) with terms from the continuum version of the axial Ward identity. In order for the action to be invariant the following condition must be satisfied

$$m\bar{\psi}\epsilon\left[\overline{\Delta} + \Delta\right]\psi - \bar{\psi}\left[\epsilon, D\right]\Delta\psi = 0. \tag{3.18}$$

The continuum version of the AWI reads

$$2mP^\tau = \partial_\mu A^\tau_\mu \tag{3.19}$$

so the currents for a Ginsparg-Wilson action using the Lüscher-rotation can be identified as

$$\begin{aligned} P^\tau(x) = &\frac{1}{2}\left[\bar\psi(x)\tau\gamma_5\left(\left[1-\frac{a}{2}D\right]\psi\right)(x)\right. && \text{(3.20a)}\\ &\left.+\left(\bar\psi\left[1-\frac{a}{2}D\right]\right)(x)\tau\gamma_5\psi(x)\right] && \text{(3.20b)}\\ \partial_\mu A^\tau_\mu(x) = &\sum_{y,z}\left[\bar\psi(y)D(y,x)\tau\gamma_5\left[\delta_{x,z}-\frac{a}{2}D(x,z)\right]\psi(z)\right. && \text{(3.20c)}\\ &\left.+\bar\psi(y)\left[\delta_{y,x}-\frac{a}{2}D(y,x)\right]\tau\gamma_5 D(x,z)\psi(z)\right] && \text{(3.20d)} \end{aligned}$$

The commutator here play the role of the derivative in the directions in Dirac space dressed with γ_μ's. The consequences of these modified currents are worked out in Sect. 4.4.1.

Chapter 4

Propagators on the lattice

4.1 Path integral on the lattice

We now want to translate the quantization prescription from Sect. 1.2 to the lattice. In the continuum we need to integrate over all possible values of the field variables at all possible space-time points. On the lattice this functional integral is modified such that we have a product of integrations over the field variables, where the quark fields are defined on the lattice sites and the gauge fields on the links between the sites. Now the generating functional reads

$$Z = \int \prod_{x\in\Lambda} d\bar{\psi}(x) \prod_{x'\in\Lambda} d\psi(x') \prod_{x''\in\Lambda} dU(x) \mathrm{e}^{-\mathcal{S}_{\mathrm{QCD}}[\bar{\psi},\psi,U]}, \tag{4.1}$$

where $\mathcal{S}_{\mathrm{QCD}}$ contains the action we are using and the product of the internal (color, Dirac) degrees of freedom is implied. In this section we are interested in 2-point functions G; we need to evaluate an expression like

$$G(y,x) = \left\langle \psi(y)\bar{\psi}(x) \right\rangle = \int [d\bar{\psi}][d\psi][dA]\psi(y)\bar{\psi}(x)\mathrm{e}^{-\mathcal{S}_{\mathrm{QCD}}}. \tag{4.2}$$

This integration can be split into a gauge part and a fermionic part, where the latter can be evaluated in terms of Grassmann variables. Using the so-called Matthews-Salam formula

$$Z_F = \int d\eta_N d\bar{\eta}_N \ldots d\eta_1 d\bar{\eta}_1 \mathrm{e}^{\left(\sum_{i,j=1}^{N} \bar{\eta}_i M_{ij} \eta_j\right)} = detM \tag{4.3}$$

the 2-point function $G(y,x)$ can be rewritten as

$$G(y,x) = \int [dA] \mathrm{e}^{S_G} detS_F \, S_F^{-1}(y,x). \tag{4.4}$$

4.2 Quenched approximation

It is very expensive to calculate the deteminant numerically, which is why a common, although uncontrolled approximation, is to set it to unity in numerical simulations. This is called the quenched approximation. Physicswise it is equivalent to forbidding closed quark loops in propagators. For example a propagator for the η' meson involves not only a single disconnected term, but also an infinite tower of contributions with an increasing number of closed quark loops in between (see Fig. 4.1). In the quenched approximation only the leading term is present.
Quenching also violates unitarity, but still it seems to be a justifiable approximation for a large part of lattice QCD, e.g., the spectrum of hadrons (excluding pathological particles like the η') is reproduced reasonably.

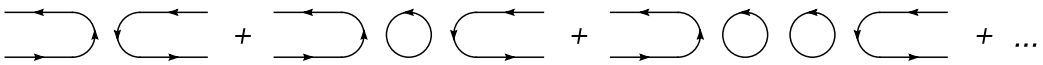

Figure 4.1: Some contributions to the η' propagator. Only the first one is present in the quenched approximation, though.

4.3 Quark propagators

In order to compute a quark propagator we have to define a quark source on a specific lattice site and then compute the correlation to a quark sink (i.e., an anti-quark) at a remote site. Point sources can easily be related to correlators from ChPT, but they are not the only possibility. We can, for example, also define sources and sinks that spread over more than one lattice point. Modified quark sources allow us to reduce the error in a propagator computation. This means introducing extended source operators S and $S^\dagger$

$$\psi_i(c\,\alpha\,x) = \sum_{c',x'} \overline{S}_i(c\,x;c'\,x')\psi(c'\,\alpha\,x') = \left(S_i^\dagger\psi\right)(c\,\alpha\,x), \tag{4.5a}$$

$$\bar{\psi}_i(c\,\alpha\,x) = \sum_{c',x'} S_i(c\,x;c'\,x')\bar{\psi}(c'\,\alpha\,x') = \left(\bar{\psi}S_i\right)(c\,\alpha\,x), \tag{4.5b}$$

which are diagonal in Dirac space. The smearing operators we use here is a Jacobi-type smeared one [26]. It starts out with a point source operator

$$S_P(c_0\,\alpha_0\,x_0;c\,\alpha\,x) = \delta_{c_0\,c}\delta_{\alpha_0\,\alpha}\delta_{x_0\,x}. \tag{4.6}$$

By applying the smearing kernel $H = H^\dagger$

$$S_i(c\,x; c'\,x') = H_i(c'\,x'; c''\,x'')S_P(c\,x; c''\,x''), \tag{4.7}$$

with

$$H_i(c'\,x'; c''\,x'') = \sum_{n=0}^{N_i} \kappa_i^n K^n \tag{4.8}$$

we end up with a smearing operator with a smearing parameter κ_i. The kernel has been applied N_i times. The two parameters κ_i and N_i determine the width of the quark source. For each gauge configuration the smearing kernel can be constructed from the gauge fields

$$K(c\,\vec{x}; c'\,\vec{x'}) = \sum_{\mu=2,3,4} U_\mu(\vec{x}\,c; \vec{x'}\,c')\delta(\vec{x}+\mu, \vec{x'}) + U_\mu^\dagger(\vec{x}\,c; \vec{x'}\,c')\delta(\vec{x}-\mu, \vec{x'}). \tag{4.9}$$

The operator K is hermitian and therefore also H is hermitean. Let us now compute a quark propagator between for two smeared quark sources.

$$\begin{aligned}
\langle\psi_j(d\,\beta\,y\,)\,\bar{\psi}_i(c\,\alpha\,x)\rangle_\psi &= \langle\sum_{d',y'} \overline{S}_j(d\,y; d'\,y')\psi(d'\,\beta, y')\sum_{c',x'} S_i(c\,x; c'\,x')\bar{\psi}(c'\,\alpha\,x')\rangle_\psi \\
&= \sum_{d',y',c',x'} S_j(c\,x; c'\,x')\overline{S}_i(d\,y; d'\,y')\langle\psi(d'\,\beta\,y')\,\bar{\psi}(c'\,\alpha\,x')\rangle_\psi \\
&= \sum_{d',y',c',x'} S_j(c\,x; c'\,x')\overline{S}_i(d\,y; d'\,y')D^{-1}(d'\,\beta\,y'; c'\,\alpha\,x') \\
&= G(d\,\beta\,y\,j; c\,\alpha\,x\,i)
\end{aligned} \tag{4.10}$$

In order to find a propagator for point sources we replace the smearing operators S_j and $\overline{S}_i$ by identity matrices (which is equal to setting the smearing indices to zero) and find

$$G(d\,\beta\,y\,0; c\,\alpha\,x\,0) = D^{-1}(d\,\beta\,y; c\,\alpha\,x). \tag{4.11}$$

For typical lattice sizes it is much too expensive to invert the full Dirac operator from all to all sites. Due to translation invariance of the theory it is sufficient to compute the propagator for a quark source at a fixed site. The inversion is then done for each component of the 12-component spinor

separately by solving the equation

$$\sum_{c''\alpha''x''} D(c'\,\alpha'\,x';c''\,\alpha''\,x'')\,v(c''\,\alpha''\,x'') = S_i(c\,\alpha\,x;c'\,\alpha'\,x') \\ \text{where } v(c''\,\alpha''\,x'') \equiv G(c''\,\alpha''\,x''\,0;c\,\alpha\,x\,i) \tag{4.12}$$

with the center of the source at $(c\,\alpha\,x)$.

4.4 Meson propagators

For all computations in this text we use flavor non-singlet bilinear interpolators. Therefore we define U and D as fields for up and down quark flavors. Sandwiching a Dirac structure Γ_a between the two quark fields leads to a meson interpolator for this Dirac structure with the quantum numbers of that very operator

$$M_a(x) = \overline{D}(c\,\alpha\,x)\,\Gamma_a(\alpha\,\alpha')\,U(c\,\alpha'\,x). \tag{4.13}$$

Analogously let us define an operator for smeared quark sources

$$M_{ai}(x) = \sum_{c'\,c''\,x'\,x''} \overline{D}(c'\,\alpha\,x')\,S_i(c'\,x';c\,x)\,\Gamma_a(\alpha\,\alpha')\,\overline{S}_i(c''\,x'';c\,x)U(c''\,\alpha'\,x''). \tag{4.14}$$

Using flavor non-singlets only ensures that there are only correlators without backtracking loops. This means we only simulate pions (or also kaons and the η), but not the η' (see Fig. 4.2 and Fig. 4.3). The correlator of the meson operator then reads

$$\begin{aligned}\langle M_b(y)\,M_a^\dagger(x)\rangle_\psi &= \sum_{a,b,\alpha,\alpha',\beta,\beta'} \langle\overline{D}(b\,\beta\,y)\,\Gamma_b(\beta\,\beta')\,U(b\,\beta'\,y) \\ &\quad\times \overline{U}(c\,\alpha'\,x)\,\overline{\Gamma}_b(\alpha'\,\alpha)\,D(c\,\alpha\,x)\rangle_\psi \\ &= -\sum_{a,b,\alpha,\alpha',\beta,\beta'} \Gamma_b(\beta\,\beta')\,\overline{\Gamma}_b(\alpha'\,\alpha) \\ &\quad\times D^{-1}(c\,\alpha\,y;b\,\beta\,x)D^{-1}(b\,\beta'\,x;c\,\alpha'\,y)\end{aligned} \tag{4.15}$$

With the γ_5-hermiticity property

$$D^{-1}(c\,\alpha\,x;d\,\beta\,y) = \gamma_5(\alpha\,\delta)\,\overline{D^{-1}}(d\,\gamma\,y;c\,\delta\,x)\,\gamma_5(\gamma\,\beta) \tag{4.16}$$

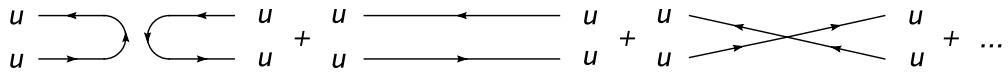

Figure 4.2: Some of the contributions to the singlet meson propagator.

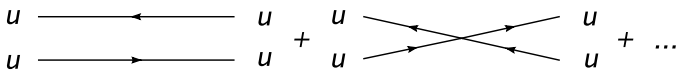

Figure 4.3: The only contribution to the nonsinglet meson propagator at the same order as in Fig. 4.2.

we can rewrite the correlator such that we only use quark propagators that run from site x to site y

$$\begin{aligned}\langle M_b(y)\, M_a^\dagger(x)\rangle_\psi = &- D^{-1}(d\,\beta'\,y; c\,\alpha'\,x)\,\overline{D^{-1}}(d\,\gamma\,y; c\,\delta\,x) \\ &\times (\gamma_5\Gamma_b)(\gamma\beta')\,(\gamma_5\Gamma_a)^\dagger(\alpha'\delta)\end{aligned} \tag{4.17}$$

Having the quark propagators on a gauge configuration we can compute all the interpolating meson correlators. Again for smeared sources the expression has to be somewhat altered. Analogous to the quark propagators we can make use of the smeared propagators G to find

$$\begin{aligned}\langle M_{bj}(y)\, M_{ai}^\dagger(x)\rangle_\psi = &- G(d\,\beta'\,y\,j; c\,\alpha'\,x\,i)\,\overline{G}(d\,\gamma\,y\,j; c\,\delta\,x\,i) \\ &\times (\gamma_5\Gamma_b)(\gamma\beta')\,(\gamma_5\Gamma_a)^\dagger(\alpha'\delta)\end{aligned} \tag{4.18}$$

4.4.1 Pseudoscalar propagator

Let us investigate the correlation between pseudoscalar currents. To this end we use the lattice version of the currents Eq. (3.20)

$$\begin{aligned}G_{PP}(t) =& \sum_{\vec{x}} \Big\langle P(\vec{x},t)P(\vec{0},0)\Big\rangle \\ =& \sum_{\vec{x}}\sum_{y,z} \Big\langle \bar{\psi}(x)\tau\gamma_5\left[\delta(x-y) - \frac{a}{2}D(x,y)\right]\psi(y) \\ &\times \bar{\psi}(0)\tau\gamma_5\left[\delta(z) - \frac{a}{2}D(0,z)\right]\psi(z)\Big\rangle \\ =& -\sum_{\vec{x}}\sum_{y,z} D^{-1}_{\beta'\alpha}(z,x)D^{-1}_{\alpha'\beta}(y,0)\left(\gamma_5\left[\delta(x-y) - \frac{a}{2}D(x,y)\right]\right)_{\alpha\alpha'} \\ &\times \left(\gamma_5\left[\delta(z) - \frac{a}{2}D(0,z)\right]\right)_{\beta\beta'}\end{aligned}$$

$$
\begin{aligned}
&= -\sum_{\vec{x}} Tr\left[D^{-1}(\vec{0},0;\vec{x},t)\gamma_5 D^{-1}(\vec{x},t;\vec{0},0)\gamma_5\right] \\
&+ \frac{a}{2}\sum_{\vec{x}}\sum_{\vec{z},v} Tr\left[D^{-1}(\vec{z},v;\vec{x},t)\gamma_5 D^{-1}(\vec{x},t;\vec{0},0)\gamma_5 D(\vec{0},0;\vec{z},v)\right] \\
&+ \frac{a}{2}\sum_{\vec{x}}\sum_{\vec{y},u} Tr\left[D^{-1}(\vec{0},0;\vec{x},t)\gamma_5 D(\vec{x},t;\vec{y},u) D^{-1}(\vec{y},u;\vec{0},0)\gamma_5\right] \\
&- \frac{a^2}{4}\sum_{\vec{x}}\sum_{\vec{y},u,\vec{z},v} Tr\left[D^{-1}(\vec{z},v;\vec{x},t)\gamma_5 D(\vec{x},t;\vec{y},u)\right. \\
&\left.\times\ D^{-1}(\vec{y},u;\vec{0},0)\gamma_5 D(\vec{0},0;\vec{z},v)\right]
\end{aligned}
\tag{4.19}
$$

The first term gives the contribution

$$
-\sum_{\vec{x}} Tr\left[D^{-1}(\vec{0},0;\vec{x},t)\gamma_5 D^{-1}(\vec{x},t;\vec{0},0)\gamma_5\right] \tag{4.20}
$$

which is what we would expect for an unimproved current. The mixing terms result at order a in

$$
\begin{aligned}
&\frac{a}{2}\sum_{\vec{x}} Tr\left[\delta(\vec{x})\delta(t)\gamma_5 D^{-1}(\vec{x},t;\vec{0},0)\gamma_5 + D^{-1}(\vec{0},0;\vec{x},t)\gamma_5\delta(\vec{x})\delta(t)\gamma_5\right] \\
&\qquad = a\delta(t)\sum_{\vec{x}}\delta(\vec{x}) Tr\left[D^{-1}(\vec{0},0;\vec{0},0)\right].
\end{aligned}
\tag{4.21}
$$

and the a^2 term yields

$$
\begin{aligned}
-\frac{a^2}{4}\sum_{\vec{x}} Tr\left[\gamma_5\delta(\vec{x})\delta(t)\gamma_5\delta(\vec{x})\delta(t)\right] &= -\frac{a^2}{4}\delta(t) Tr\left[\mathbb{1}\right] \\
&= -3a^2\delta(t).
\end{aligned}
\tag{4.22}
$$

Putting all together the pseudoscalar correlator for a GW operator reads

$$
\begin{aligned}
G_{PP}(t) = &-\sum_{\vec{x}} Tr\left[D^{-1}(\vec{0},0;\vec{x},t)\gamma_5 D^{-1}(\vec{x},t;\vec{0},0)\gamma_5\right] \\
&+ a\delta(t) Tr\left[D^{-1}(\vec{0},0;\vec{0},0)\right] - 3a^2\delta(t)
\end{aligned}
\tag{4.23}
$$

Hence the only terms that are modified are contact terms at $t = 0$.

4.4.2 Kaon propagators

In first approximation we can build a kaon propagator from a pion propagator with higher mass, namely taking for the quark mass the average of light and strange quark masses. For kaons we can also fix the mass of the strange quark to a "physical" value and vary the other mass. The pseudoscalar masses squared depend linearly on the quark masses at first order due to the GMOR relation Eq. (5.32). For a given coupling constant we fix the strange quark mass parameter such that the kaon obtains its physical mass value when we extrapolate to the physical light quark mass, i.e. the point, where the pion has its physical mass [27].

Chapter 5

Chiral perturbation theory for mesons

Results in lattice QCD are typically obtained at unphysically high quark masses. In order to connect those results with physical quantities at zero or finite, but realistic quark masses, we can make use of Chiral Perturbation Theory (ChPT). This is believed to be a valid low energy effective theory for QCD defined in the chiral limit. In this section we collect the important results for ChPT for mesons at leading order. In this case pseudoscalar fields are treated as the fundamental degrees of freedom of the theory. This section mainly follows [28].

5.1 Definition of the fields

The fundamental fields of this effective field theory are

$$\mathcal{U}(x) = \exp\left(i\frac{\phi(x)}{\mathcal{F}}\right), \tag{5.1a}$$

$$\phi(x) = \sum_{a=1}^{N_f^2-1} \lambda_a \phi_a, \tag{5.1b}$$

where the constant $\mathcal{F}$ can be connected to the experimentally known pion decay constant $f_\pi \approx 93\,\mathrm{MeV}$ via the weak decay. The number of flavors is denoted by N_f and governs the symmetry, i.e., which matrices λ_a are used. Two flavors implies using Pauli matrices A.1.2, 3 flavors means Gell-Mann

matrices A.1.3. The matrix $\phi(x)$ for $SU(2)$ and $SU(3)$ respectively looks like

$$\phi(x) = \begin{pmatrix} \phi_3 & \phi_1 - i\phi_2 \\ \phi_1 + i\phi_2 & -\phi_3 \end{pmatrix} = \begin{pmatrix} \pi^0 & \sqrt{2}\,\pi^+ \\ \sqrt{2}\,\pi^- & -\pi^0 \end{pmatrix}, \tag{5.2a}$$

$$\begin{aligned} \phi(x) &= \begin{pmatrix} \phi_3 + \frac{1}{\sqrt{3}}\phi_8 & \phi_1 - i\phi_2 & \phi_4 - i\phi_5 \\ \phi_1 + i\phi_2 & -\phi_3 + \frac{1}{\sqrt{3}}\phi_8 & \phi_6 - i\phi_7 \\ \phi_4 + i\phi_5 & \phi_6 + i\phi_7 & -\frac{2}{\sqrt{3}}\phi_8 \end{pmatrix} \\ &= \begin{pmatrix} \pi^0 + \frac{1}{\sqrt{3}}\eta & \sqrt{2}\,\pi^+ & \sqrt{2}\,K^+ \\ \sqrt{2}\,\pi^- & -\pi^0 + \frac{1}{\sqrt{3}}\eta & \sqrt{2}\,K^0 \\ \sqrt{2}\,K^- & \sqrt{2}\,\bar{K}^0 & -\frac{2}{\sqrt{3}}\eta \end{pmatrix}. \end{aligned} \tag{5.2b}$$

The fields can be projected out using

$$\phi_a = \frac{1}{2} Tr\left[\lambda_a \phi\right] \tag{5.3}$$

with the following particles

$$\pi^0 = \phi_3, \qquad \pi^+ = \frac{1}{\sqrt{2}}\left(\phi_1 - i\phi_2\right), \qquad \pi^- = \frac{1}{\sqrt{2}}\left(\phi_1 + i\phi_2\right), \tag{5.4a}$$

$$K^0 = \frac{1}{\sqrt{2}}\left(\phi_6 - i\phi_7\right), \qquad \bar{K}^0 = \frac{1}{\sqrt{2}}\left(\phi_6 + i\phi_7\right), \tag{5.4b}$$

$$K^+ = \frac{1}{\sqrt{2}}\left(\phi_4 + i\phi_5\right), \qquad K^- = \frac{1}{\sqrt{2}}\left(\phi_4 - i\phi_5\right), \tag{5.4c}$$

$$\eta = \phi_8. \tag{5.4d}$$

5.2 The Lagrangian and its transformation properties

The effective Lagrangian density $\mathcal{L}_{\text{eff}}$ at lowest order is given by

$$\mathcal{L}_{\text{eff}} = \frac{\mathcal{F}^2}{4} Tr\left(\partial_\mu \mathcal{U} \partial^\mu \mathcal{U}^\dagger\right). \tag{5.5}$$

The fields have to satisfy certain transformation properties under left and right handed transformation L and R. For the moment let us just consider global $SU(N_f)$ transformations.

$$\mathcal{U} \mapsto R\mathcal{U}L^\dagger, \tag{5.6a}$$

$$\mathcal{U}^\dagger \mapsto L\mathcal{U}^\dagger R^\dagger, \tag{5.6b}$$

$$\begin{aligned}\partial_\mu \mathcal{U} \mapsto \partial_\mu \left(R\mathcal{U}L^\dagger\right) &= (\underbrace{\partial_\mu R}_{0})\mathcal{U}L^\dagger + R\left(\partial_\mu \mathcal{U}\right)L^\dagger + R\mathcal{U}(\underbrace{\partial_\mu L^\dagger}_{0}) \\ &= R\left(\partial_\mu \mathcal{U}\right)L^\dagger,\end{aligned} \tag{5.6c}$$

$$\partial_\mu \mathcal{U}^\dagger \mapsto L\left(\partial_\mu \mathcal{U}^\dagger\right)R^\dagger. \tag{5.6d}$$

This leaves $\mathcal{L}_{\text{eff}}$ invariant

$$\begin{aligned}\mathcal{L}_{\text{eff}} &= \frac{\mathcal{F}^2}{4} Tr\left[R\partial_\mu \mathcal{U}L^\dagger L\partial^\mu \mathcal{U}^\dagger R^\dagger\right] \\ &= \frac{\mathcal{F}^2}{4} Tr\left[\partial_\mu \mathcal{U}\partial^\mu \mathcal{U}^\dagger\right].\end{aligned} \tag{5.7}$$

In the last line we used the cyclic property of the trace. As mesons have baryon number $B = 0$ they transform trivially under a global $U(1)_V$ transformation, i.e., $\phi \mapsto \phi$. In principle there are also other terms with the same number of derivatives, but we can show that they can be expressed in terms of the free part of $\mathcal{L}_{\text{eff}}$. Such a term is evaluated in the following lines:

$$\begin{aligned}\partial_\mu Tr\left[(\partial^\mu \mathcal{U})\mathcal{U}^\dagger\right] &= \partial_\mu Tr\left[U\frac{i}{\mathcal{F}}\lambda_a \partial^\mu \phi_a \mathcal{U}^\dagger\right] \\ &= \partial_\mu Tr\left[\frac{i}{\mathcal{F}}\lambda_a \partial^\mu \phi_a\right] = 0 \\ &= Tr\left[(\partial_\mu \partial^\mu \mathcal{U})\mathcal{U}^\dagger\right] + Tr\left[\partial^\mu \mathcal{U}\partial_\mu \mathcal{U}^\dagger\right]\end{aligned} \tag{5.8a}$$

$$\Rightarrow Tr\left[(\partial_\mu \partial^\mu \mathcal{U})\mathcal{U}^\dagger\right] = -Tr\left[\partial^\mu \mathcal{U}\partial_\mu \mathcal{U}^\dagger\right]. \tag{5.8b}$$

So all terms with two derivatives either evaluate to zero or can be rewritten to be equal to the terms in $\mathcal{L}_{\text{eff}}$ we already have.

5.2.1 Expansion of $\mathcal{L}_{\text{eff}}$

Let us now expand the effective Lagrangian in terms of the fields ϕ

$$\begin{aligned}
\mathcal{L}_{\text{eff}} &= \frac{\mathcal{F}^2}{4} Tr\left[\left(\frac{i}{\mathcal{F}}\partial_\mu\phi\right)\left(-\frac{i}{\mathcal{F}}\partial^\mu\phi\right)\right] + \mathcal{O}\left(\phi^4\right) \\
&= \frac{1}{4} Tr\left[\partial_\mu\left(\lambda_a\phi_a\right)\partial^\mu\left(\lambda_b\phi_b\right)\right] + \mathcal{O}\left(\phi^4\right) \\
&= \frac{1}{4} Tr\left[\lambda_a\lambda_b\right]\partial_\mu\phi_a\partial^\mu\phi_b + \mathcal{O}\left(\phi^4\right) \\
&= \frac{1}{2}\delta_{ab}\partial_\mu\phi_a\partial^\mu\phi_b + \mathcal{O}\left(\phi^4\right) \\
&= \frac{1}{2}\partial_\mu\phi_a\partial^\mu\phi_a + \mathcal{L}_{\text{int}}.
\end{aligned} \tag{5.9}$$

The first term resembles the free Klein-Gordon Lagrangian and all higher order terms can be absorbed into the interaction term $\mathcal{L}_{\text{int}}$.

5.2.2 Local symmetries

Let us now turn our attention towards local symmetries. We define the operators L and R with local parameters $\Theta_a^L = \Theta_a^L(x)$ and $\Theta_a^R = \Theta_a^R(x)$ respectively.

$$L = \exp\left(-i\Theta_a^L\frac{\lambda_a}{2}\right), \tag{5.10a}$$

$$R = \exp\left(-i\Theta_a^R\frac{\lambda_a}{2}\right). \tag{5.10b}$$

We can examine left- and right-handed rotations separately by, i.e., setting $\Theta_a^R = 0$ for the left-handed case. The fields transform as

$$\mathcal{U} \mapsto \mathcal{U}' = R\mathcal{U}L^\dagger = \mathcal{U}\left(1 + i\Theta_a^L\frac{\lambda_a}{2} + \mathcal{O}\left(\Theta_a^L\right)^2\right), \tag{5.11a}$$

$$\mathcal{U}^\dagger \mapsto \mathcal{U}^{\dagger\prime} = L\mathcal{U}^\dagger R^\dagger = \left(1 - i\Theta_a^L\frac{\lambda_a}{2} + \mathcal{O}\left(\Theta_a^L\right)^2\right)\mathcal{U}^\dagger, \tag{5.11b}$$

$$\partial_\mu\mathcal{U} \mapsto \partial_\mu\mathcal{U}' = \partial_\mu\mathcal{U}\left[1 + i\Theta_a^L\frac{\lambda_a}{2}\right] + \mathcal{U}i\partial_\mu\Theta_a^L\frac{\lambda_a}{2} + \mathcal{O}\left(\Theta_a^L\right)^2, \tag{5.11c}$$

$$\partial_\mu\mathcal{U}^\dagger \mapsto \partial_\mu\mathcal{U}^{\dagger\prime} = \left[1 - i\Theta_a^L\frac{\lambda_a}{2}\right]\partial_\mu\mathcal{U}^\dagger - i\partial_\mu\Theta_a^L\frac{\lambda_a}{2}\mathcal{U}^\dagger + \mathcal{O}\left(\Theta_a^L\right)^2. \tag{5.11d}$$

In order to extract symmetry currents we need to consider the variation of the Lagrangian utilizing $\partial^\mu \left(\mathcal{U}^\dagger \mathcal{U}\right) = \left(\partial^\mu \mathcal{U}^\dagger\right)\mathcal{U} + \mathcal{U}^\dagger \left(\partial^\mu \mathcal{U}\right) = 0$

$$\begin{aligned}
\delta\mathcal{L}^L_{\text{eff}} &= \mathcal{L}_{\text{eff}}(\mathcal{U}', \mathcal{U}^{\dagger\prime}) - \mathcal{L}_{\text{eff}}(\mathcal{U}, \mathcal{U}^\dagger) \\
&= \frac{\mathcal{F}^2}{4} Tr\left[\left(\mathcal{U} i\partial_\mu \Theta^L_a \frac{\lambda_a}{2}\right)\partial^\mu \mathcal{U}^\dagger + \partial_\mu \mathcal{U}\left(-i\partial_\mu \Theta^L_a \frac{\lambda_a}{2}\mathcal{U}^\dagger\right)\right] \\
&= \frac{\mathcal{F}^2}{4} i\partial_\mu \Theta^L_a Tr\left[\frac{\lambda_a}{2}\left((\partial^\mu \mathcal{U}^\dagger)\mathcal{U} - \mathcal{U}^\dagger(\partial^\mu \mathcal{U})\right)\right] \\
&= \frac{\mathcal{F}^2}{4} i\partial_\mu \Theta^L_a Tr\left[\lambda_a (\partial^\mu \mathcal{U}^\dagger)\mathcal{U}\right].
\end{aligned} \tag{5.12}$$

For the right-handed case we just set $\Theta^L_a = 0$ and end up with

$$\delta\mathcal{L}^R_{\text{eff}} = -\frac{\mathcal{F}^2}{4} i\partial_\mu \Theta^R_a Tr\left[\lambda_a (\partial^\mu \mathcal{U}^\dagger)\mathcal{U}\right]. \tag{5.13}$$

The symmetry currents then turn out to be

$$J^{\mu,a}_L = \frac{\partial \delta\mathcal{L}^L_{\text{eff}}}{\partial(\partial_\mu \Theta^L_a)} = i\frac{\mathcal{F}^2}{4} Tr\left[\lambda_a (\partial^\mu \mathcal{U}^\dagger)\mathcal{U}\right], \tag{5.14a}$$

$$J^{\mu,a}_R = \frac{\partial \delta\mathcal{L}^R_{\text{eff}}}{\partial(\partial_\mu \Theta^R_a)} = -i\frac{\mathcal{F}^2}{4} Tr\left[\lambda_a \mathcal{U}(\partial^\mu \mathcal{U}^\dagger)\right]. \tag{5.14b}$$

5.2.3 Axial vector and vector currents

The axial vector and vector currents are combinations of the left and right handed currents

$$\mathcal{V}^{\mu,a} = J^{\mu,a}_R + J^{\mu,a}_L = -i\frac{\mathcal{F}^2}{4} Tr\left[\lambda_a \left[\mathcal{U}, \partial^\mu \mathcal{U}^\dagger\right]\right], \tag{5.15a}$$

$$\mathcal{A}^{\mu,a} = J^{\mu,a}_R - J^{\mu,a}_L = -i\frac{\mathcal{F}^2}{4} Tr\left[\lambda_a \left\{\mathcal{U}, \partial^\mu \mathcal{U}^\dagger\right\}\right], \tag{5.15b}$$

where the script symbols are used for the currents in ChPT. They have the same quantum numbers as their counterparts in QCD. Note that under the transformation $\phi \mapsto -\phi$ the currents transform in the expected manner (with $\mathcal{U}' = \mathcal{U}^\dagger$ and $\mathcal{U}^{\dagger\prime} = \mathcal{U}$)

$$\mathcal{V}^{\mu,a} \mapsto \mathcal{V}^{\mu,a} \tag{5.16a}$$

$$\mathcal{A}^{\mu,a} \mapsto -\mathcal{A}^{\mu,a} \tag{5.16b}$$

Let us now expand the axial current

$$\begin{aligned}\mathcal{A}^{\mu,a} &= -i\frac{\mathcal{F}^2}{4}Tr\left[\lambda_a\left\{1+\mathcal{O}\left(\phi\right),-i\frac{\lambda_b\partial^\mu\phi_b}{\mathcal{F}}+\mathcal{O}\left(\phi\right)^2\right\}\right] \\ &= -\mathcal{F}\partial^\mu\phi_a+\mathcal{O}\left(\phi\right)^2.\end{aligned} \tag{5.17}$$

On the other hand for the vector current we find

$$\begin{aligned}\mathcal{V}^{\mu,a} &= -i\frac{\mathcal{F}^2}{4}Tr\left[\lambda_a\left[1+\frac{i}{\mathcal{F}}\lambda_b\phi_b+\mathcal{O}\left(\phi\right)^2,-i\frac{\lambda_c\partial^\mu\phi_c}{\mathcal{F}}-\frac{\lambda_b\phi_b\lambda_c\partial^\mu\phi_c}{\mathcal{F}^2}+\mathcal{O}\left(\phi\right)^3\right]\right] \\ &= -i\frac{1}{4}\phi_b\partial^\mu\phi_c Tr\left[\lambda_a\left[\lambda_b,\lambda_c\right]\right]+\mathcal{O}\left(\phi\right)^4 \\ &= \phi_b\partial^\mu\phi_c f_{bca}+\mathcal{O}\left(\phi\right)^4,\end{aligned} \tag{5.18}$$

where we have used

$$Tr\left[\lambda_a\left[\lambda_b,\lambda_c\right]\right]=Tr\left[2if_{bcd}\lambda_a\lambda_d\right]=4if_{bca}. \tag{5.19}$$

This knowledge allows us to check the coupling of the axial current to the meson field. To this end we compute the matrix element

$$\begin{aligned}\left\langle 0|\mathcal{A}^{\mu,a}(x)|\phi^b(p)\right\rangle &= \left\langle 0|-\mathcal{F}\partial^\mu\phi_a(x)|\phi^b(p)\right\rangle \\ &= -\mathcal{F}\partial^\mu\left\langle 0|\phi_a(x)|\phi^b(p)\right\rangle \\ &= -\mathcal{F}\partial^\mu\exp\left(-ipx\right)\delta_{ab} \\ &= i\mathcal{F}p^\mu\exp\left(-ipx\right)\delta_{ab}.\end{aligned} \tag{5.20}$$

The π^+ and π^- have a dominant decay channel (99.99% [29]) to muon and anti-neutrino (or their anti-particles) via the weak interaction. The weak decay constant measured in the experiment is equal to our coupling to the axial current. In fact, taking the derivative of the above gives the PCAC relation

$$\begin{aligned}\left\langle 0|\partial_\mu\mathcal{A}^{\mu,a}(x)|\phi^b(p)\right\rangle &= \mathcal{F}p^\mu p_\mu\exp\left(-ipx\right)\delta_{ab} \\ &= \mathcal{F}M_\pi^2\exp\left(-ipx\right)\delta_{ab}.\end{aligned} \tag{5.21}$$

5.3 The symmetry breaking term

In QCD the mass term that accounts for explicit symmetry breaking looks like

$$\mathcal{L}_{\mathrm{M}} = -\bar{\psi}_R \mathcal{M} \psi_L - \bar{\psi}_L \mathcal{M}^\dagger \psi_R, \quad \mathcal{M} = \begin{pmatrix} m_u & 0 & 0 \\ 0 & m_d & 0 \\ 0 & 0 & m_s \end{pmatrix}. \tag{5.22}$$

Quark masses in the Lagrangian of QCD are bare masses, but ChPT is an effective theory. We can introduce a symmetry breaking term inspired by QCD, but already with a renormalized mass matrix

$$\mathcal{M}^{(r)} = \begin{pmatrix} m_u^{(r)} & 0 & 0 \\ 0 & m_d^{(r)} & 0 \\ 0 & 0 & m_s^{(r)} \end{pmatrix}. \tag{5.23}$$

The lowest order Lagrangian that is invariant under the transformations

$$\mathcal{U} \mapsto R \mathcal{U} L^\dagger, \tag{5.24a}$$
$$\mathcal{U}^\dagger \mapsto L \mathcal{U}^\dagger R^\dagger, \tag{5.24b}$$
$$\mathcal{M}^{(r)} \mapsto R \mathcal{M}^{(r)} L^\dagger \tag{5.24c}$$

is

$$\begin{aligned} \mathcal{L}_{\text{s.b.}} = \frac{\mathcal{F}^2 \mathcal{B}}{2} Tr\left[\mathcal{M}^{(r)} \mathcal{U}^\dagger + \mathcal{U} M^\dagger\right] \mapsto & \frac{\mathcal{F}^2 \mathcal{B}}{2} Tr\Big[R \mathcal{M}^{(r)} L^\dagger L \mathcal{U}^\dagger R^\dagger \\ & + R \mathcal{U} L^\dagger L \mathcal{M}^{(r)\dagger} R^\dagger\Big] \\ = & \frac{\mathcal{F}^2 \mathcal{B}}{2} Tr\left[\mathcal{M}^{(r)} \mathcal{U}^\dagger + \mathcal{U} \mathcal{M}^{(r)\dagger}\right]. \end{aligned} \tag{5.25}$$

We have introduced a new parameter $\mathcal{B}$ into the theory here. Of course we could also use the unrenormalized mass matrix $\mathcal{M}$, which would just lead to a different $\mathcal{B}$. Note that a term like $Tr\mathcal{M}^{(r)}$ is excluded as it is not invariant under those transformations. Also a term like $Tr\left[\mathcal{M}^{(r)} \mathcal{U}^\dagger - \mathcal{U} \mathcal{M}^{(r)\dagger}\right]$ is not allowed due to non-invariance under parity and the property $\mathcal{M}^{(r)} = \mathcal{M}^{(r)\dagger}$ requires us to only use terms even in ϕ in the expansion. The zeroth order

term in expanding $\mathcal{L}_{\text{s.b.}}$ is just a constant and can therefore be neglected, but the second order term exposes the masses of the Goldstone bosons (here only shown for the $\pi^+\pi^-$ and $\pi^0\pi^0$ contributions)

$$\begin{aligned}\mathcal{L}_{\text{s.b.}} &= -\frac{\mathcal{B}}{2} Tr\left[\phi^2 \mathcal{M}^{(r)}\right] + \mathcal{O}\left(\phi\right)^4 \\ &= -\frac{\mathcal{B}}{2}\left[2(m_u^{(r)} + m_d^{(r)})\pi^+\pi^- + (m_u^{(r)} + m_d^{(r)})\pi^0\pi^0\right] + \mathcal{O}\left(\phi\right)^4 .\end{aligned} \tag{5.26}$$

Comparing mass terms in the effective Hamiltonian and the QCD-Hamiltonian in the chiral limit allows us to give a meaning to the parameter $\mathcal{B}$. The vacuum in the effective theory corresponds to $\mathcal{U} = 1$, i.e., the energy ground state is (from Eq. (5.25))

$$\langle 0|\mathcal{H}_{\text{eff}}|0\rangle = \langle \mathcal{H}_{\text{eff}}\rangle = -\mathcal{F}^2 \mathcal{B} Tr \mathcal{M}^{(r)} = -\mathcal{F}^2 \mathcal{B}(m_u^{(r)} + m_d^{(r)} + m_s^{(r)}). \tag{5.27}$$

Let us now consider the mass terms in the ground state of QCD in some renormalization scheme

$$\langle 0|\mathcal{H}_{\text{QCD}}|0\rangle_m^{(r)} = \langle \mathcal{H}_{\text{QCD}}\rangle_m^{(r)} = \sum_{f=1}^{N_f} m_f^{(r)} \left\langle \bar{\psi}_f \psi_f \right\rangle^{(r)} . \tag{5.28}$$

We can also take the derivative of the QCD ground state with respect to quark masses and set them to zero afterwards

$$\left.\frac{\partial \langle 0|\mathcal{H}_{\text{QCD}}|0\rangle_m^{(r)}}{\partial m_f}\right|_{m_f=0} = \Sigma^{(r)}, \tag{5.29}$$

with the renormalized quark or chiral condensate defined as

$$\Sigma^{(r)} = \frac{1}{N_f} \left\langle \bar{\psi}\psi \right\rangle^{(r)} . \tag{5.30}$$

This allows us to identify two of the above terms

$$\mathcal{F}^2 \mathcal{B} = -\Sigma^{(r)}. \tag{5.31}$$

For the pion mass we then find (using Eq. (5.26))

$$\begin{aligned} M_\pi^2 &= -\frac{2\Sigma^{(r)}}{\mathcal{F}^2} \bar{m}^{(r)}, \\ &= 2\mathcal{B}\bar{m}^{(r)}, \end{aligned} \tag{5.32}$$

which is the Gell-Mann–Oakes–Renner (GMOR) relation. The average renormalized light quark mass is denoted as

$$\bar{m}^{(r)} = \frac{m_u^{(r)} + m_d^{(r)}}{2}. \tag{5.33}$$

If we extend this calculation to also include the strange sector the kaon receives a mass of

$$\begin{aligned} M_K^2 &= -\frac{\Sigma^{(r)}}{\mathcal{F}^2}\left(\bar{m}^{(r)} + m_s^{(r)}\right), \\ &= \mathcal{B}\left(\bar{m}^{(r)} + m_s^{(r)}\right), \end{aligned} \tag{5.34}$$

Setting $m_u = m_d = \bar{m}$ suppresses $\eta\,\pi^0$ mixing and the η acquires a mass of

$$M_\eta^2 = \frac{2}{3}\mathcal{B}\left(\bar{m}^{(r)} + 2m_s^{(r)}\right). \tag{5.35}$$

Independent of the value of the parameter $\mathcal{B}$the meson masses satisfy the so-called Gell-Mann–Okubo relation

$$4M_K^2 = 4\mathcal{B}(\bar{m}^{(r)} + m_s^{(r)}) = 2\mathcal{B} + 2\mathcal{B}(\bar{m}^{(r)} + 2m_s^{(r)}) = 3M_\eta^2 + M_\pi^2. \tag{5.36}$$

We can now combine these to the second order Lagrangian

$$\mathcal{L}_{\text{eff}} = \frac{1}{2}\partial_\mu\phi\partial^\mu\phi - \frac{\Sigma^{(r)}}{2}Tr\left[\phi^2\mathcal{M}^{(r)}\right] + \mathcal{O}\left(\phi\right)^4. \tag{5.37}$$

5.3.1 The pion coupling constant G

Let us first normalize the fields by defining

$$\langle 0|\phi^a(x)|\phi^c(p)\rangle = \delta_{ac}e^{-ipx}. \tag{5.38}$$

If we now take an arbitrary operator Φ satisfying

$$\langle 0|\Phi^a(x)|\phi^c(p)\rangle = \delta_{ac}e^{-ipx} \tag{5.39}$$

we have an operator containing the pion, i.e., an interpolating pion operator. The pseudoscalar operator can serve as such an interpolator for our purposes if we introduce a normalization constant, namely the pion coupling constant G. The matrix element then reads

$$\langle 0|\mathcal{P}^a(x)|\phi^c(p)\rangle = G\delta_{ac}e^{-ipx}, \tag{5.40}$$

i.e.,

$$\mathcal{P}^a(x) = G\Phi^a(x). \tag{5.41}$$

The axial Ward identity relates the local operators A_μ and P in QCD. Written in matrix elements this means

$$\frac{\left\langle 0|\partial^\mu A_\mu^{a,(r)}|\phi^b\right\rangle}{\langle 0|P^{a,(r)}|\phi^b\rangle} = 2m^{(r)}. \tag{5.42}$$

Note that we don't need to worry about renormalization in ChPT as it is an effective theory. Borrowing this result and applying it to the matrix elements computed from ChPT yields

$$\frac{\left\langle 0|\partial^\mu \mathcal{A}_\mu^{a,(r)}|\phi^b\right\rangle}{\langle 0|\mathcal{P}^{a,(r)}|\phi^b\rangle} = \frac{G}{\mathcal{F}M_\pi}, \tag{5.43}$$

hence we can identify

$$\frac{G}{\mathcal{F}M_\pi} = 2m^{(r)}. \tag{5.44}$$

5.3.2 The decay constant $\mathcal{F}$

Also correlations between the axial-vector components can be evaluated in the framework of ChPT. The pion decay constant is the wave function of the pion in the origin and related to the derivative of the axial current. Using the axial Ward identity Eq. (5.21) and the PCAC relation Eq. (5.21) together with the definition of G we end up with

$$2m^{(r)}G = 2\mathcal{B}\mathcal{F} = M_\pi^2\mathcal{F}. \tag{5.45}$$

5.3.3 Useful matrix elements

For calculating propagators later on we need to know elements of operators sandwiched between the vacuum and a meson field. We want to concentrate directly on components defining the $\pi^\pm$ that are built up from elements of the $su(N)$ algebra. The modified pseudoscalar operators in QCD are given

by

$$\begin{aligned} P^{\pm} &= \bar{\psi}\gamma_5 \frac{\lambda^{\pm}}{2}\psi \\ &= \bar{\psi}\gamma_5 \frac{\lambda^1 \pm i\lambda^2}{2}\psi \\ &= P^1 \pm iP^2, \end{aligned} \tag{5.46}$$

with

$$P^{\pm\dagger} = P^{\mp}. \tag{5.47}$$

The axial-vector operators $A^{\mu,\mp}$ are constructed analogously. The same is true for ChPT with

$$\mathcal{P}^{\pm} = \mathcal{P}^1 \pm i\mathcal{P}^2 \tag{5.48a}$$

$$\mathcal{A}_{\mu}^{\pm} = \mathcal{A}_{\mu}^1 \pm i\mathcal{A}_{\mu}^2 \tag{5.48b}$$

$$\phi^{\pm} = \phi^1 \pm i\phi^2 \tag{5.48c}$$

Let us now evaluate matrix elements for the field, the pseudoscalar operator, the axial-vector current and the derivative of the latter

$$\left\langle 0|\phi^{\pm}(x)|\phi^b(p)\right\rangle = e^{-ipx}\left[\delta^{1b} \pm i\delta^{2b}\right] \tag{5.49a}$$

$$\begin{aligned} \left\langle 0|\mathcal{P}^{\pm}(x)|\phi^b(p)\right\rangle &= Ge^{-ipx}\left[\delta^{1b} \pm i\delta^{2b}\right] \\ &= \frac{\mathcal{F}M_\pi^2}{2m^{(r)}}e^{-ipx}\left[\delta^{1b} \pm i\delta^{2b}\right] \end{aligned} \tag{5.49b}$$

$$\left\langle 0|\mathcal{A}_{\mu}^{\pm}(x)|\phi^b(p)\right\rangle = i\mathcal{F}p_\mu e^{-ipx}\left[\delta^{1b} \pm i\delta^{2b}\right] \tag{5.49c}$$

$$\left\langle 0|\left(\partial^\mu \mathcal{A}_{\mu}^{\pm}\right)(x)|\phi^b(p)\right\rangle = \mathcal{F}M_\pi^2 e^{-ipx}\left[\delta^{1b} \pm i\delta^{2b}\right]. \tag{5.49d}$$

5.4 Propagators

Let us first define what a complete set of pseudoscalar fields is supposed to look like. The typical definition of the integration measure is that each momentum differential dp_i comes with a factor of 2π and that we restrict the

states to the mass shell and positive energies. This means

$$\begin{aligned}\mathbb{1} &= \int \frac{d^4p}{(2\pi)^4} 2\pi\delta(p_\mu p^\mu - M_\pi^2)\Theta(p_0) \sum_a |\phi^a(\vec{p})\rangle \langle\phi^a(\vec{p})| \\ &= \int \frac{d^3p}{(2\pi)^3} \int dp_0 \delta(p_\mu p^\mu - M_\pi^2)\Theta(p_0) \sum_a |\phi^a(\vec{p})\rangle \langle\phi^a(\vec{p})| \\ &= \int \frac{d^3p}{(2\pi)^3} \frac{1}{2\sqrt{\vec{p}\cdot\vec{p} + M_\pi^2}} \sum_a |\phi^a(\vec{p})\rangle \langle\phi^a(\vec{p})|\,,\end{aligned} \tag{5.50}$$

where in the last line we used the properties of the delta distribution. Correlators between operators $\mathcal{X}(x)$ and $\mathcal{Y}(y)$ can be computed in both frameworks, the one of ChPT and lattice QCD. Let us define

$$\mathcal{G}_{\mathcal{X}\mathcal{Y}}(x,y) = \big\langle 0|\mathcal{X}(x)^\dagger \mathcal{Y}(y)|0\big\rangle = \big\langle \mathcal{X}(x)^\dagger \mathcal{Y}(y)\big\rangle\,. \tag{5.51}$$

Inserting a complete set of fields ϕ yields

$$\mathcal{G}_{\mathcal{X}\mathcal{Y}}(x,y) = \int \frac{d^3p}{(2\pi)^3} \frac{1}{2\sqrt{\vec{p}\cdot\vec{p} + M_\pi^2}} \sum_c \big\langle 0|\mathcal{X}(x)^\dagger|\phi^c(p)\big\rangle \langle\phi^c(p)|\mathcal{Y}(y)|0\rangle\,. \tag{5.52}$$

In order to extract masses it is appropriate to project the object to 3-momentum zero. Utilizing translational invariance we can shift the space variables in the propagator such that $y = 0$

$$\mathcal{G}_{\mathcal{X}\mathcal{Y}}(t) = \int \frac{d^3z\, d^3p}{(2\pi)^3} \frac{1}{2\sqrt{\vec{p}\cdot\vec{p} + M_\pi^2}} \sum_c \big\langle 0|\mathcal{X}(\vec{z},t)^\dagger|\phi^c(p)\big\rangle \Big\langle \phi^c(p)|\mathcal{Y}(\vec{0},0)|0\Big\rangle\,. \tag{5.53}$$

Using the matrix elements from Sect. 5.3.3 we can find expressions for the different combinations of pseudoscalar and axial-vector current and the derivative of the latter. Also the propagator for the fields can be evaluated

$$\begin{aligned}\mathcal{G}_{\phi^a\phi^b}(t) &= \int \frac{d^3p\, d^3x}{(2\pi)^3} \frac{1}{2\sqrt{\vec{p}\cdot\vec{p} + M_\pi^2}} \sum_c \langle 0|\phi^a(x)|\phi^c(p)\rangle \big\langle \phi^c(p)|\phi^b(0)|0\big\rangle \\ &= \int \frac{d^3p\, d^3x}{(2\pi)^3} \frac{1}{2\sqrt{\vec{p}\cdot\vec{p} + M_\pi^2}} e^{-i\sqrt{\vec{p}\cdot\vec{p}+M_\pi^2}t} e^{i\vec{p}\vec{x}} \sum_c \delta_{ac}\delta_{cb} \\ &= \int d^3p \frac{1}{2\sqrt{\vec{p}\cdot\vec{p} + M_\pi^2}} e^{-i\sqrt{\vec{p}\cdot\vec{p}+M_\pi^2}t} \delta_{ab}\delta(\vec{p}) \\ &= \frac{1}{2M_\pi} e^{-iM_\pi t}\delta_{ab}.\end{aligned} \tag{5.54}$$

The axial current correlator can also be calculated

$$\begin{aligned}
\mathcal{G}_{\mathcal{A}^{\mu,a}\mathcal{A}^{\nu,b}}(t) &= \left\langle \mathcal{A}^{\mu,a}(x)\mathcal{A}^{\nu,b}(0)\right\rangle = \left\langle 0|\mathcal{A}^{\mu,a}(x)\mathcal{A}^{\nu,b}(0)|0\right\rangle \\
&= \int \frac{d^3p}{(2\pi)^3}\frac{1}{2\sqrt{\vec{p}\cdot\vec{p}+M_\pi^2}}\sum_c \langle 0|\mathcal{A}^{\mu,a}(x)|\phi^c(\vec{p})\rangle \left\langle \phi^c(\vec{p})|\mathcal{A}^{\nu,b}(0)|0\right\rangle \\
&= \int \frac{d^3p}{(2\pi)^3}\frac{1}{2\sqrt{\vec{p}\cdot\vec{p}+M_\pi^2}}\sum_c i\mathcal{F}p^\mu e^{-ipx}\delta_{ac}(-i\mathcal{F}p^\nu)\delta_{cb} \\
&= \delta_{ab}\int \frac{d^3p}{(2\pi)^3}\frac{\mathcal{F}^2}{2\sqrt{\vec{p}\cdot\vec{p}+M_\pi^2}}p^\mu p^\nu e^{-ipx} \\
&= \delta_{ab}\int \frac{d^3p}{(2\pi)^3}\frac{\mathcal{F}^2}{2\sqrt{\vec{p}\cdot\vec{p}+M_\pi^2}}p^\mu p^\nu e^{-i\sqrt{\vec{p}\cdot\vec{p}+M_\pi^2}t}e^{-i\vec{p}\vec{x}}.
\end{aligned} \tag{5.55}$$

Again, we are interested in the correlators depending only on time separation

$$\begin{aligned}
\mathcal{G}_{\mathcal{A}^{\mu,a}\mathcal{A}^{\nu,b}}(t) &= \int d^3x \left\langle \mathcal{A}^{\mu,a}(x)\mathcal{A}^{\nu,b}(0)\right\rangle \\
&= \frac{\mathcal{F}^2}{2}\delta_{ab}\int \frac{d^3x\, d^3p}{(2\pi)^3}\frac{p^\mu p^\nu}{\sqrt{\vec{p}\cdot\vec{p}+M_\pi^2}}\, e^{i\vec{p}\cdot\vec{x}}\, e^{-i\sqrt{\vec{p}\cdot\vec{p}+M_\pi^2}\,t} \\
&= \frac{\mathcal{F}^2}{2}\delta_{ab}\int d^3p\frac{p^\mu p^\nu}{\sqrt{\vec{p}\cdot\vec{p}+M_\pi^2}}\, e^{-i\sqrt{\vec{p}\cdot\vec{p}+M_\pi^2}\,t}\delta\left(\vec{p}\right) \\
&= \frac{\mathcal{F}^2}{2}\,\delta_{ab}M_\pi\,\delta_{0\mu}\,\delta_{0\nu}\, e^{-iM_\pi t} \\
&= \begin{cases} \dfrac{\mathcal{F}^2}{2}\delta_{ab}\, M_\pi e^{-iM_\pi t} & \mu = 0 \wedge \nu = 0 \\ 0 & \mu \neq 0 \vee \nu \neq 0 \end{cases}.
\end{aligned} \tag{5.56}$$

The correlators that are used in this work are listed below

$$\mathcal{G}_{\phi^\mp\phi^\pm}(t) = \frac{1}{M_\pi}e^{-iM_\pi t}, \tag{5.57a}$$

$$\begin{aligned}
\mathcal{G}_{\mathcal{P}^\mp\mathcal{P}^\pm}(t) &= \frac{G^2}{M_\pi}e^{-iM_\pi t} \\
&= \frac{1}{M_\pi}\left(\frac{\mathcal{F}M_\pi^2}{2m^{(r)}}\right)^2 e^{-iM_\pi t} \\
&= \frac{M_\pi\Sigma^{(r)}}{2m^{(r)}}\, e^{-iM_\pi t},
\end{aligned} \tag{5.57b}$$

$$\mathcal{G}_{\mathcal{A}_0^\mp \mathcal{A}_0^\pm}(t) = \mathcal{F}^2 M_\pi e^{-iM_\pi t}, \tag{5.57c}$$

$$\begin{aligned}\mathcal{G}_{\mathcal{A}_0^\mp \mathcal{P}^\pm}(t) &= i\mathcal{F}Ge^{-iM_\pi t} \\ &= i\mathcal{F}\frac{\mathcal{F}M_\pi^2}{2m^{(r)}}\, e^{-iM_\pi t} \\ &= -i\Sigma^{(r)} e^{-iM_\pi t},\end{aligned} \tag{5.57d}$$

$$\begin{aligned}\mathcal{G}_{\partial^\mu \mathcal{A}_\mu^\mp \mathcal{P}^\pm}(t) &= \mathcal{F}M_\pi Ge^{-iM_\pi t} \\ &= \mathcal{F}M_\pi \frac{\mathcal{F}M_\pi^2}{2m^{(r)}}\, e^{-iM_\pi t} \\ &= -\Sigma^{(r)} M_\pi e^{-iM_\pi t},\end{aligned} \tag{5.57e}$$

$$\begin{aligned}\mathcal{G}_{\partial^\mu \mathcal{A}_\mu^\mp \partial^\nu \mathcal{A}_\nu^\pm}(t) &= (\mathcal{F}M_\pi^2)^2 G_{\phi^\mp \phi^\pm}(t) \\ &= \frac{(\mathcal{F}M_\pi^2)^2}{G^2}\mathcal{G}_{P^\mp P^\pm}(t) \\ &= (2m^{(r)})^2 \mathcal{G}_{P^\mp P^\pm}(t).\end{aligned} \tag{5.57f}$$

The propagators in ChPT are worked out as correlation functions between two local pointlike operators in the continuum. Propagators on the lattice can be connected to the ones in ChPT as soon as they are normalized to pointlike propagators and translated to a continuum scheme. Let us introduce renormalized lattice correlators with renormalization factors Z_X (see Sect. 6.2). We make the following identifications

$$\mathcal{G}_{\mathcal{X}\mathcal{Y}}(t) \sim G_{XY}^{(r)}(t) = \frac{1}{Z_X Z_Y} G_{XY}(t) = \sum_{\vec{x}} \langle X(\vec{x}, t) Y(\vec{0}, 0)\rangle \tag{5.58}$$

where we have to be aware that the correlators in ChPT are worked out in Minkowski metric and our correlators are in Euclidean metric. The main difference is the additional imaginary unit in the exponent and in front of Eq. (5.57d). We can also relate

$$\mathcal{F} = f_\pi \quad \text{and} \tag{5.59a}$$

$$G = G_\pi^{(r)} \tag{5.59b}$$

used later on.

Chapter 6

Results

6.1 Lattice ensembles

In Table 6.1 we present the different parameter sets for the lattices we use in this work. Note that all of them are in the quenched approximation using the D_{CI} action for the fermions and Lüscher-Weiss action for the gaugefields. Note that β denotes the coupling β_1 in Eq. (2.17). The remaining couplings are computed using Eq. (2.18). For the two largest lattices in physical units we have data for degenerate and non-degenerate quarks in the meson propagators, that are computed using Eq. (4.18).

6.2 Renormalization

Quantities like the quark mass, the decay constants and the chiral condensate are not directly accessable by experiment. Instead they are defined in some theory and can be determined by analyzing processes there is experimental data for in this theoretical framework. The results are typically scheme and scale dependent, so one needs to specify which renormalization scheme and at which renormalization scale one is working in. In [2] conversion factors for the D_{CI} action in the quenched case were computed. These conversion factors allow us to relate meson correlators in our lattice formulation to the according point to point meson correlators in the continuum theory in the modified minimal subtraction scheme ($\overline{\mathrm{MS}}$) at the renormalization scale $\mu = 2\,\mathrm{GeV}$. In Table 6.2 the results for quark bilinears in the different Clifford sectors are collected. Note that for the pseudoscalar renormalization factor

$L^3 \times T$	β	a[fm]	$L^3 \times T$[fm^4]	# cf.	$a\,m$ ($a\,m_s$)	$m^{(r)}[MeV]$
$8^3 \times 24$	7.90	0.148	$1.2^3 \times 3.6$	200	$0.02 - 0.20$	24-236
$12^3 \times 24$	7.90	0.148	$1.8^3 \times 3.6$	100	$0.02 - 0.20$	24-236
$12^3 \times 24$	8.35	0.102	$1.2^3 \times 2.5$	100	$0.02 - 0.20$	37-372
$16^3 \times 32$	7.90	0.148	$2.4^3 \times 4.7$	99	$0.02 - 0.20$	24-236
$16^3 \times 32$	8.35	0.102	$1.6^3 \times 3.3$	100	$0.02 - 0.20$	37-372
$16^3 \times 32$	8.70	0.078	$1.3^3 \times 2.5$	100	$0.02 - 0.20$	53-528
$16^3 \times 32$	7.90	0.148	$2.4^3 \times 4.7$	100	$0.02 - 0.20$	24-245
					$(0.08, 0.10)$	
$20^3 \times 32$	8.15	0.119	$2.4^3 \times 3.8$	100	$0.017 - 0.16$	26-236
					(0.06)	

Table 6.1: Different parameter sets the computations are based on. The coupling β is actually the coupling β_1 in the Lüscher-Weiss action Eq. (2.17), the other couplings are computed therefrom using Eq. (2.18).

the influence from the pion pole has been subtracted, hence the notation Z_P^{Sub}. For $\beta = 8.15$ we use interpolation between the other values of the coupling, as there are no explicit values available.

β	Z_S	Z_V	Z_T	Z_A	Z_P^{Sub}
7.90	1.1309(9)	0.9586(2)	0.9944(3)	1.0087(4)	1.0281(5)
8.15*	1.081(1)	0.967(1)	1.014(1)	1.011(1)	1.012(3)
8.35	1.039(1)	0.973(1)	1.028(2)	1.012(1)	0.987(4)
8.70	0.959(2)	0.979(1)	1.049(1)	1.0095(7)	0.915(1)

Table 6.2: Renormalization constants taken from [2]. The values for $\beta = 8.15$ have been obtained by interpolation.

6.3 Quark norm evaluation

In Sect. 4.3 smearing operators for quark and anti-quark sources have been introduced. In order to compute prefactors of exponential decaying functions in a meaningful way, i.e., such that we can compare them to the definitions

usually made in the continuum theory, we need to relate the quantities calculated from smeared sources to ones from point sources. Depending on the configurations we have either one (denoted as n(arrow), Table 6.1) or two different widths (n and w(ide)) of smeared sources available. In addition we have pointlike sinks (p(oint)) in our datasets. The smearing parameters are chosen such that the effective size of a given source is approximately the same for all lattice spacings [30]. Let us denote a mesonic operator by $X_{s_1 s_2}$, built up from an antiquark of smearing type s_1 and a quark of smearing type s_2 with $s_i = n, w, p$. First we compute the ratio of meson correlators

$$C^X_{s_1 s_2 s_3 s_4} = \frac{\langle X_{s_1 s_2} X_{s_3 s_4} \rangle}{\langle X_{s_1 s_2} X_{pp} \rangle}. \tag{6.1}$$

It turns out that the ratios for a given set s_3 and s_4 are relatively independent of the choices of s_1 and s_2, which can be seen in Fig. 6.1. We also demand the ratios to be symmetric under exchange of s_3 and s_4 due to the symmetries of the meson propagator. We find excellent plateaus for the time range

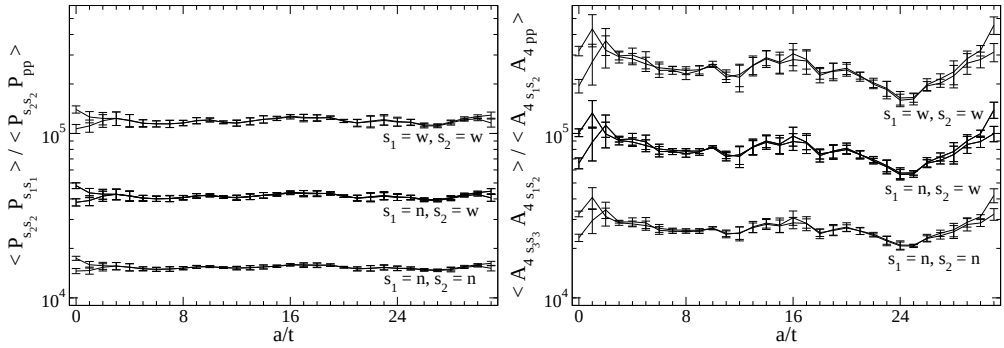

Figure 6.1: The ratios $C^X_{s_3 s_3 s_1 s_2}$ in Eq. (6.1) for $X = P$ on the left and $X = A_4$ on the right on a $16^3 \times 32$ lattice at $\beta = 7.90$ and $am = 0.02$. One can see small differences in the behavior at small time separations and at the symmetry point depending on which smearing width s_3 is used.

$t, t' \in [4, T-4]$ and perform plateau fits to those. We want to check if the normalization factors for mesons factorize into a product of normalization factors for quark sources such that

$$X_{s_1 s_2} = C^X_{s_1 s_2} X_{pp} = C^X_{s_1} C^X_{s_2} X_{pp}. \tag{6.2}$$

Using the numbers for C^X_{nn}, C^X_{ww} and C^X_{nw} and performing an exponential fit to those we find an agreement of the factorization hypothesis up to $\mathcal{O}(1.2\%)$

for $\beta = 7.90$ and $\mathcal{O}(2.2\%)$ for $\beta = 8.15$. In Fig. 6.2 the results for C_s^X are displayed. For large physical lattice sizes we find only $\mathcal{O}(1\%)$ dependence of the coefficients on the quark mass, which goes up to $\mathcal{O}(5-10\%)$ for the smallest volumes. The statistical errors are so small that we neglect them in the further analysis.

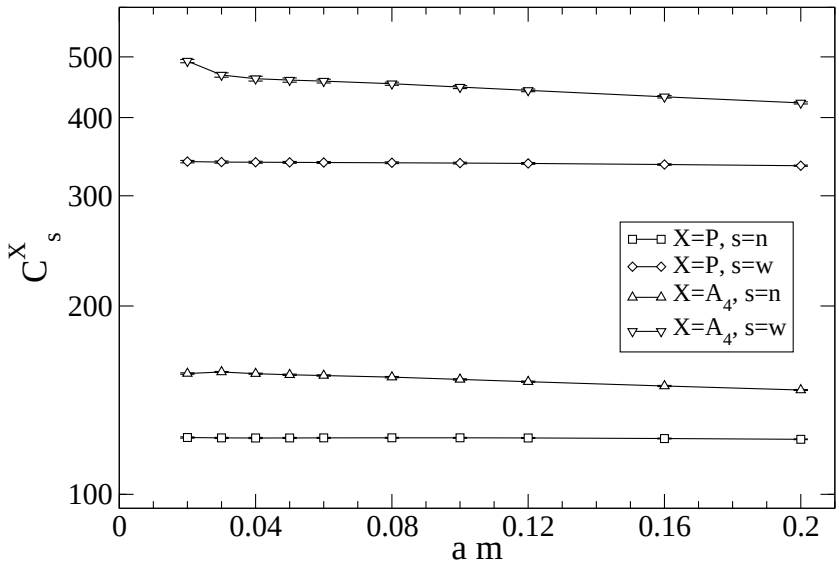

Figure 6.2: The normalization factors for operators P and A_4 for a $16^3 \times 32$ lattice at $\beta = 7.90$ computed from Eq. (6.1) and Eq. (6.2).

6.4 Masses

As mentioned before all the quantities in lattice computations appear with the regularization scale a attached, i.e., masses only appear in products like aM_π. One physical quantity has to be sacrificed to set the scale of the calculation. We use the string tension to assign a physical value to the parameter a [31]. Furthermore for quantities that cannot be observed directly we have to agree to a certain renormalization scheme in order to compare the values. In this case we quote the values for the $\overline{\text{MS}}$ scheme at the scale 2 GeV.

6.4.1 Meson masses

In Fig. 6.3 we show the masses of pseudoscalar mesons determined from the axial correlator. M_π^2 and M_K^2 are obtained directly from the fit, and M_η is computed therefrom using the Gell-Mann–Okubo relation (5.36). Also a linear fit and extrapolation to the squared meson mass suggested by the Gell-Mann–Oakes–Renner relation is included. It is interesting to note that there is a small residual pion mass at $m_q = 0$ in the extrapolation, which indicates a small residual additive mass. In Fig. 6.4 the behavior of the kaon mass and

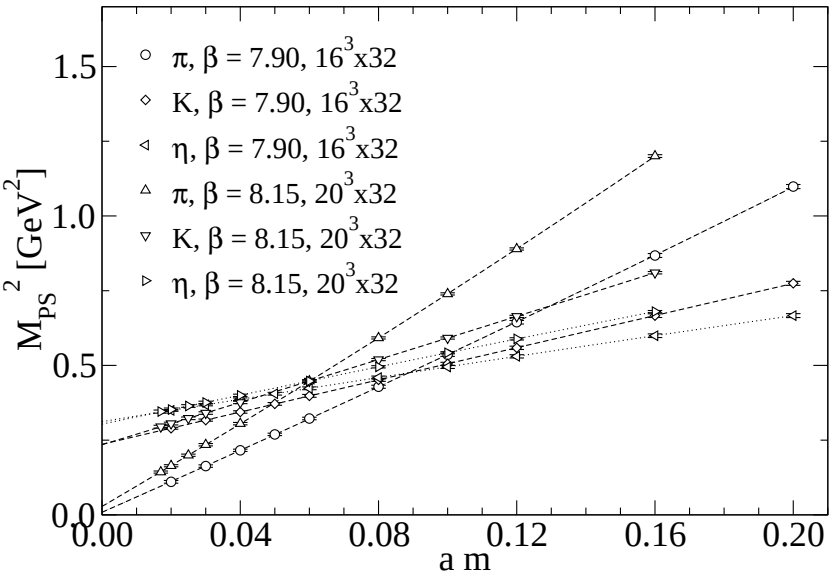

Figure 6.3: M_π^2, M_K^2 and M_η^2 determined from the asymptotic behavior of the axial correlator. M_π^2 and M_K^2 are obtained directly from the fit, M_η^2 is computed from the Gell-Mann–Okubo relation (5.36). The strange quark mass for the $\beta = 7.90$ and $\beta = 8.15$ is $am_s = 0.089$ and $am_s = 0.06$ respectively.

the determination of the strange quark mass according to the prescription in 4.4.2 is displayed. For the $16^3 \times 32$ lattice at $\beta = 7.90$ we interpolate M_K^2 linearly between the two values of the strange quark mass ($a\,m_s = 0.08$ and $a\,m_s = 0.10$) neighboring the physical point at $a\,m_s = 0.089$ whereas for the $20^3 \times 32$ lattice at $\beta = 8.15$ the physical point is at $a\,m_s = 0.06$.

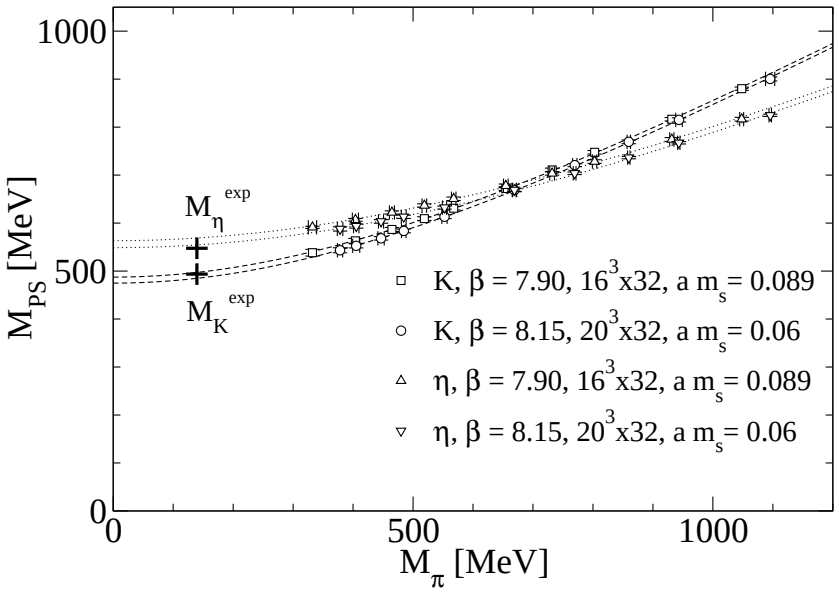

Figure 6.4: M_K^2 and M_η^2 plotted vs M_π^2. For the $16^3 \times 32$ lattice we have an interpolation between two values of the strange quark mass, while for the $20^3 \times 32$ the value $am = 0.06$ already corresponds to the physical value. The curves correspond to the linear fits in Fig. 6.3.

Topological finite size effects

Exact GW Dirac operators have exact zero modes. In contrary to full QCD these are not suppressed by the fermionic determinant in quenched situations. However, their effects for, e.g., the pion correlators [32], are hard to detect unless one approaches very small pion masses $\mathcal{O}(250$ MeV) [33]. We don't have an exact GW-operator, but only an approximate one, where there is the possibility that slightly misplaced zero modes occur. These lie on the real axis and lead to divergencies in the quark propagator already at some positive, but usually small mass. The effect is stronger the smaller the mass parameter in the Dirac operator gets and is often referred to as topological finite size effect. There have been various suggestions on how to deal with this problem [34, 35, 36, 37]. One of them is based on the fact that iso-non-singlet pseudoscalar and scalar correlators receive the same contributions from such zero modes, but the masses of the propagated ground states is separated by roughly an order of magnitude. Hence one can consider the difference between pseudoscalar and scalar correlators, which leads to a cancellation of the contributions

and extract the mass from the resulting correlator. For exactly chiral Dirac operators one expects a different behavior of contributions from topological finite size effects for the axial and the pseudoscalar correlator, that both mediate the pion as lowest lying state, A_4-correlators are supposed to have $\mathcal{O}(1/m)$ terms whereas P-correlators only come with $\mathcal{O}(1/m^2)$ terms. In Fig. 6.5 we plot the ratios of the pion mass obtained from $\langle PP \rangle$ and $\langle A_4 A_4 \rangle$ for two different lattice ensembles at the same physical volume with two different types of sources. Additionally there is one determination from the variational method [30] included in the plot. In this method we have a set of sources as an operator basis and then perform a diagonalization in order to find optimal combinations of these sources for the ground and excited states, such that the wave functions are orthonormal and the sum of exponentials appearing in the correlator can be disentangled. A fit to the function $\frac{a}{m} + b + cm$ is included in order to account for the different behavior of the correlators at small masses. Even for our smallest quark mass parameters the deviation from one is only 3% for the $16^3 \times 32$ and 1% for the $20^3 \times 32$ lattice, hence we can use either operator for measuring the pion mass.

Finite size dependence

ChPT calculations can also be performed in a finite volume, just as we have on the lattice. In this case we can distinguish between two regimes of expansion [38, 39, 40]. The p-regime is where $M_\pi L > 1$ holds. The expansion parameters are the same as we had in the infinite volume case discussed in Sect. 5. In the case $M_\pi L < 1$ the expansion breaks down and one has to use a different expansion parameter leading to the so-called ϵ-expansion. The physical interpretation of this case is that the pion Compton wave length is of the order of the lattice extent and correlations that are mediated over the periodic boundaries become important. We work in the p-regime here. In Fig. 6.6 we show the dimensionless unrenormalized pion coupling constant for the pion $a^2 G_\pi = a^2 \, G_\pi^{(r)} / Z_P$ determined from Eq. (5.57b) for three volumes with but at the same lattice spacing. The values of the bare quark mass parameter range down to $a\,m \geq 0.01$, but already at $a\,m = 0.06$ we find strong volume effects for the smallest lattice. This is to be expected since the inverse mass of the pion is already in the range of half the spatial lattice size, i.e., we are around the transition to the ϵ-regime. For larger lattices the effect is significant only for $a\,m < 0.02$. In the subsequent discussion we therefore only use the largest lattices in physical units, namely the sets with

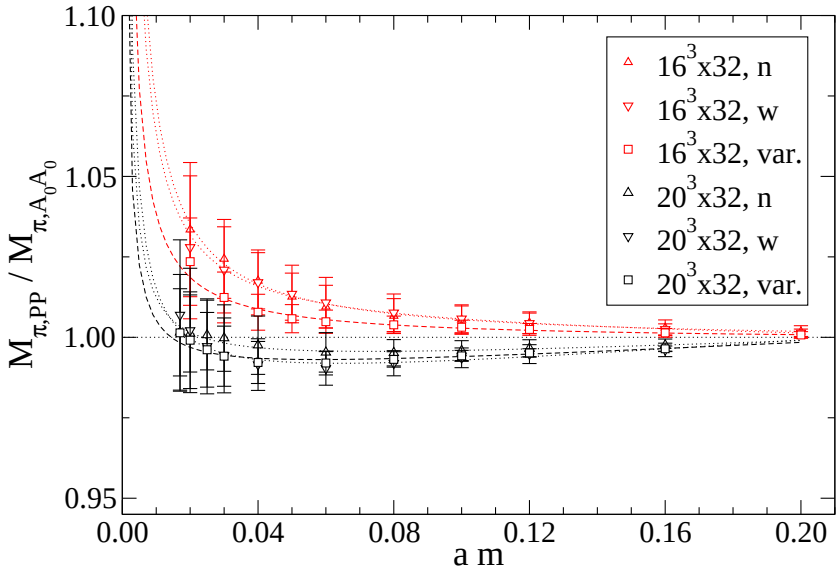

Figure 6.5: Ratio of the pion masses obtained from the pseudoscalar propagator $\langle PP \rangle$ and the axial propagator $\langle A_4 A_4 \rangle$ for the same physical volumes but two different lattice spacings. We display results for n(arrow) and w(ide) sources as well as for the variational method. A fit to a function $\frac{a}{m} + b + cm$ (dotted lines: standard sources, dashed lines: variational method) is included to check for topological finite size effects.

$16^3 \times 32$ at $\beta = 7.90$ ($a = 0.148$ fm) and $20^3 \times 32$ at $\beta = 8.15$ ($a = 0.119$ fm). In the latter we allow quark mass parameters of $a\,m \geq 0.017$.

Chiral logs

As discussed in Sect. 4.2 quenched QCD does not include closed quark loops. Quenched chiral perturbation theory (QChPT) [41, 42, 43] accounts for those missing graphs and new singular correction terms to standard ChPT arise, the so-called quenched chiral logs. It is hard to identify these correction terms in numerical simulations, though [37, 33, 44], due to the fact that one needs to go to relatively small pion masses (usually well below 300 MeV) in order to observe them. Additionally the role of zero modes and variation in the fit range obscure the effects. For the pseudoscalar mass the expected behavior in the quenched situation is [32, 45]

$$(a\,M_P)^2 \propto (a\,m)^{1/(1+\delta)}, \tag{6.3}$$

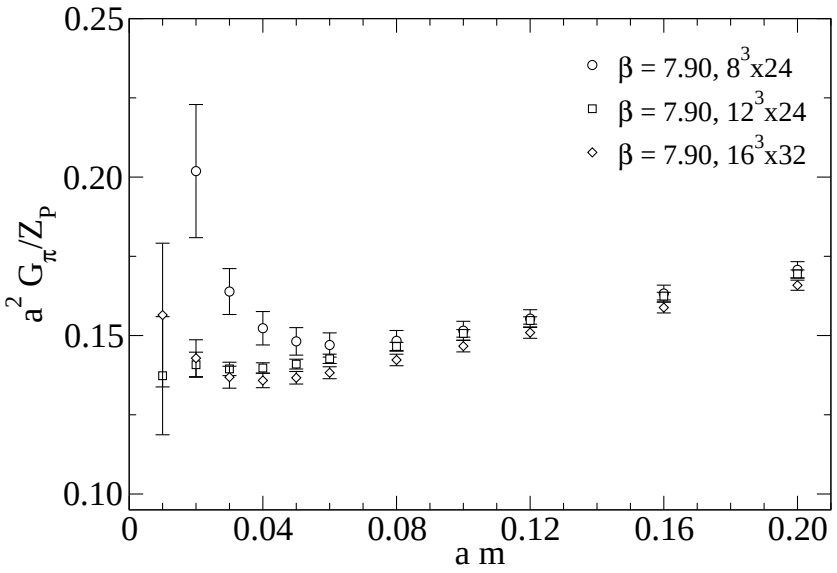

Figure 6.6: $a^2\, G_\pi^{(r)}/Z_P$ from Eq. (5.57b) for $\beta = 7.90$ and lattice sizes $8^3 \times 24$, $12^3 \times 24$ and $16^3 \times 32$. The finite size significantly affects the small volume data ($8^3 \times 24$) for $a\, m \leq 0.06$. For the other volumes finite size effects become important for $a\, m < 0.02$.

where the parameter δ ranges from 0.19 to 0.23 in the simulations mentioned above. Consequently we do not attempt to determine δ here.

6.4.2 Quark masses

For determining the quark mass we utilize the AWI (see Sect. 3.3). We can use a plateau

$$\frac{Z_A}{Z_P}\frac{\langle \partial_t A_4 X\rangle}{\langle PX\rangle} = Z_m 2m = 2m^{(r)} \tag{6.4}$$

with X being either P or A_4. In Fig. 6.7 we show data for the two choices. $X = A_4$ means we have to take the ratio of two correlators with hyperbolic sine shape that leads to numerical instabilities especially around the symmetry point in t. Thus we cannot reliably determine the plateau values for this choice at small quark masses. At mass values we can compare the results, they are in excellent agreement, though. For further analysis we stick to the more stable choice $X = P$. In Fig. 6.8 we plot the renormalized quark mass against the pion mass squared for the two lattices with largest physical size.

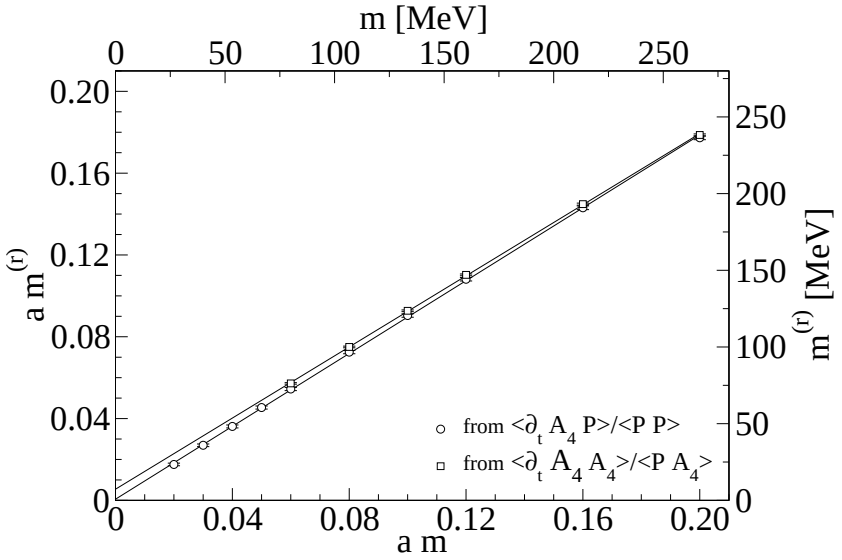

Figure 6.7: The renormalized quark mass $am^{(r)}$ (in the $\overline{\text{MS}}$ scheme) vs the bare mass parameter on a $16^3 \times 32$, $\beta = 7.90$ lattice determined from Eq. (6.4). The circles show the data with $X = P$ and the squares with $X = A_4$. For the second choice values below $am = 0.06$ have been ommited due to numerical instabilities in the fits.

The linear extrapolations to the physical point are in good agreement with the Particle Data Group [29] average for the light quark mass. Logarithmic corrections due to quenching are not taken into account here. Averaging over the extrapolated values at the physical point leads us to a value of

$$\frac{1}{2}\left(m_u^{(r)} + m_d^{(r)}\right) \equiv \bar{m}^{(r)} \simeq 4.1(2.4)\,\text{MeV} \tag{6.5}$$

in the $\overline{\text{MS}}$ scheme for the average light quark mass. The error is mainly due to the residual quark mass (see Fig. 6.3 and Fig. 6.7). The mass parameter for the strange quark has been fixed such that the kaon gets the correct physical mass for the light quark at physical mass. In Fig. 6.9 we display the corresponding renormalized strange quark mass in lattice units. The fitted lines for the strange quark are close to being parallel with negative intercepts. The fit touches the negative x-axis at the bare strange quark mass indicating very little additive mass renormalization of the Chiral Improved Dirac operator. In Fig. 6.8 we display the renormalized mass again in physical units. The fits for light and strange quarks coincide and give us our estimate

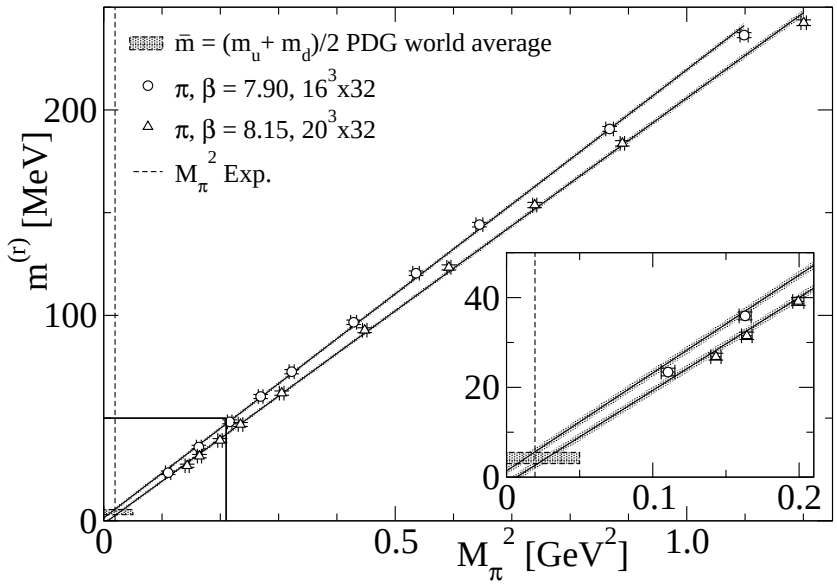

Figure 6.8: The renormalized quark mass $m^{(r)}$ vs M_π^2 for the two largest lattices. The extrapolation is in good agreement with the expected light current quark mass.

for the strange quark mass in the $\overline{\rm MS}$ scheme. Our average of renormalized light and strange quark obtained from the fit is

$$\frac{1}{2}\left(m_s^{(r)} + \bar{m}^{(r)}\right) \simeq 52(3)\,\mathrm{MeV} \tag{6.6}$$

and with Eq. (6.5) we find

$$m_s^{(r)} = 101(8)\,\mathrm{MeV} \tag{6.7}$$

in the $\overline{\rm MS}$ scheme at 2 GeV . We did not consider possible finite size, quenching or other systematic effects on the chiral extrapolation here. The error is given, just as in the case of the light quark mass, by the standard error and deviations on different lattice spacings. The pion data on the slope of $m^{(r)}$ also gives us the mass renormalization constant (according to Eq. (6.4)) which is given in Table 6.3. For actions respecting chiral symmetry we expect $Z_S = 1/Z_m$, which is indeed well realized. The PCAC relations lets us also expect that for the kaon data we find

$$am^{(r)} \simeq Z_m a \frac{(m_s + m)}{2} \tag{6.8}$$

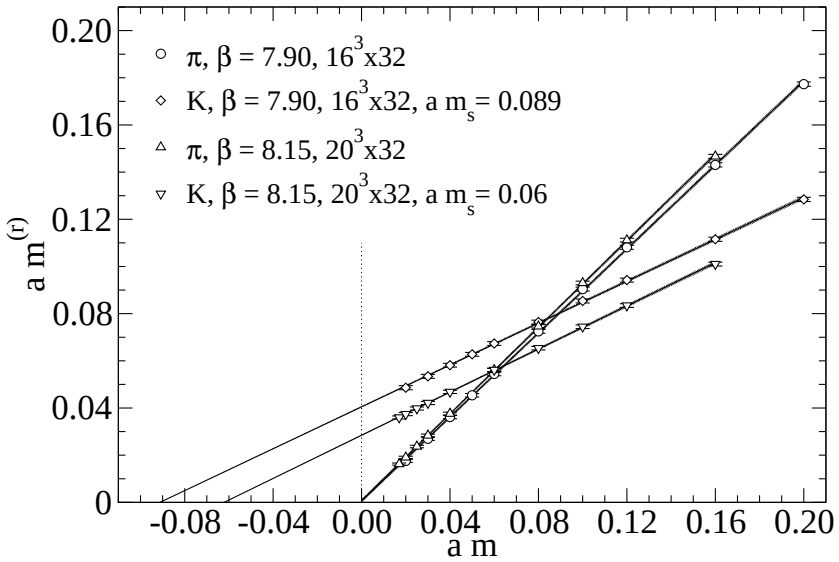

Figure 6.9: $a\,m^{(r)}$ vs. $a\,m$ from (6.4) using $X = P$. The slope of $m^{(r)}$ for the pion data provides Z_m.

which is indeed observed. The numbers obtained here are in good agreement with determinations from the overlap action in [46, 47] and also to a lesser extent with [48].

6.5 Low energy parameters

6.5.1 Decay constants

The pseudoscalar decay constants have been extracted from the axial correlation function according to (5.57c) for pion and kaon. In Fig. 6.10 we display the dimensionless pseudoscalar decay constants af_{PS}. A quadratic extrapolation to the chiral limit is also shown with the error bands coming from

β	a[fm]	a[GeV^{-1}]	Z_S	$1/Z_S$	Z_m	$Z_m Z_S$
7.90	0.148	0.750	1.1309(9)	0.8842(7)	0.891(4)	1.007(5)
8.15	0.119	0.605	1.081(1)	0.9250(9)	0.916(5)	0.991(6)

Table 6.3: Renormalization constant Z_S from [2] (see Table 6.2) compared to the values of Z_m as derived from the slope of the renormalized quark mass.

the jackknife analysis. In Fig. 6.11 the decay constant is plotted versus the according pseudoscalar mass. The data for pion and kaon essentially overlap and exhibit a universal functional behavior. This again confirms that for mesons the strategy to use two moderately heavy quarks to simulate states with one light and one strange quark is a reasonable one. For full QCD the

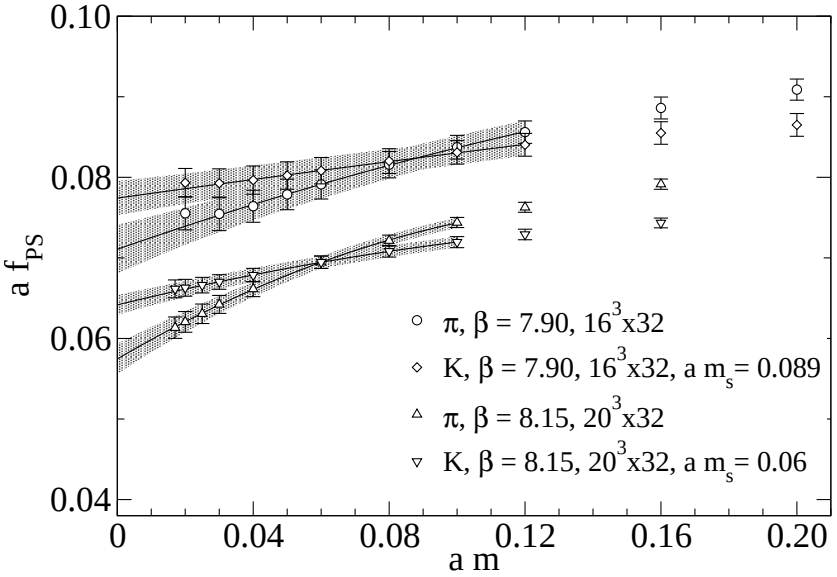

Figure 6.10: The dimensionless decay constants $a\,f_\pi$ and $a\,f_K$, determined with Eq. (5.57c), vs. $a\,m$.

chiral expansion of the pion decay constant reads [49]

$$\frac{f_\pi}{f} = 1 + \xi\,\bar{\ell}_4 + \mathcal{O}(\xi^2) \quad \text{with} \quad \xi = \left(\frac{M_\pi}{4\,\pi\,F_\pi}\right)^2, \tag{6.9}$$

where f denotes the decay constant at the chiral limit and f_π and M_π denotes the corresponding values at the physical point. The parameter $\bar{\ell}_4 = -\ln(M_\pi^2/\Lambda^2)$ depends on the intrinsic QCD scale Λ with the value $\Lambda \approx 4\,\pi\,f_\pi$ suggested in [49]. In [50] a value of $\bar{\ell}_4 \approx 4.0 \pm 0.6$ is quoted. ChPT also relates the decay constant of both, the pion and the kaon to the scalar charge radius by

$$f_{\pi,K}/f = 1 + \frac{1}{6}\langle r^2\rangle_s M_{\pi,K}^2 + \frac{13}{12}\xi + \mathcal{O}(\xi^2). \tag{6.10}$$

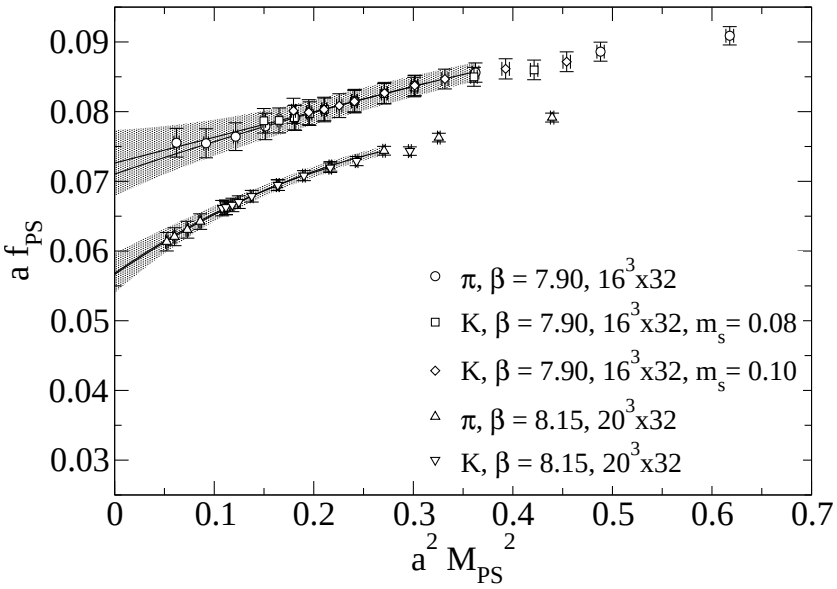

Figure 6.11: $a\, f_{\pi,K}$ vs. $(a\, M_{PS})^2$ with error bands for chiral extrapolations as discussed in the text. The fit includes only data in the indicated range.

The scalar charge radius is then given by

$$\langle r^2 \rangle_s = \frac{3}{8\,\pi^2\, f_\pi^2}, \left(\bar{\ell}_4 - \frac{13}{12} + \mathcal{O}(\xi) \right) \tag{6.11}$$

with an expected value of $\langle r^2 \rangle_s = 0.61(4)\,\mathrm{fm}^2$ at $f_\pi / f = 1.072(4)$ [50]. We use results from quenched calculations where one expects correction terms with a logarithmic singularity in the valence quark mass m. On the other hand the leading order logarithmic terms $m \log m$ involves quark loops that are absent in the quenched case and only higher order logarithmic terms may play a role [42]. In addition to the linear term in our extrapolation we also allow a term $m^2 \log m$ (as discussed in [33]), but the deviance from a quadratic fit is only of the order of $\frac{1}{10}\sigma$.
In Fig. 6.12 we display the decay constants in physical units. The values extrapolated to the chiral limit agree quite well, but away from the chiral limit we still have considerable dependence on the lattice spacing a. Using (6.9) we can assign values of $\langle r^2 \rangle_s = 0.08\,\mathrm{fm}^2$ and $\langle r^2 \rangle_s = 0.13\,\mathrm{fm}^2$ to the scalar charge radius, which are much smaller than expected from full QCD. This intriguing fact is also somewhat confirmed by studies of the scalar form factor, which also contains the scalar charge radius as the slope. The authors

of [51] quote a value of $\langle r^2 \rangle_s = 0.054(16)\,\mathrm{fm}^2$. Since the D_{CI} is not an exact

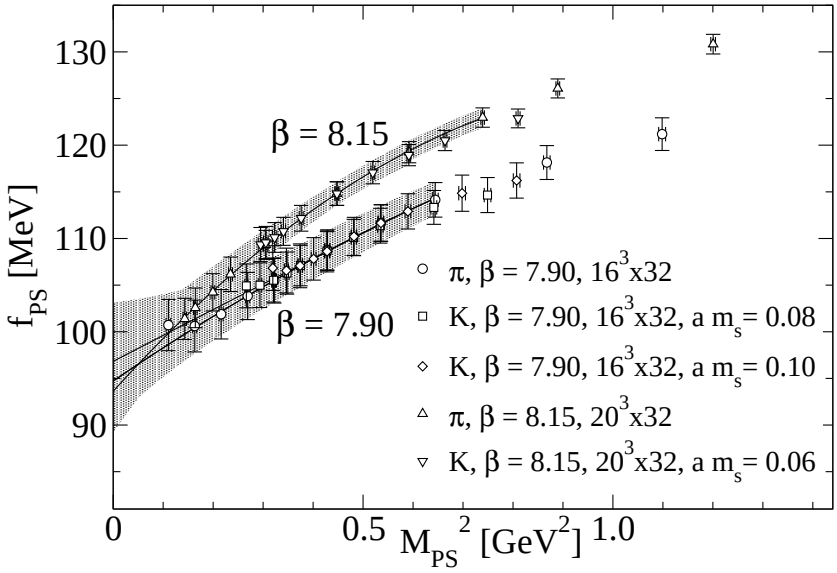

Figure 6.12: Chiral limit of $f_{\pi,K}$ vs. M_{PS}^2. Error bands for quadratic extrapolation.

GW operator we cannot exclude linear corrections to the scaling behavior. In the comparison of our results from different lattice sizes we therefore perform a constant fit in order to get our continuum limit result and statistical error bar and take the deviation from a linear fit as our systematic error. The corresponding data and both extrapolations, as well as the data for the ratio f_π/f_K are displayed in 6.13. In this ratio we expect the leading order scaling corrections to cancel. For the two largest lattices we had data for pions and kaons, while for the smaller ones we used the pion decay constant at the kaon mass as our result for the kaon decay constant, which is justified by the universal behavior shown in Fig. 6.11. We find values of $f_\pi = 96(2)\,\mathrm{MeV}$ for a constant fit and $f_\pi = 100(10)\,\mathrm{MeV}$ for a linear fit which gives us the final continuum extrapolation value of

$$f_\pi = 96(2)(4)\,\mathrm{MeV}. \tag{6.12}$$

In the same manner we find a continuum value for the kaon decay constant of

$$f_K = 106(1)(8)\,\mathrm{MeV}. \tag{6.13}$$

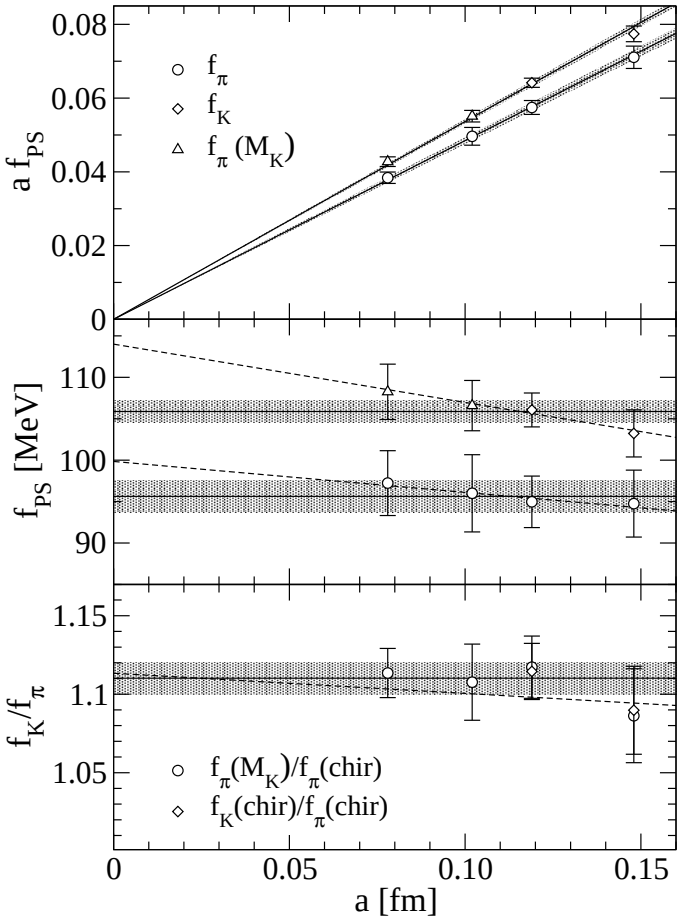

Figure 6.13: $a\,f_{\pi,K}$, $f_{\pi,K}$ and f_K/f_π vs. a.

The ratio f_π/f_K is indeed compatible with a constant and has a value of

$$f_K/f_\pi = 1.11(1)(2) \tag{6.14}$$

in the continuum limit. Studies using the overlap operator give similar results for f_π [33, 52, 53, 54, 55, 56, 48, 44]. The experimental values from [29] are $f_\pi = 92.4(0.3)\,\mathrm{MeV}$ and $f_K = 113.0(1.3)\,\mathrm{MeV}$, where we have adjusted the values to the definition used here by dividing by a factor of $\sqrt{2}$.

6.5.2 Condensate

One method for determining the chiral condensate for exact GW-operators is to use the trace of the inverse Dirac operator, which has been successfully applied to calculations using the overlap operator [57, 58]. For the D_{CI} this does not work, because the subtraction constant is not known to a high enough precission, which was shown in [59]. Another method is to derive the condensate's value from the density distribution of the low-lying complex eigenvalues of the Dirac operator, which is rather involved concerning computational efford. Instead we use the GMOR ((5.32)) and the quantities therein, Eq. (5.57e) and a combination of Eq. (5.57b) and Eq. (5.57c) reading

$$Z_A Z_P \sqrt{\langle A_4 A_4 \rangle \langle PP \rangle} \sim |\Sigma^{(r)}| \mathrm{e}^{-M_\pi t}. \tag{6.15}$$

For the first determination we use the decay constant, quark mass and the pion mass determined previously. For relation two and three, which implicitely use the GMOR as well, we perform an exponential fit and the prefactor gives us the renormalized chiral condensate. Numerous studies were performed in the ϵ-regime [57, 52, 53, 54], but again, we want to work in the p-regime here, though. In Fig. 6.14 we show data and results for all three determination methods including linear extrapolations to the chiral limit. We find excellent agreement of all three methods. In Fig. 6.15 the same quantities are displayed in physical units. Here we can see that also the values for the two largest lattices are consistent within error bars. The dependence on the quark mass is also compatible with the leading linear chiral behavior. So far we have restricted ourselves to the discussion of the two lattices with largest physical volume. Just like in Sect. 6.5.1 we now want to analyze the scaling behavior and continuum limit of the chiral condensate. To this end we also include lattices with smaller lattice spacing and smaller physical volume. In Fig. 6.16 we plot the dimensionless results as well as results in physical units against the lattice spacing. Again, as we cannot exclude linear corrections to the constant scaling behavior, we perform both, a constant and a linear extrapolation. We use the mean value and error from the first fit to claim our value in the continuum limit with the statistical error, whereas the deviation of constant and linear fit gives us the systematic error. We do this for all three types of derivations and end up with $|\Sigma^{(r)}| = (286(4)\ \mathrm{MeV})^3$ for the constant fit. The linear fit leads to a larger value of $|\Sigma^{(r)}| \approx (318(25)\ \mathrm{MeV})^3$. Combining the two we find a value of

$$|\Sigma^{(r)}| = (286(4)(32)\,\mathrm{MeV})^3 \tag{6.16}$$

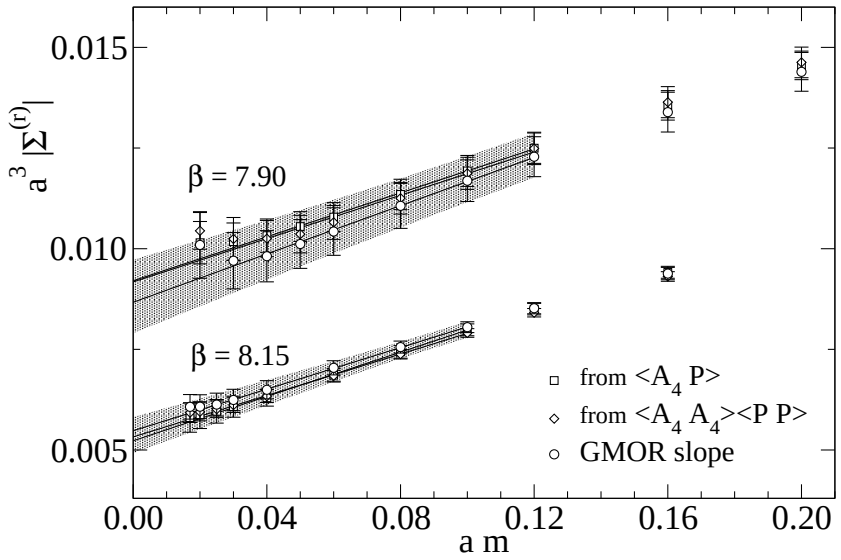

Figure 6.14: $a^3\,|\Sigma^{(r)}|$ vs. $a\,m$ for $16^3 \times 32$, $\beta = 7.90$ and $20^3 \times 32$, $\beta = 8.15$ comparing different way of extraction; circles: GMOR-slope Eq. (5.32), boxes: $\langle A_4 P\rangle$ Eq. (5.57b), diamonds: $\langle A_4 A_4\rangle\langle PP\rangle$ Eq. (6.15). We also show linear extrapolations to the chiral limit.

for the renormalized chiral condensate in the continuum limit. This value is slightly larger, but still within the error limits of a determination using the overlap operator [44] and larger than results in [47, 55, 56]. Results in the ϵ-regime [52, 53, 54] also agree well. In [60] a study using spectral decomposition of the overlap operator was performed and our result is in agreement with a continuum extrapolation of the results therein.

6.5.3 Collection of the results and concluding remarks

Within the Bern-Graz-Regensburg collaboration two Ginsparg-Wilson type Dirac operators, namely the so-called fixed-point operator [61] and the $D_{\rm CI}$ operator, have been studied. Both of them do not obey the GW-relation exactly, but to a good approximation. For the $D_{\rm CI}$ action we know the quark bilinear renormalization constants [2], which enables us to determine basic low energy constants for both, the light- and the strange-quark sector. All the computations were done in the quenched case, because only recently first results for the $D_{\rm CI}$ in full QCD became available [62, 63, 64, 65]. Also

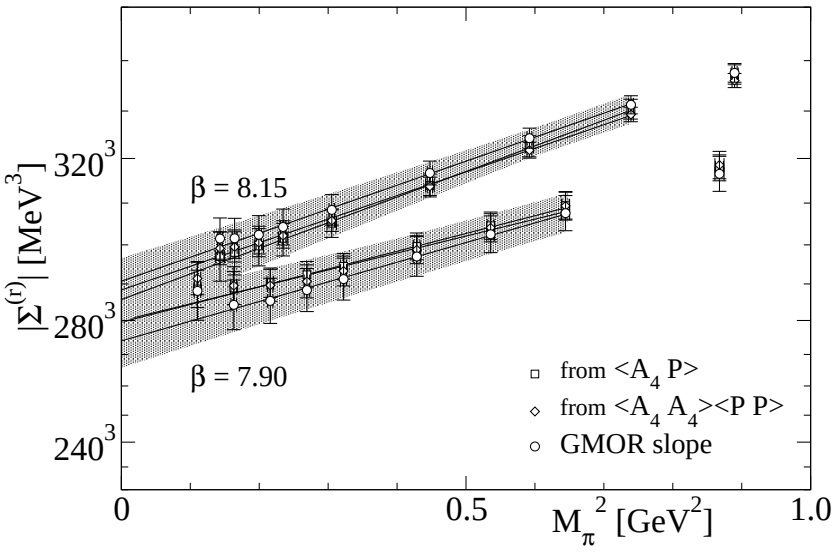

Figure 6.15: $|\Sigma^{(r)}|$ vs. M_π^2 as in Fig. 6.14, but in physical units.

the condensate was worked out using a different method [66]. Since the $D_{\rm CI}$ provides good chiral properties, but is much less expensive than the overlap operator, it was possible to work at several lattice spacings ranging from 0.15 fm to 0.08 fm with different lattice sizes and different physical volumes. The results are mainly based on the two physically largest lattice ensembles with spacings 0.15 fm and 0.12 fm with a spatial extent of 2.4 fm. Only for the study of finite-size effects and scaling behavior we used data from lattices with smaller extent. We used quark mass parameters corresponding to pion masses ranging between 330 MeV and roughly 1 GeV. All quantities have been converted to the $\overline{\rm MS}$ scheme at 2 GeV and the final list of renormalized physical values in the chiral limit reads:

$$\begin{aligned}
\text{Quark masses:} \quad \bar{m} &= 4.1(2.4)\,\text{MeV}\,, \\
m_s &= 101(8)\ \text{MeV}\,, \\
\text{Condensate:} \quad \Sigma &= -(286(4)(32)\ \text{MeV})^3\,, \\
\text{Decay constants:} \quad f_\pi &= 96(2)(4)\,\text{MeV}\,, \\
f_K &= 105(2)(8)\,\text{MeV}\,, \\
f_K/f_\pi &= 1.11(1)(2)\,.
\end{aligned} \tag{6.17}$$

Like many quenched results, these numbers are surprisingly close to experimental values [29]. Still, it would be very interesting to perform such calculations also for full QCD. By the time of writing gauge configurations and

meson propagators for three different lattice sizes and up to five different parameter sets are available. The renormalization constants are yet unknown, but a determination is in progress.

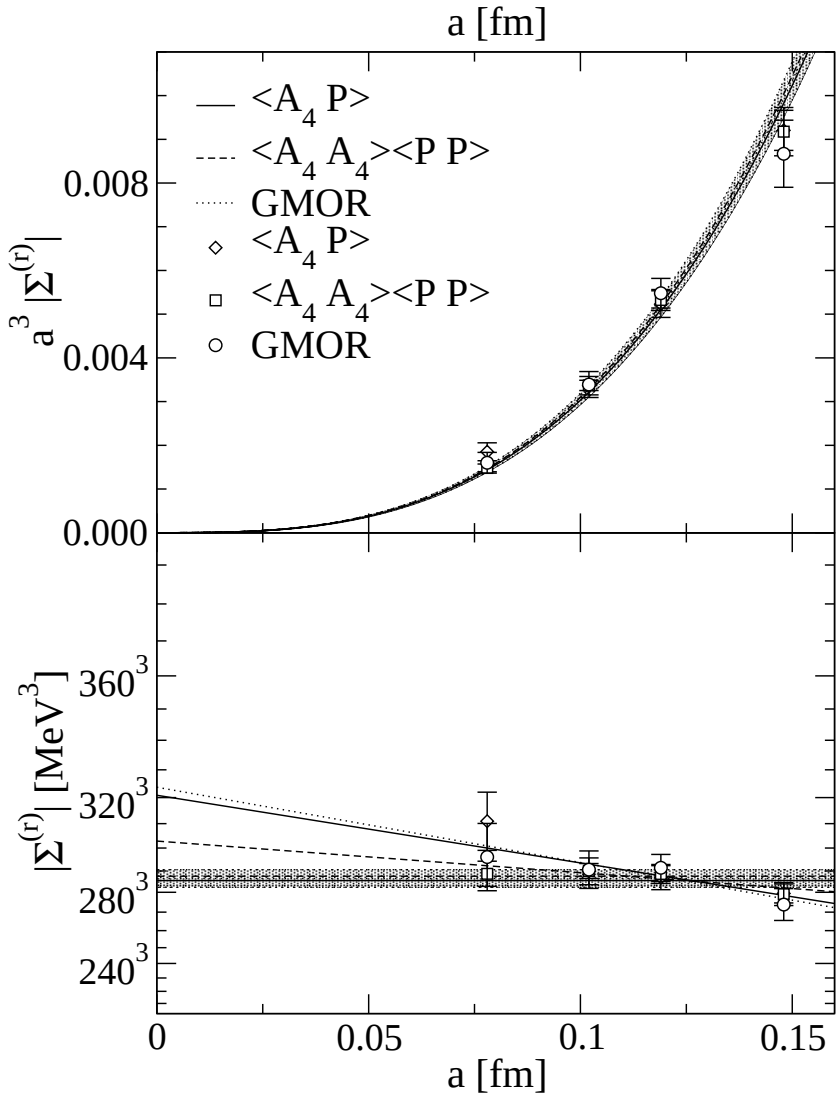

Figure 6.16: $a^3\,|\Sigma^{(r)}|$ and $|\Sigma^{(r)}|$ vs. a. In the legends we indicate the quantities used in the derivation of the condensate value. In the bottom plot we show a constant extrapolation (horizontal error bands) and compare it to a linear one.

6.5.4 Tables

In Tables 6.4, 6.5, 6.6, 6.7, 6.8 and 6.9 we collect the results for meson and quark masses, the decay constants and the condensate in the $\overline{\text{MS}}$ scheme at 2 GeV.

$a\,m$	$a^2\,M_\pi^2$	M_π^2[GeV^2]	M_π[MeV]	$a^2\,M_K^2$	M_K^2[GeV^2]	M_K[MeV]
0.02	0.062(3)	0.110(5)	332(7)	0.163(2)	0.290(3)	538(3)
0.03	0.092(2)	0.163(4)	404(5)	0.178(2)	0.317(4)	563(3)
0.04	0.121(2)	0.216(4)	465(4)	0.194(2)	0.344(4)	586(4)
0.05	0.151(2)	0.269(4)	519(4)	0.209(2)	0.371(4)	609(4)
0.06	0.181(2)	0.322(4)	568(4)	0.224(3)	0.398(5)	631(4)
0.08	0.241(3)	0.429(5)	655(4)	0.254(3)	0.452(5)	672(4)
0.10	0.301(3)	0.536(6)	732(4)	0.284(3)	0.505(5)	711(4)
0.12	0.362(3)	0.644(6)	803(4)	0.314(3)	0.559(6)	747(4)
0.16	0.488(4)	0.868(7)	931(4)	0.375(3)	0.666(6)	816(4)
0.20	0.618(4)	1.098(7)	1048(3)	0.436(4)	0.775(7)	880(4)

Table 6.4: The pion and kaon masses computed from Eq. (5.57b) on the $16^3 \times 32$, $\beta = 7.90$ lattice. As soon as the light quark mass exceeds the (fixed) strange quark mass, the kaon becomes lighter than the pion.

$a\,m$	$a^2\,M_\pi^2$	M_π^2[GeV^2]	M_π[MeV]	$a^2\,M_K^2$	M_K^2[GeV^2]	M_K[MeV]
0.017	0.052(1)	0.143(4)	378(5)	0.108(2)	0.295(5)	543(4)
0.02	0.060(1)	0.164(4)	405(4)	0.112(2)	0.305(5)	553(4)
0.025	0.073(1)	0.199(4)	447(4)	0.118(2)	0.323(4)	568(4)
0.03	0.086(1)	0.235(4)	484(4)	0.125(2)	0.341(4)	584(4)
0.04	0.112(1)	0.305(4)	552(4)	0.138(1)	0.376(4)	613(3)
0.06	0.164(1)	0.448(4)	669(3)	0.164(1)	0.448(4)	669(3)
0.08	0.217(1)	0.592(4)	769(2)	0.190(1)	0.519(4)	721(3)
0.10	0.271(1)	0.739(4)	860(2)	0.217(1)	0.592(4)	769(2)
0.12	0.326(1)	0.890(4)	943(2)	0.243(1)	0.664(4)	815(2)
0.16	0.439(2)	1.200(5)	1096(2)	0.297(1)	0.810(4)	900(2)

Table 6.5: The pion and kaon masses computed from Eq. (5.57b) on the $20^3 \times 32$, $\beta = 8.15$ lattice.

$a\,m$	$a\,f_\pi/Z_A$	$a\,f_\pi$	f_π[MeV]	$a\,f_K/Z_A$	$a\,f_K$	f_K[MeV]
0.02	0.076(2)	0.076(2)	101(3)	0.080(2)	0.079(2)	106(2)
0.03	0.076(2)	0.075(2)	101(3)	0.080(2)	0.079(2)	106(2)
0.04	0.077(2)	0.076(2)	102(3)	0.080(2)	0.080(2)	106(2)
0.05	0.079(2)	0.078(2)	104(3)	0.081(2)	0.080(2)	107(2)
0.06	0.080(2)	0.079(2)	105(2)	0.082(2)	0.081(2)	108(2)
0.08	0.082(2)	0.082(2)	109(2)	0.083(2)	0.082(2)	109(2)
0.10	0.084(1)	0.084(1)	112(2)	0.084(1)	0.083(1)	111(2)
0.12	0.086(1)	0.086(1)	114(2)	0.085(1)	0.084(1)	112(2)
0.16	0.089(1)	0.089(1)	118(2)	0.086(1)	0.085(1)	114(2)
0.20	0.092(1)	0.091(1)	121(2)	0.087(1)	0.087(1)	115(2)
(semi-)chir.	0.072(3)	0.071(8)	95(4)	0.078(2)	0.077(2)	103(3)

Table 6.6: Pion and kaon decay constants (from Eq. (5.57c)) for $16^3 \times 32$, $\beta = 7.90$ lattice. In the last line we give the extrapolation to the (semi-)chiral limit (where the light quark masses vanish) as it is discussed in the text.

$a\,m$	$a\,f_\pi/Z_A$	$a\,f_\pi$	f_π[MeV]	$a\,f_K/Z_A$	$a\,f_K$	f_K[MeV]
0.017	0.062(1)	0.061(1)	101(2)	0.067(1)	0.066(1)	109(2)
0.02	0.063(1)	0.062(1)	103(2)	0.067(1)	0.066(1)	110(2)
0.025	0.064(1)	0.063(1)	104(2)	0.067(1)	0.067(1)	110(2)
0.03	0.065(1)	0.064(1)	106(2)	0.0678(9)	0.0670(9)	111(1)
0.04	0.067(1)	0.0661(9)	109(2)	0.0686(8)	0.0679(8)	112(1)
0.06	0.0703(8)	0.0695(8)	115(1)	0.0703(8)	0.0695(8)	115(1)
0.08	0.0730(7)	0.0721(7)	119(1)	0.0716(7)	0.0708(7)	117(1)
0.10	0.0752(6)	0.0744(6)	123(1)	0.0728(7)	0.0720(7)	119(1)
0.12	0.0772(6)	0.0763(6)	126(1)	0.0737(7)	0.0729(7)	121(1)
0.16	0.0801(6)	0.0792(6)	131(1)	0.0752(6)	0.0743(6)	123(1)
(semi-)chir.	0.058(2)	0.058(2)	95(3)	0.065(1)	0.064(1)	106(2)

Table 6.7: Pion and kaon decay constants (from Eq. (5.57c)) for $20^3 \times 32$, $\beta = 8.15$ lattice.

$a\,m$	$a^3\,\lvert\Sigma_1\rvert$	$a^3\,\lvert\Sigma_2\rvert$	$a^3\,\lvert\Sigma_3\rvert$	$\sqrt[3]{\lvert\Sigma_1\rvert}$[MeV]	$\sqrt[3]{\lvert\Sigma_2\rvert}$[MeV]	$\sqrt[3]{\lvert\Sigma_3\rvert}$[MeV]
0.02	0.0101(5)	0.0101(8)	0.0104(5)	289(5)	288(8)	291(4)
0.03	0.0102(5)	0.0097(7)	0.0102(5)	289(4)	284(7)	290(5)
0.04	0.0103(4)	0.0098(6)	0.0103(5)	290(4)	285(6)	290(4)
0.05	0.0105(4)	0.0101(6)	0.0104(5)	292(3)	288(6)	291(4)
0.06	0.0108(4)	0.0104(6)	0.0107(4)	295(3)	291(5)	293(4)
0.08	0.0113(4)	0.0111(6)	0.0113(4)	300(3)	297(5)	299(3)
0.10	0.0119(4)	0.0117(5)	0.0119(4)	305(3)	303(4)	304(3)
0.12	0.0125(4)	0.0123(5)	0.0125(4)	309(3)	308(4)	309(3)
0.16	0.0136(4)	0.0134(5)	0.0136(4)	318(3)	317(4)	319(3)
0.20	0.0146(4)	0.0144(5)	0.0146(4)	326(3)	324(4)	326(3)
chir.	0.0092(5)	0.0087(8)	0.0092(6)	279(5)	274(8)	279(6)

Table 6.8: The light quark condensate as derived from different observables (lattice size $16^3 \times 32$, $\beta = 7.90$). We use the abbreviations $\Sigma_1 = \Sigma_{\langle A_4 P\rangle}$, $\Sigma_2 = \Sigma_{\mathrm{GMOR}}$ and $\Sigma_3 = \Sigma_{\langle PP\rangle\langle A_4 A_4\rangle}$. In the last line we give the extrapolation to the chiral limit as discussed in the text.

$a\,m$	$a^3\,\lvert\Sigma_1\rvert$	$a^3\,\lvert\Sigma_2\rvert$	$a^3\,\lvert\Sigma_3\rvert$	$\sqrt[3]{\lvert\Sigma_1\rvert}$[MeV]	$\sqrt[3]{\lvert\Sigma_2\rvert}$[MeV]	$\sqrt[3]{\lvert\Sigma_3\rvert}$[MeV]
0.017	0.0058(4)	0.0061(3)	0.0059(2)	297(6)	302(5)	299(4)
0.02	0.0059(3)	0.0061(3)	0.0059(2)	298(6)	302(5)	299(4)
0.025	0.0060(3)	0.0061(3)	0.0060(2)	300(5)	302(5)	301(3)
0.03	0.0061(3)	0.0062(3)	0.0061(2)	302(4)	304(4)	302(3)
0.04	0.0063(2)	0.0065(2)	0.0063(2)	305(3)	308(4)	306(3)
0.06	0.0069(2)	0.0070(2)	0.0068(1)	314(3)	317(3)	314(2)
0.08	0.0074(2)	0.0076(1)	0.0074(1)	323(2)	324(2)	322(2)
0.10	0.0080(1)	0.0081(1)	0.0079(1)	330(2)	331(2)	329(1)
0.12	0.0085(1)	0.0085(1)	0.0084(1)	337(2)	338(2)	336(1)
0.16	0.0094(1)	0.0094(2)	0.0093(1)	349(2)	349(2)	348(1)
chir.	0.0052(3)	0.0055(3)	0.0053(2)	287(6)	291(6)	289(4)

Table 6.9: The light quark condensate as derived from different observables (lattice size $20^3 \times 32$, $\beta = 8.15$). We use the abbreviations $\Sigma_1 = \Sigma_{\langle A_4 P\rangle}$, $\Sigma_2 = \Sigma_{\mathrm{GMOR}}$ and $\Sigma_3 = \Sigma_{\langle PP\rangle\langle A_4 A_4\rangle}$.

Appendix A

Appendix

A.1 Useful matrices

A.1.1 $su(N)$

Elements of the algebra $su(N)$ obey the commutator relation

$$\left[\frac{\lambda_i}{2}, \frac{\lambda_j}{2}\right] = i f_{ijk} \frac{\lambda_k}{2} \tag{A.1}$$

with the so-called structure constants f_{ijk}. Due to the commutator they have to be antisymmetric in the first two indices

$$f_{ijk} = -f_{jik}. \tag{A.2}$$

A.1.2 Pauli matrices

The structure constants for the algebra $su(2)$ are the elements of the antisymmetric tensor ϵ_{ijk}. The non-trivial entries are

$$\epsilon_{123} = \epsilon_{231} = \epsilon_{312} = 1, \tag{A.3a}$$
$$\epsilon_{132} = \epsilon_{321} = \epsilon_{213} = -1. \tag{A.3b}$$

The canonical basis are the Pauli matrices

$$\sigma_1 = \begin{pmatrix} 0 & 1 \\ 1 & 0 \end{pmatrix}, \qquad \sigma_2 = \begin{pmatrix} 0 & -i \\ i & 0 \end{pmatrix}, \qquad \sigma_3 = \begin{pmatrix} 1 & 0 \\ 0 & -1 \end{pmatrix}. \tag{A.4a}$$

All of those are traceless matrices and an expression for the product of two matrices can be established

$$\sigma_i \sigma_j = \delta_{ij} + i\epsilon_{ijk}\sigma_k. \tag{A.5}$$

A.1.3 Gell-Mann matrices

The algebra $su(3)$ is more complicated. The non-trivial entries for the structure constants are given in Table A.1. Here the canonical basis are the Gell-

f_{123}	f_{147}	f_{156}	f_{246}	f_{257}	f_{345}	f_{367}	f_{458}	f_{678}
1	$\frac{1}{2}$	$-\frac{1}{2}$	$\frac{1}{2}$	$\frac{1}{2}$	$\frac{1}{2}$	$-\frac{1}{2}$	$-\frac{\sqrt{3}}{2}$	$-\frac{\sqrt{3}}{2}$

Table A.1: Structure constants for $su(3)$

Mann or flavor matrices

$$\lambda_1 = \begin{pmatrix} 0 & 1 & 0 \\ 1 & 0 & 0 \\ 0 & 0 & 0 \end{pmatrix}, \quad \lambda_2 = \begin{pmatrix} 0 & -i & 0 \\ i & 0 & 0 \\ 0 & 0 & 0 \end{pmatrix}, \quad \lambda_3 = \begin{pmatrix} 1 & 0 & 0 \\ 0 & -1 & 0 \\ 0 & 0 & 0 \end{pmatrix}, \tag{A.6a}$$

$$\lambda_4 = \begin{pmatrix} 0 & 0 & 1 \\ 0 & 0 & 0 \\ 1 & 0 & 0 \end{pmatrix}, \quad \lambda_5 = \begin{pmatrix} 0 & 0 & -i \\ 0 & 0 & 0 \\ i & 0 & 0 \end{pmatrix}, \quad \lambda_6 = \begin{pmatrix} 0 & 0 & 0 \\ 0 & 0 & 1 \\ 0 & 1 & 0 \end{pmatrix}, \tag{A.6b}$$

$$\lambda_7 = \begin{pmatrix} 0 & 0 & 0 \\ 0 & 0 & -i \\ 0 & i & 0 \end{pmatrix}, \quad \lambda_8 = \begin{pmatrix} \frac{1}{\sqrt{3}} & 0 & 0 \\ 0 & \frac{1}{\sqrt{3}} & 0 \\ 0 & 0 & -\frac{2}{\sqrt{3}} \end{pmatrix}. \tag{A.6c}$$

A.2 Clifford algebra

The connection between Dirac matrices in Euclidean γ_μ and Minkowski space γ_μ^M is

$$\gamma_{1,2,3} \equiv i\gamma_{1,2,3}^M, \tag{A.7a}$$

$$\gamma_4 \equiv -i\gamma_4^M = \gamma_0^M. \tag{A.7b}$$

The Euclidean Dirac matrices are chosen to be Hermitian

$$\gamma_\mu = \gamma_\mu^\dagger \tag{A.8}$$

and satisfy

$$\{\gamma_\mu, \gamma_\nu\} = 2\delta_{\mu\nu}. \tag{A.9}$$

A.2.1 Chiral representation

Although the unit matrix is no element of the representations, as it does not satisfy Eq. (A.9), but it is often referred to as Γ_0 or Γ_S, as it is responsible for the scalar density

$$\Gamma_S = \mathbb{1} = \begin{pmatrix} 1 & 0 & 0 & 0 \\ 0 & 1 & 0 & 0 \\ 0 & 0 & 1 & 0 \\ 0 & 0 & 0 & 1 \end{pmatrix}. \tag{A.10}$$

We refer to Γ_1-Γ_4 as the vector, often denoted as Γ_V or Γ_{V_μ}. The matrices are

$$\Gamma_1 = \gamma_1 = \begin{pmatrix} 0 & 0 & 0 & -i \\ 0 & 0 & -i & 0 \\ 0 & i & 0 & 0 \\ i & 0 & 0 & 0 \end{pmatrix}, \tag{A.11}$$

$$\Gamma_2 = \gamma_2 = \begin{pmatrix} 0 & 0 & 0 & -1 \\ 0 & 0 & 1 & 0 \\ 0 & 1 & 0 & 0 \\ -1 & 0 & 0 & 0 \end{pmatrix}, \tag{A.12}$$

$$\Gamma_3 = \gamma_3 = \begin{pmatrix} 0 & 0 & -i & 0 \\ 0 & 0 & 0 & i \\ i & 0 & 0 & 0 \\ 0 & -i & 0 & 0 \end{pmatrix}, \tag{A.13}$$

$$\Gamma_4 = \gamma_4 = \begin{pmatrix} 0 & 0 & 1 & 0 \\ 0 & 0 & 0 & 1 \\ 1 & 0 & 0 & 0 \\ 0 & 1 & 0 & 0 \end{pmatrix}. \tag{A.14}$$

There are several ways to construct the matrices for the anti-symmetric tensor $\sigma_{\mu\nu}$. Commonly used combinations are

$$\sigma_{\mu\nu} = \gamma_\mu \gamma_\nu, \tag{A.15a}$$

$$\sigma_{\mu\nu} = \frac{1}{2}\left[\gamma_\mu, \gamma_\nu\right], \tag{A.15b}$$

$$\sigma_{\mu\nu} = \frac{i}{2}\left[\gamma_\mu, \gamma_\nu\right]. \tag{A.15c}$$

We use

$$\Gamma_5 = \gamma_1\gamma_2 = \begin{pmatrix} i & 0 & 0 & 0 \\ 0 & -i & 0 & 0 \\ 0 & 0 & i & 0 \\ 0 & 0 & 0 & -i \end{pmatrix}, \tag{A.16}$$

$$\Gamma_6 = \gamma_1\gamma_3 = \begin{pmatrix} 0 & -1 & 0 & 0 \\ 1 & 0 & 0 & 0 \\ 0 & 0 & 0 & -1 \\ 0 & 0 & 1 & 0 \end{pmatrix}, \tag{A.17}$$

$$\Gamma_7 = \gamma_1\gamma_4 = \begin{pmatrix} 0 & -i & 0 & 0 \\ -i & 0 & 0 & 0 \\ 0 & 0 & 0 & i \\ 0 & 0 & i & 0 \end{pmatrix}, \tag{A.18}$$

$$\Gamma_8 = \gamma_2\gamma_3 = \begin{pmatrix} 0 & i & 0 & 0 \\ i & 0 & 0 & 0 \\ 0 & 0 & 0 & i \\ 0 & 0 & i & 0 \end{pmatrix}, \tag{A.19}$$

$$\Gamma_9 = \gamma_2\gamma_4 = \begin{pmatrix} 0 & -1 & 0 & 0 \\ 1 & 0 & 0 & 0 \\ 0 & 0 & 0 & 1 \\ 0 & 0 & -1 & 0 \end{pmatrix}, \tag{A.20}$$

$$\Gamma_{10} = \gamma_3\gamma_4 = \begin{pmatrix} -i & 0 & 0 & 0 \\ 0 & i & 0 & 0 \\ 0 & 0 & i & 0 \\ 0 & 0 & 0 & -i \end{pmatrix}. \tag{A.21}$$

Just like before, we have a bunch of options how to define the axial vector denoted as Γ_{A_μ}. Common choices are $\gamma_\mu\gamma_5$, $\gamma_5\gamma_\mu$ or combinations like

$\gamma_1\gamma_2\gamma_3, \ldots$, where we use the first one

$$\Gamma_{11} = \gamma_1\gamma_5 = \begin{pmatrix} 0 & 0 & 0 & -1 \\ 0 & 0 & 1 & 0 \\ 0 & 1 & 0 & 0 \\ -1 & 0 & 0 & 0 \end{pmatrix}, \tag{A.22}$$

$$\Gamma_{12} = \gamma_2\gamma_5 = \begin{pmatrix} 0 & 0 & 0 & i \\ 0 & 0 & i & 0 \\ 0 & -i & 0 & 0 \\ -i & 0 & 0 & 0 \end{pmatrix}, \tag{A.23}$$

$$\Gamma_{13} = \gamma_3\gamma_5 = \begin{pmatrix} 0 & 0 & 1 & 0 \\ 0 & 0 & 0 & 1 \\ -1 & 0 & 0 & 0 \\ 0 & -1 & 0 & 0 \end{pmatrix}, \tag{A.24}$$

$$\Gamma_{14} = \gamma_4\gamma_5 = \begin{pmatrix} 0 & 0 & i & 0 \\ 0 & 0 & 0 & -i \\ i & 0 & 0 & 0 \\ 0 & -i & 0 & 0 \end{pmatrix}. \tag{A.25}$$

The pseudoscalar is defined as the product of the basic 4 γ-matrices. Note, that while the γ_μ are defined in every space-time dimensionality from 3 on upwards (even in non-integer cases used in dimensional regularization), γ_5 only exists in even dimensions. The matrix γ_5 is also the kernel for the pseudoscalar current and reads

$$\Gamma_{15} = \gamma_5 = \gamma_1\gamma_2\gamma_3\gamma_4 = \begin{pmatrix} 1 & 0 & 0 & 0 \\ 0 & 1 & 0 & 0 \\ 0 & 0 & -1 & 0 \\ 0 & 0 & 0 & -1 \end{pmatrix}. \tag{A.26}$$

To check γ_5-hermiticity of the Dirac operator we need to know the anticommutator of γ_5 and the vector components of the Clifford-algebra. The matrix $gamma_5$ consists of the basic four γ-matrices, so γ_μ will anticommute with three of them and pick up an additional term from the one, where the index is equal. Let us consider the anticommutator with γ_1

$$\{\gamma_1, \gamma_5\} = \gamma_2\gamma_3\gamma_4 - \left(-\gamma_1^2 + 2\mathbb{1}\right)\gamma_2\gamma_3\gamma_4 = 0. \tag{A.27}$$

The same applies for the other three vector components and we end up with

$$\{\gamma_\mu, \gamma_5\} = 0. \tag{A.28}$$

A.3 Coefficients for the D_{CI}

In Table A.2 the coefficients used in Eq. (3.8) for the D_{CI} operator are collected.

	free case	$\beta = 7.90$, hyp smeared
s_1	$0.1409870061 \times 10^{1}$	$0.1435242205 \times 10^{1}$
s_2	$-0.4063348276 \times 10^{-1}$	$-0.4423977491 \times 10^{-1}$
s_3	$-0.1328179378 \times 10^{-1}$	$-0.1388845602 \times 10^{-1}$
s_5	$-0.1707793316 \times 10^{-2}$	$-0.1857941213 \times 10^{-2}$
s_6	$0.1707277975 \times 10^{-2}$	$0.1844693091 \times 10^{-2}$
s_8	$-0.2995931667 \times 10^{-2}$	$-0.3297305313 \times 10^{-2}$
s_{10}	$-0.4097715677 \times 10^{-3}$	$-0.4380561498 \times 10^{-3}$
s_{11}	$-0.7711930549 \times 10^{-3}$	$-0.8385459928 \times 10^{-3}$
s_{13}	$0.6542013926 \times 10^{-2}$	$0.6910343703 \times 10^{-2}$
v_1	0.2526693368	0.2359524603
v_2	$0.4483311559 \times 10^{-2}$	$0.5478266870 \times 10^{-2}$
v_4	$0.3493344361 \times 10^{-2}$	$0.4024272445 \times 10^{-2}$
v_5	$0.1077099799 \times 10^{-2}$	$0.1277439335 \times 10^{-2}$
t_1	$-0.7464002396 \times 10^{-1}$	$-0.7931477422 \times 10^{-1}$
t_2	$-0.1947456954 \times 10^{-2}$	$-0.2132367624 \times 10^{-2}$
t_3	$0.1702447555 \times 10^{-2}$	$0.1832223642 \times 10^{-2}$
t_5	$-0.4273892564 \times 10^{-2}$	$-0.4671766610 \times 10^{-2}$
t_{15}	$-0.2924376836 \times 10^{-2}$	$-0.3103630192 \times 10^{-2}$
p_1	$-0.6927076246 \times 10^{-2}$	$-0.7366668038 \times 10^{-2}$

Table A.2: Coefficients for the D_{CI} operator.

A.4 Fitting correlators

Correlators for mesons have the following behavior

$$C(t) = \sum_{i}^{\infty} D_i \left(\mathrm{e}^{-M_i\, t} \pm \mathrm{e}^{-M_i\, (T-t)} \right) \quad \text{with} \quad M_0 < M_1 < \ldots, \tag{A.29}$$

where the sign of the second term depends on the quantity in use. In principle we have many contributions to the correlator, but for determining the

quantities we are interested in it is sufficient to consider only the lowest lying state. Hence let us denote the prefactor and mass for the ground state as $D = D_0$ and $M = M_0$.

Fitting procedure

At larger t, where excited state contributions become negligible, the correlators have a cosh or sinh functional behavior. Therefore we may extract the prefactor D and the meson mass M performing a correlated least-squares fit of the correlation function $C(t)$ to

$$D(M)\, f(M,\, t) \quad \text{with} \quad f(M,\, t) \equiv \left(\mathrm{e}^{-M\, t} \pm \mathrm{e}^{-M\,(T-t)}\right) \tag{A.30}$$

by minimizing the merit function

$$\chi^2 = [C - Df(M), C - Df(M)]\,. \tag{A.31}$$

The abbreviation

$$[A, B] = \sum_{t,t'} A(t)\mathrm{Cov}^{-1}(t, t')B(t') \tag{A.32}$$

with $t, t' \in [t_a, t_b]$ and

$$\mathrm{Cov}_{t,t'} = \delta_{t,t'} \tag{A.33a}$$

$$\mathrm{Cov}_{t,t'} = \delta_{t,t'}\sigma(t)^2 \tag{A.33b}$$

$$\mathrm{Cov}_{t,t'} = \sum_{i}^{N} \left(C_i(t) - \overline{C}(t)\right)^2 \sum_{j}^{N} \left(C_j(t') - \overline{C}(t')\right)^2 \tag{A.33c}$$

is used here. We use Eq. (A.33a) for a fit without error information, Eq. (A.33b) for a fit with error bars present and Eq. (A.33c) for a fit with the full covariance information, e.g., if we have different jackknife blocks. The minimization may be simplified by observing, that for given M the minimum of χ^2 is obtained for

$$\frac{\partial \chi^2}{\partial D} = -2\,[f(M), C - Df(M)] = 0 \tag{A.34}$$

resulting in

$$D(M) = \frac{[C, f(M)]}{[f(M), f(M)]}. \tag{A.35}$$

Using this relation one performs the one-dimensional minimization of Eq. (A.31) with regard to M. In Fig. A.1 we display the merit function χ^2 for the original two dimensional case and the reduced case.

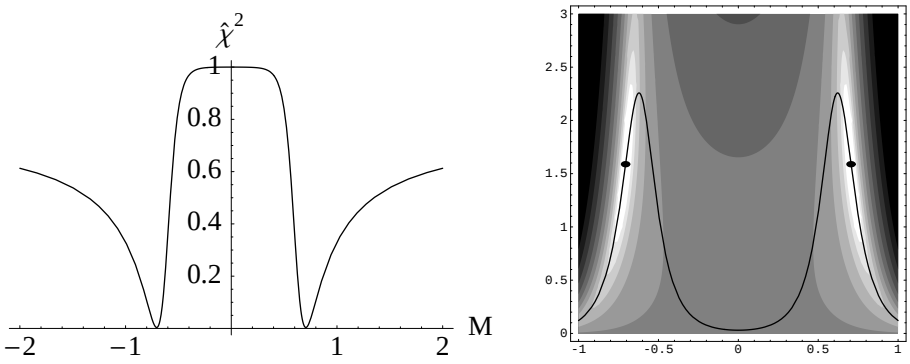

Figure A.1: (a) Normalized χ^2 for sample data using the reduction to one parameter. (b) A contour plot of $\log(\chi^2)$ for M on the x-axis and $\frac{D}{10^5}$ on the y-axis. The path in parameter space of the reduced problem is displayed as a solid line. The dots mark the two minimal values.

Error estimation

The correlator values are arranged in overlapping blocks according to the standard jackknife algorithm. Each block consists of typically 95% of all hadron propagators for a given set of lattice parameters. For each such jackknife block we then determine the values of the propagator and the requested ratios at various t, as well as the covariance matrix for the propagator and the variance for the ratios. These are then fitted as discussed, i.e., either to asymptotic cosh- or sinh-behavior or to a constant. For this fit the relative weights (as defined from the covariance and variance) are important. We also need variances for the correlators involving derivatives with regard to t, as they also enter some of the ratios. Since we need these for each jackknife set we estimate the variance of the derivatives by performing another jackknife analysis within the given set. The fits are then repeated for all jackknife blocks and the variation of the results for coefficients, mass values and ratios leads to the estimate for the corresponding errors.

Numerical derivatives

For some of the ratios of correlators we need derivatives of the correlator with regard to the time t. Numerical derivatives are always based on assumptions on the interpolating function. Usual simple 2- or 3- point formulas assume polynomials as interpolating functions. We can do better by utilizing the

information on the expected cosh- and sinh-dependence. In fact, we may use these functions for local 3-point interpolation and get the derivative therefrom. A two point derivative based only on function values y_t and y_{t-1} is not suitable since it provides values at half-integer t. We therefore use a local 3-point fit to y_{t-1}, y_t and y_{t+1} to the functional form (A.30) (depending on whether the correlator is symmetric or anti-symmetric in t), where the parameters $\overline{D}$ and $\overline{M}$ now depend on the actual value of t. We then reconstruct the derivative as

$$\partial_t f(\overline{M},\, t) \equiv \overline{M} \left(-\mathrm{e}^{-\overline{M}\, t} \pm \mathrm{e}^{-\overline{M}\, (T-t)} \right) \tag{A.36}$$

Then the desired ratios can be computed in a straightforward manner and the plateau values obtained by fits. When analyzing not ratios but the correlators of type $\langle (\partial_t A_4) X \rangle$ directly we perform a global fit to $\langle A_4 X \rangle$ according to Eq. (A.30) and take the analytic derivative.

List of Tables

List of Figures

Bibliography

[1] P. Huber, Chiral properties and renormalization constants in qcd, Master's thesis, University of Graz, 2003.

[2] C. Gattringer, M. Göckeler, P. Huber, and C. B. Lang, Nucl. Phys. **B694**, 170 (2004), hep-lat/0404006.

[3] Bern-Graz-Regensburg (BGR), C. Gattringer, P. Huber, and C. B. Lang, Phys. Rev. **D72**, 094510 (2005), hep-lat/0509003.

[4] C. Gattringer, P. Huber, and C. B. Lang, PoS **LAT2005**, 121 (2006), hep-lat/0509059.

[5] H. Fritzsch, M. Gell-Mann, and H. Leutwyler, Phys. Lett. **B47**, 365 (1973).

[6] E. Seiler, Lect. Notes Phys. **159**, 1 (1982).

[7] G. 't Hooft, Nucl. Phys. **B61**, 455 (1973).

[8] W. A. Bardeen, A. J. Buras, D. W. Duke, and T. Muta, Phys. Rev. **D18**, 3998 (1978).

[9] R. P. Feynman, Rev. Mod. Phys. **20**, 367 (1948).

[10] S. Elitzur, Phys. Rev. **D12**, 3978 (1975).

[11] K. G. Wilson, Phys. Rev. **D10**, 2445 (1974).

[12] G. Curci, P. Menotti, and G. Paffuti, Phys. Lett. **B130**, 205 (1983).

[13] M. Lüscher and P. Weisz, Phys. Lett. **B158**, 250 (1985).

[14] G. P. Lepage and P. B. Mackenzie, Phys. Rev. **D48**, 2250 (1993), hep-lat/9209022.

[15] M. G. Alford, W. Dimm, G. P. Lepage, G. Hockney, and P. B. Mackenzie, Phys. Lett. **B361**, 87 (1995), hep-lat/9507010.

[16] K. G. Wilson, New Phenomena In Subnuclear Physics. Part A. Proceedings of the First Half of the 1975 International School of Subnuclear Physics, Erice, Sicily, July 11 - August 1, 1975, ed. A. Zichichi, Plenum Press, New York, 1977, p. 69, CLNS-321.

[17] H. B. Nielsen and M. Ninomiya, Phys. Lett. **B105**, 219 (1981).

[18] H. B. Nielsen and M. Ninomiya, Nucl. Phys. **B193**, 173 (1981).

[19] P. H. Ginsparg and K. G. Wilson, Phys. Rev. **D25**, 2649 (1982).

[20] R. Narayanan and H. Neuberger, Phys. Rev. Lett. **71**, 3251 (1993), hep-lat/9308011.

[21] R. Narayanan and H. Neuberger, Phys. Lett. **B302**, 62 (1993), hep-lat/9212019.

[22] R. Narayanan and H. Neuberger, Nucl. Phys. **B443**, 305 (1995), hep-th/9411108.

[23] C. Gattringer, Phys. Rev. **D63**, 114501 (2001), hep-lat/0003005.

[24] C. Gattringer, I. Hip, and C. B. Lang, Nucl. Phys. **B597**, 451 (2001), hep-lat/0007042.

[25] M. Lüscher, Phys. Lett. **B428**, 342 (1998), hep-lat/9802011.

[26] C. Best *et al.*, Phys. Rev. **D56**, 2743 (1997), hep-lat/9703014.

[27] C. Hagen, Spectroscopy of baryons and exotic hadrons on the lattice, Master's thesis, University of Regensburg, 2005.

[28] S. Scherer, (2002), hep-ph/0210398.

[29] Particle Data Group, S. Eidelman *et al.*, Phys. Lett. **B592**, 1 (2004).

[30] Bern-Graz-Regensburg, T. Burch *et al.*, Phys. Rev. **D70**, 054502 (2004), hep-lat/0405006.

[31] R. Sommer, Nucl. Phys. **B411**, 839 (1994), hep-lat/9310022.

[32] S. R. Sharpe, Phys. Rev. **D56**, 7052 (1997), hep-lat/9707018.

[33] Y. Chen *et al.*, Phys. Rev. **D70**, 034502 (2004), hep-lat/0304005.

[34] T. Blum *et al.*, Phys. Rev. **D69**, 074502 (2004), hep-lat/0007038.

[35] L. Giusti, C. Hölbling, and C. Rebbi, Phys. Rev. **D64**, 114508 (2001), hep-lat/0108007.

[36] S. J. Dong *et al.*, Phys. Rev. **D65**, 054507 (2002), hep-lat/0108020.

[37] BGR, C. Gattringer *et al.*, Nucl. Phys. **B677**, 3 (2004), hep-lat/0307013.

[38] J. Gasser and H. Leutwyler, Phys. Lett. **B188**, 477 (1987).

[39] F. C. Hansen, Nucl. Phys. **B345**, 685 (1990).

[40] F. C. Hansen and H. Leutwyler, Nucl. Phys. **B350**, 201 (1991).

[41] C. W. Bernard and M. F. L. Golterman, Phys. Rev. **D46**, 853 (1992), hep-lat/9204007.

[42] S. R. Sharpe, Phys. Rev. **D46**, 3146 (1992), hep-lat/9205020.

[43] C. W. Bernard, M. Golterman, J. Labrenz, S. R. Sharpe, and A. Ukawa, Nucl. Phys. Proc. Suppl. **34**, 334 (1994).

[44] R. Babich *et al.*, JHEP **01**, 086 (2006), hep-lat/0509027.

[45] ALPHA, J. Heitger, R. Sommer, and H. Wittig, Nucl. Phys. **B588**, 377 (2000), hep-lat/0006026.

[46] L. Giusti, C. Hölbling, and C. Rebbi, Nucl. Phys. Proc. Suppl. **106**, 739 (2002), hep-lat/0110184.

[47] T.-W. Chiu and T.-H. Hsieh, Nucl. Phys. **B673**, 217 (2003), hep-lat/0305016.

[48] S. Dürr and C. Hölbling, Phys. Rev. **D72**, 071501 (2005), hep-ph/0508085.

[49] G. Colangelo, J. Gasser, and H. Leutwyler, Nucl. Phys. **B603**, 125 (2001), hep-ph/0103088.

[50] B. Ananthanarayan, I. Caprini, G. Colangelo, J. Gasser, and H. Leutwyler, Phys. Lett. **B602**, 218 (2004), hep-ph/0409222.

[51] Bern-Graz-Regensburg (BGR), S. Capitani, C. Gattringer, and C. B. Lang, Phys. Rev. **D73**, 034505 (2006), hep-lat/0511040.

[52] L. Giusti, P. Hernandez, M. Laine, P. Weisz, and H. Wittig, JHEP **01**, 003 (2004), hep-lat/0312012.

[53] L. Giusti, P. Hernandez, M. Laine, P. Weisz, and H. Wittig, JHEP **04**, 013 (2004), hep-lat/0402002.

[54] H. Fukaya, S. Hashimoto, and K. Ogawa, Prog. Theor. Phys. **114**, 451 (2005), hep-lat/0504018.

[55] W. Bietenholz and S. Shcheredin, PoS **LAT2005**, 138 (2006), hep-lat/0508016.

[56] S. Shcheredin and W. Bietenholz, PoS **LAT2005**, 134 (2006), hep-lat/0508034.

[57] P. Hernandez, K. Jansen, and L. Lellouch, Phys. Lett. **B469**, 198 (1999), hep-lat/9907022.

[58] P. Hasenfratz, S. Hauswirth, T. Jorg, F. Niedermayer, and K. Holland, Nucl. Phys. **B643**, 280 (2002), hep-lat/0205010.

[59] M. Hofmayer, Hadronic properties of chirally improved dirac operators, Master's thesis, University of Graz, 2004.

[60] J. Wennekers and H. Wittig, JHEP **09**, 059 (2005), hep-lat/0507026.

[61] P. Hasenfratz and F. Niedermayer, Nucl. Phys. **B414**, 785 (1994), hep-lat/9308004.

[62] C. B. Lang, P. Majumdar, and W. Ortner, (2004), hep-lat/0412016.

[63] C. B. Lang, P. Majumdar, and W. Ortner, PoS **LAT2005**, 124 (2006), hep-lat/0509004.

[64] C. B. Lang, P. Majumdar, and W. Ortner, PoS **LAT2005**, 131 (2006), hep-lat/0509005.

[65] C. B. Lang, P. Majumdar, and W. Ortner, Phys. Rev. **D73**, 034507 (2006), hep-lat/0512014.

[66] C. B. Lang, P. Majumdar, and W. Ortner, (2006), hep-lat/0611010.

Acknowledgment

I am deeply grateful to so many people for being part of my life and helping me to finish this thesis.
First of all I want to thank Prof. Dr. Christian Lang for guiding me through this work, for having the time to sit down and discuss even the most trivial questions of mine and for giving me the freedom I needed to work.
Prof. Dr. Christof Gattringer for working together on different projects, for showing me how beautiful and also useful it can be to sit down and do a calculation with pencil and paper, and for developing this crazy set of rules for ping-pong that can really calm you down before you have to give a talk.
Prof. Thomas DeGrand for being willing to accept me as a visitor in Boulder, teaching me and discussing subjects from finite-size effects to backcountry skiing. The stay in Colorado was really great fun.
The "Zeitschriftenzimmer-Crew" provided the best possible office to have your desk in, but in more detail that means: I want to thank Alex for your enthusiasm and interest that you transfer to all the people around you and all the time we've spent together, both, on and off campus.
Reini for always having a smile on your face and a tune on your lips.
Andi for all the curious questions and crazy ideas that always make me lough and think at the same time.
All my dear colleagues here in Graz, or wherever you are right now, hopefully I don't forget anyone. Kai, Wolfgang, Michi, Erek, Markus, Elmar, Vreni, Roland, Rafael, Daniel, Julia, Markus, Reini, Kathi, it is really cool that I met you all. Maybe I should also thank the coffee maker next door for rarely letting us down when we were on our more or less extensive breaks... Maybe not.
Now to my two roommates. Chris I want to thank you for your motivation and positive energy that you have and pass on to me and for all the trips to the rocks, both past and future ones.

Roli for all the deep conversations and amusing activities... I am ready for the road trip.
I want to thank all of my climbing buddies, Heli (especially for getting me into bouldering), Steff, Paul, Martin, Flo, Jörg.
Georges, I want to thank you for letting me experience what lived serenity means.
My beloved parents, for everything that you did in the past 27 years. You supported me in the best possible way and I will never forget that.
Marlis, I want to thank you for your positive and kind nature and all the beautiful time we've spent together. Tell you the rest later on when we talk... I love you!